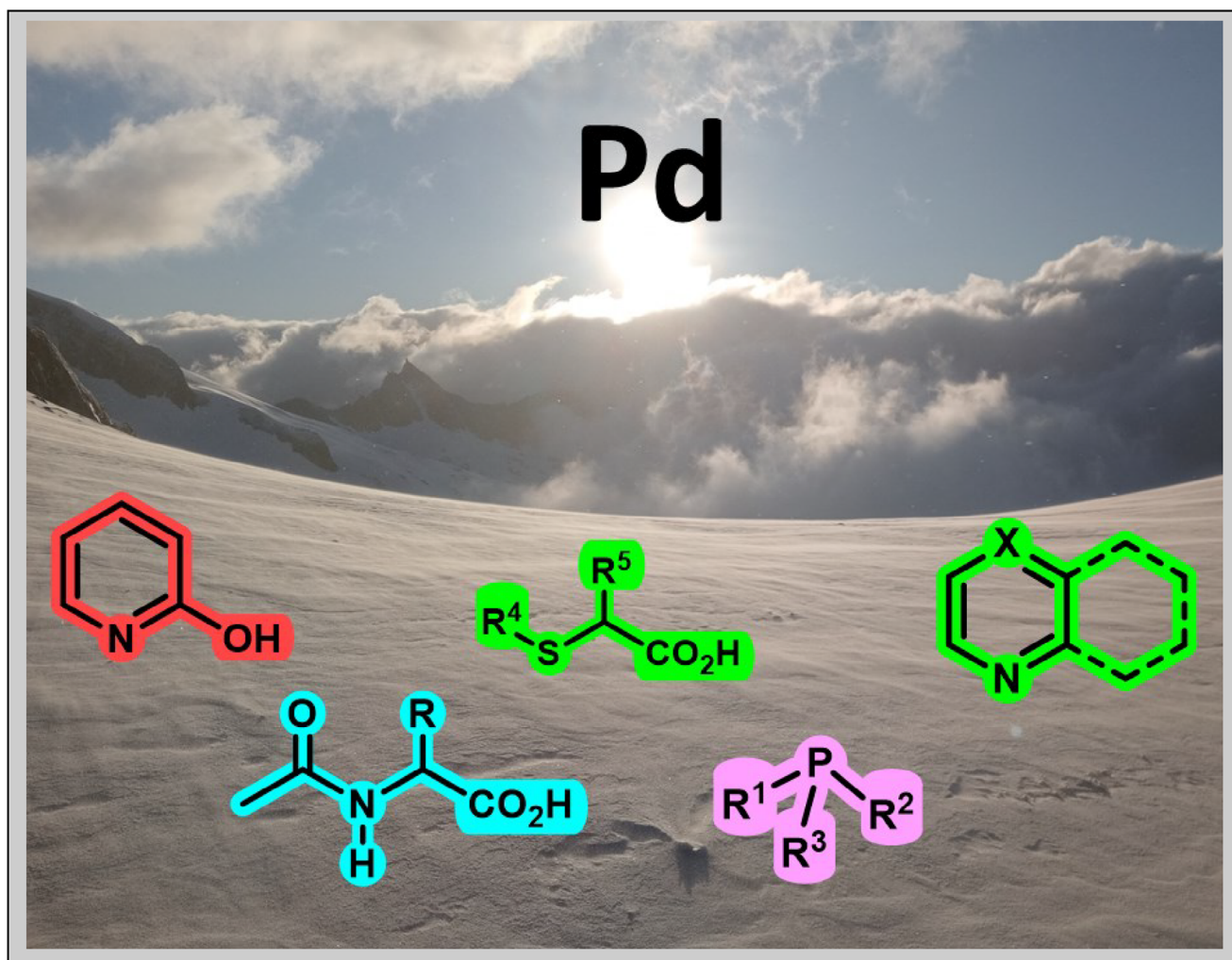


Advances in Ligand-Driven Pd-Catalyzed C–H Functionalizations: Recent Insights and Updates

Jesús Moradell,^[a] Cosmina Bohan,^[b] Alexandra Pop,^[b] and Esteban P. Urriolabeitia*^[a]



The activation of C—H bonds mediated by transition metals has become an essential tool for synthetic chemists, enabling more efficient, selective, and sustainable processes. This progress has been driven by the elimination of precursor prefunctionalization, shortening and reducing the cost of syntheses. However, challenges remain in this methodology, both in terms of activity and selectivity. The introduction of DG to achieve maximum selectivity represents the core of this issue, as it fails to overcome the problem of prefunctionalization, and reaction control remains dependent on substrate design. Recently, we have witnessed a revolution in this field, as activity and selectivity of

new processes are no longer controlled by the substrate but by the catalyst. It is the design of the catalyst itself—particularly the ligands—that determines whether the reaction occurs, its rate, and selectivity. This review analyzes the crucial role of ligands in Pd-catalyzed C—H functionalizations in the period from 2022 to the present, focusing on five types of ligands: (i) mono-*N*-protected amino acids (MPAAs); (ii) pyridones; (iii) pyridines, related *N*-heterocycles; (iv) thioacids; (v) phosphines and NHCs. For each category, its role, how the reaction is accelerated, and the origin of its selectivity is analyzed.

1. Introduction

C—C and C—Heteroatom coupling processes (C—N, C—O, C—Hal, C—P, C—S, among the most relevant) are the primary tool for constructing more elaborate new molecules from simple substrates found in raw materials. Under ideal conditions, the introduction of complex functional groups should be carried out at selected positions in a selective manner, using the fewest possible steps, consuming the least amount of energy, and generating minimal amounts of waste. In other words, following the principles of green chemistry, which were established more than 25 years ago.^[1] Developing a process that meets all these principles simultaneously is challenging and some green chemistry recommendations have been studied and implemented much more extensively than others.

The use of catalysts is one of these recommendations, as their application is extensive and they are present in all types of processes, making this one of the research areas where the number of contributions continues to grow year after year. This ongoing interest is also driven by the recent introduction of new methodologies, such as photocatalysis, electrocatalysis, or mechanocatalysis among others.^[2–9] There are numerous and diverse types of catalysts, but transition-metal coordination complexes are perhaps among the most widely studied for different reasons: their robustness and stability under demanding reaction conditions, as well as their high activity and selectivity in a wide range of catalyzed processes, to name the most outstanding features. Additionally, the properties of these catalysts can be easily fine-tuned, whether in terms of electronic factors

(such as net charge, formal charge of the metal, oxidation state, or ligand characteristics) or steric factors (such as coordination index, geometry, or ligand volume). All of this makes transition-metal coordination complexes an almost infinitely versatile tool for synthesis.

However, achieving high reactivity and selectivity in most cases comes at a cost. The classic Pd-catalyzed C—C cross-coupling processes, such as Heck, Suzuki, or Sonogashira, among others are clear examples of this statement.^[10,11] Although Pd catalysts are by far the most widely used for constructing C—C bonds, both reactivity and selectivity in these processes are achieved by introducing functional groups into the substrates, such as halides, boron, tin, lithium, magnesium, or zinc derivatives (Figure 1a). This prefunctionalization of substrates extends the synthetic route, increases the cost of preparing starting materials, and requires the removal of equimolar amounts of waste after the reaction, which undermines the sustainability that catalytic processes aim to achieve. Furthermore, in many cases, prefunctionalization is not feasible due to synthetic constraints, significantly limiting the range of available starting materials.

One of the most extensively studied approaches to overcoming the drawbacks associated with the use of pre-functionalized substrates and one that has demonstrated remarkable efficacy, is the use of catalytic processes based on C—H bond activation.^[12–20] C—H bonds are ubiquitous in organic molecules, which eliminates the need for substrate pre-functionalization, prevents unnecessary extension of precursor synthesis, and, at the same time, does not limit the scope of accessible starting materials. Moreover, this organometallic methodology provides new retrosynthetic routes that are not accessible otherwise, as the possible disconnections differ from those offered by classical organic chemistry. Maintaining the delicate balance between accessibility, sustainability, reactivity, and selectivity, it is evident that the absence of pre-functionalization directly results in low reactivity and necessitates the design of strategies to achieve selective activation. The lack of reactivity and the chemical inertia of C—H bonds are once again overcome through the use of transition-metal coordination complexes, as these are capable of activating and ultimately cleaving C—H bonds. Achieving high selectivity has proven to be more challenging, and various approaches have been employed. The first of these is the modification of starting materials by introducing directing groups

[a] J. Moradell, Dr. E. P. Urriolabeitia
Instituto de Síntesis Química y Catálisis Homogénea, ISQCH, CSIC –
Universidad de Zaragoza, Pedro Cerbuna 12, Zaragoza 50009, Spain
E-mail: esteban.u.a@csic.es

[b] C. Bohan, Dr. A. Pop
Supramolecular Organic and Organometallic Chemistry Centre, Department
of Chemistry, Faculty of Chemistry and Chemical Engineering, Babeş-Bolyai
University, Arany Janos 11, Cluj-Napoca 400028, Romania

© 2025 The Author(s). ChemCatChem published by Wiley-VCH GmbH. This is an open access article under the terms of the [Creative Commons Attribution-NonCommercial-NoDerivs](#) License, which permits use and distribution in any medium, provided the original work is properly cited, the use is non-commercial and no modifications or adaptations are made.

(DG, Figure 1b).^[21] Their mode of action is well understood: once installed on the substrate, they coordinate with the metal, bringing it into close proximity to the C–H bond(s) intended for activation and functionalization. This reactivity is based on the spatial proximity between the metal and the substrate, though it can also be influenced by electronic and steric factors. The paradigm of this type of reaction is functionalization at the ortho position of aromatic rings.^[22–26]

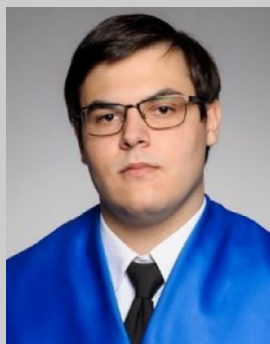
In general, DG are permanent and covalently bonded to the substrate. The most favorable scenario is one in which a functional group from the starting material (such as an amine, aldehyde, or acid) can be utilized as a DG as this avoids extending the synthesis.^[27–30] However, in some cases, they must be introduced prior to C–H activation, which once again leads to the same situation described in previous paragraphs, as it lengthens and increases the cost of the synthesis. Despite these drawbacks, the use of DG has been—and continues to be—the most widely employed method for achieving complete selectivity in functionalization.

In addition to the covalent anchoring of the DG to the substrate, several strategies have been developed to achieve the desired selectivity while minimizing the synthetic effort required for substrate preparation. For instance, traceless DG have been described; these are incorporated into the starting materials and are removed from the substrate under reaction conditions after

fulfilling their function.^[31–37] Similarly, transient DG have been extensively studied. These are bonds or functional groups that form during the catalytic cycle, act as DG, and break before the next cycle begins, releasing the catalytic product without the DG.^[38–47] Carboxylic acids, through decarbonylation processes, or silanols are excellent examples of traceless DG. Meanwhile, the in situ formation of imines from amines and aldehydes represents a classic and representative example of transient DG.

All previous strategies involving DG rely on substrate modification with the advantages and disadvantages already discussed. When the substrate lacks incorporated DG or their incorporation is synthetically unfeasible, nondirected C–H activation can follow two different scenarios. The first includes precursors that, due to their inherent electronic nature, already direct C–H activation to very specific positions in the molecule, allowing the catalytic reaction to proceed with high (even complete) selectivity naturally (innate or biased substrates).^[48–51] For example, substrates with high electron density (such as nucleophilic arenes or heterocycles like pyrrole, indole, etc.) or those with very low electron density (such as C₆F₅H and other pentafluorophenyl derivatives) fall into this category.

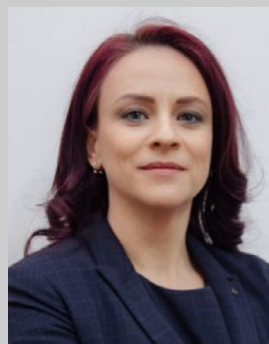
When the substrate does not exhibit this type of inherent reactivity and selectivity (unbiased), the control of both reactivity and selectivity must be exerted by the catalyst, making its design a significant challenge. The advantage of unmodified substrates



Jesus Moradell received his BSc in chemistry in 2023 and his MSc in molecular chemistry and homogeneous catalysis in 2024 from the University of Zaragoza (Spain). Currently, he is a PhD student at the University of Zaragoza under the supervision of Dr. Esteban P. Urriolabeitia Arrondo and Dr. Juan Vicente Alegre Requena. His current research focuses on the development of new fluorescent probes using a data-driven approach.



Cosmina Bohan graduated in chemistry in 2022 from Babeş-Bolyai University (Romania) and she received her MSc in advanced chemistry in 2024. Currently, she is a PhD student at the Babeş-Bolyai University under the supervision of Prof. Dr. Anca Silvestru. Her scientific research focuses on synthesis, chemical reactivity, and applications of organochalcogen compounds.



Dr. Alexandra Pop is currently a lecturer at the Faculty of Chemistry and Chemical Engineering at Babeş-Bolyai University of Cluj-Napoca, Romania. She obtained her PhD at Babeş-Bolyai University in 2012 under the supervision of Acad. Prof. Dr. Cristian Silvestru. Her research focuses on the synthesis, structural characterization, and investigation of the photophysical properties of some transition-metal complexes containing organochalcogen (S, Se, Te) ligands.



Dr. Esteban P. Urriolabeitia completed his PhD (1991) at the University of Zaragoza and undertook a postdoctoral stay (1993–1994) at the University of Strasbourg with Prof. Michel Pfeffer, working on organic synthesis through organometallic intermediates. After rejoining ICMA, he became a permanent staff member of CSIC in 2000 and was promoted to CSIC research scientist in 2007. His research focuses on organometallic chemistry with particular emphasis on the application of organometallic compounds as intermediates in organic synthesis via CH activation and luminescent devices.

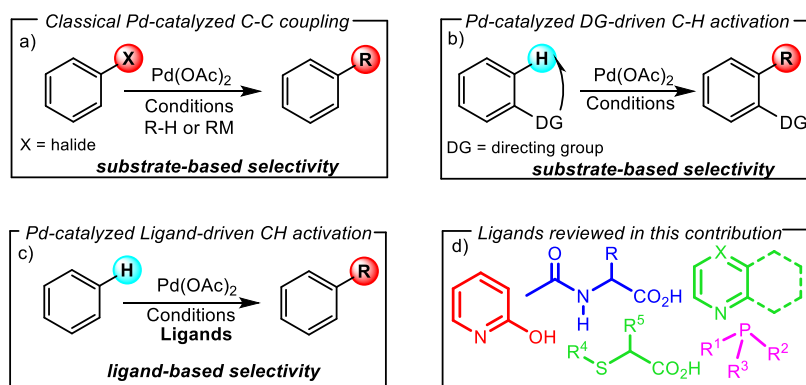


Figure 1. (a–c) Different approaches to achieve functionalization and (d) ligands that provide the best results for functionalization type, which are reviewed in this contribution.

without DG is that their reactivity is not constrained by a functional group, potentially broadening the scope of the reaction. Additionally, selectivity may differ and in some cases, even complement that of the prefunctionalized substrate. Both aspects represent a clear improvement over previous approaches. However, there is a major drawback: the unbiased substrate to be functionalized (typically an arene) must be present in a large excess, even as a co-solvent, and this is not very sustainable.

At this point, the role of ancillary ligands surrounding the transition metal becomes even more critical. In the case of palladium catalysis, achieving a reactivity increase to the point where the arene becomes the limiting reagent while maintaining selectivity control has been a relatively unexplored topic, with only a few ligands proving particularly effective. In recent years, this field has seen remarkable progress, where the presence of a specific type of ligand—or at most, a combination of two ligands—has led to significant acceleration of the reaction rate while ensuring high selectivity across a broad and diverse range of precursors. A selection of the most important ligands is shown in Figure 1d.

This contribution will review Pd-catalyzed processes enabled by these ligands (or their combinations), focusing on the most recent developments (mid-2022 to present). Although several reviews on this topic have been published more or less recently,^[52–69] the rapid pace of advancements calls for frequent updates. Moreover, most reviews focus on a single ligand, whereas this work aims to provide a broader overview of the state-of-the-art, covering all relevant Pd ligands that have emerged within the specified timeframe.

2. Mono-Protected Amino Acid Ligands (MPAA)

Amino acid-type ligands that possess an *N*-acyl protecting group (MPAA) as represented in Figure 2a have been and continue to be widely used in Pd-catalyzed C–H functionalization processes on substrates that lack DG. There are two fundamental reasons for this. The first is that the coordination of MPAA to the metal generates reactive intermediates that significantly accelerate the reaction rate. This acceleration is explained by considering that the MPAA ligand acts as an internal base through the carbonyl

group to assist the C–H activation step when it occurs via a concerted metalation-deprotonation (CMD) mechanism.^[52,54] The second reason lies in the fact that the rigid N,O-coordination of MPAA and the presence of stereogenic centers within it create chiral pockets around the metal—well-defined spatial environments that enable highly effective enantioselective catalysis. The performance of these two functions—acceleration and selectivity—leads to their classification as *bifunctional ligands*.

The coordination mode of these MPAA ligands can vary according to the requirements imposed by the metal's environment at any given moment, being accesible monoanionic $\kappa^1\text{-O}$, $\kappa^2\text{-N,O}$ and $\mu^2\text{-O,O}$ and dianionic $\kappa^2\text{-N,O}$ bonding modes. However, to effectively fulfill their role as bifunctional ligands, they must act as $\kappa^2\text{-N,O}$ dianionic ligands after deprotonation of the carboxyl O–H and the acyl N–H groups. The presence of the carbonyl oxygen is critical for assisting proton transfer, whereas the carboxylate group is not as crucial in this step. This statement has been experimentally demonstrated by Albéniz and coworkers.^[70] Complex **1**, shown in Figure 2b, reacts with toluene in refluxing *N,N*-dimethylacetamide (DMA) to yield the biphenyl C–C coupling product ($\text{C}_6\text{F}_5\text{--C}_6\text{H}_4\text{Me}$) as a mixture of all isomers where the *meta* is most abundant. However, complex **2**, which lacks the carbonyl group, does not react with toluene under the same reaction conditions, proving the importance of this functional group in accelerating C–H activation. In any case, the same authors demonstrate that the nature of auxiliary ligands plays a key role in determining the coordination mode, even though the reactive species is the $\kappa^2\text{-N,O}$ dianion. Once the reactive coordination mode has been established, the most important contributions published since 2022 are presented below, categorized by the type of process they catalyze.

2.1. Intramolecular Cyclization in Absence and in Presence of Alkenes

The functionalization of carboxylic acids remains a challenge since they are very common, accessible, and generally inexpensive raw materials, but the carboxylate group acts as a weak DG. Therefore, advances in this area are of great interest. Van

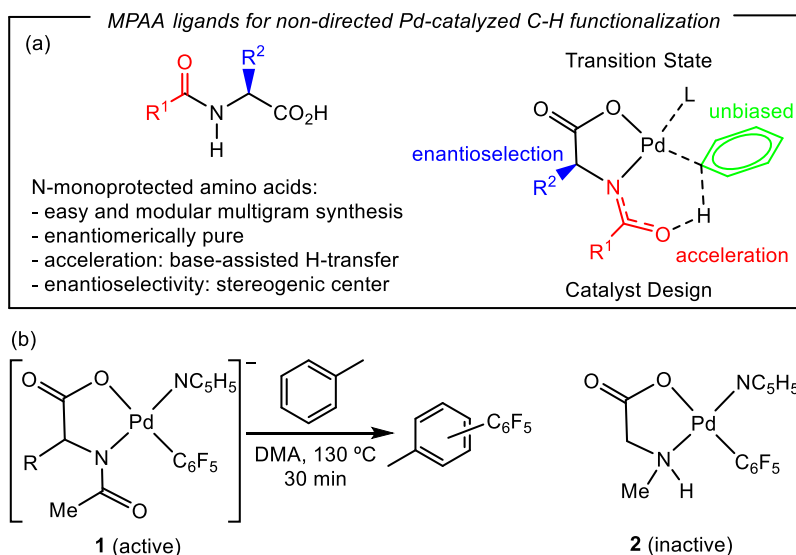


Figure 2. (a) Diagram of mono-protected amino acids (MPAAs) and their mode of action. Comparison of the reactivity of 1 and 2, and (b) demonstration of the necessity of the carbonyl group to promote C–H activation.

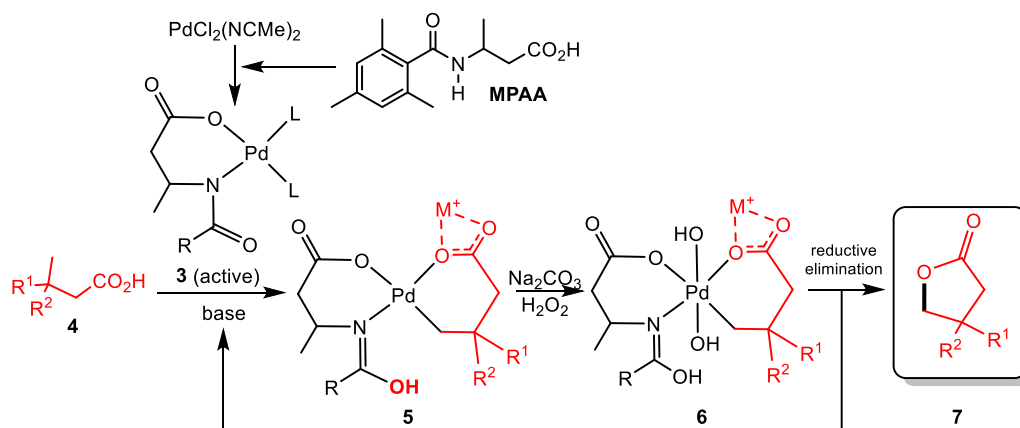


Figure 3. γ -Lactonization of aliphatic carboxylic acids 4 via C(sp³)–H bond activation.

Gemmeren and coworkers have very recently described the γ -lactonization of a wide variety of aliphatic carboxylic acids in the presence of K₂HPO₄ and Na₂CO₃·H₂O₂, with PdCl₂(NCMe)₂ (10 mol%) as the pre-catalyst, a process illustrated in Figure 3.^[71] As mentioned in previous paragraphs, this complex is not the reactive species but rather the complex formed by the coordination of MPAA to Pd represented as (3) in Figure 3. The ligand optimization process shows that 2,4,6-alkyl-substituted benzamide- β -alanine MPAA provides the highest yield, presumably because the acidity of the amide proton, the ligand's bite angle, and the increased steric hindrance favors the reductive elimination step, which is the critical step. The reaction proceeds via C(sp³)–H bond activation in the carboxylate species, formed by the reaction of acid (4) in the presence of a base. The O,O'-coordination of the carboxylate brings the γ -C–H bond close to the metal (proximity-driven functionalization), allowing activation by Pd to form intermediate (5), which then undergoes an oxidative addition process with Na₂CO₃·H₂O₂ (sodium percarbonate), yielding the dihydroxy derivative (6). The subsequent

C–O coupling through reductive elimination, facilitated by the MPAA ligand, leads to lactone (7) formation, and regenerates the active species (3).^[71]

The γ -butyrolactones obtained serve as precursors to high-value added compounds. In this regard, although the method proceeds under harsh reaction conditions (100 °C, 15 h), it exhibits a very broad scope (which is uncommon for this type of reaction) and eliminates the need for any prior prefunctionalization, a common requirement in classical lactonization reactions.

The mechanism of lactonization reactions of aliphatic carboxylic acids, catalyzed by Pd in the presence of MPAA and tert-butyl hydroperoxide (TBHP) has been thoroughly studied by Xu, Yu, and Musaev.^[72] The study shows that the reaction begins with the formation of the catalytically active species through coordination of MPAA to Pd (very similar to species 3 in Figure 3), followed by the C–H bond activation step in the substrate, where the substrate is in the form of a carboxylate. The calculated activation of the C(sp³)–H bond is not the rate-

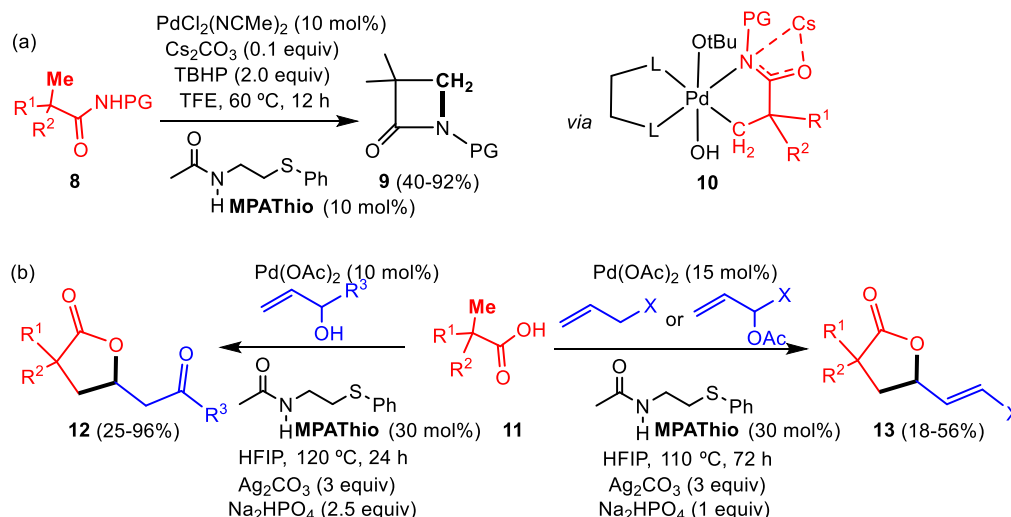


Figure 4. (a) γ -Lactamization of aliphatic carboxylic amides **8** via $C(sp^3)$ -H bond activation and (b) γ -lactonization followed by olefination of aliphatic carboxylic acids **11** via $C(sp^3)$ -H bond activation.

determining step (RDS) of the reaction, with one reason for the low activation energy of this step being the assistance of the MPAA ligand in the removal of the proton resulting from C—H activation. After $C(sp^3)$ -H activation, the formation of the C—O bond by direct reductive elimination or by intramolecular nucleophilic substitution (S_N2) is ruled out, as the reaction proceeds through oxidation of Pd(II) to Pd(IV) followed by reductive elimination back to Pd(II). The oxidation of Pd(II) to Pd(IV) is the RDS of the reaction and must be carried out with an oxidant containing hydroxyl groups. This study is crucial as it demonstrates that the MPAA ligand not only stabilizes the catalytically active species as a hydrogen acceptor during CH activation but also acts as a proton donor toward the oxidant during oxidation and reductive elimination. This assistance in proton migration stabilizes all intermediate steps and is the reason for the effectiveness of these ligands in this type of process.^[73]

Slight changes in the substrate may require significant variations in reaction conditions. Yu and collaborators have described the intramolecular cyclization of aliphatic amides (**8**) to form lactams (**9**) (lactamization), a process shown in Figure 4a.^[73] Despite the apparent similarity to the process shown in Figure 3, the ligand that enables this transformation is the amido-thioether ligand shown in the figure (MPATHio). In this case, as determined from an extensive ligand screening conducted in this study, neither MPAA nor hydroxy-pyridines are suitable, as they result in much lower conversions. Interestingly, this MPATHio ligand had not been previously used in intramolecular cyclization reactions. The reaction occurs only in the presence of TBHP, which is highly advantageous from an economic standpoint, and it is proposed to proceed through a Pd(IV) intermediate such as (**10**), whose structure is particularly stabilized by the amido-thioether ligand. Due to this stabilization, the reaction takes place under exceptionally mild conditions compared to other lactamization reactions and does not require special precautions against ambient oxygen or moisture. The reaction has a broad scope, tolerating a variety of *N*-protecting groups based on sulfonyl groups as well as gem-dimethyl ($R_1 = \text{Me}$) and mono-

methyl ($R_1 \neq R_2 \neq \text{Me}$) substituents in the aliphatic chain. The C—H activation occurs selectively at one of the β -methyl groups with no activation observed at the γ - or δ -positions.^[73]

The lactonization reaction can be combined with olefination, allowing the synthesis of highly valuable species. Jeganmohan has studied the reactivity of aliphatic carboxylic acids with olefins bearing different substituents in a Pd-catalyzed process promoted by the MPATHio ligand, as shown in Figure 4b.^[74] As observed, the outcome of the reaction depends on the olefin substituents. When allylic alcohols are used (left side of Figure 4b), γ -butyrolactones (**12**) substituted with an alkyl-ketone group at the γ -position are obtained. This reaction is general for a wide variety of allylic alcohols and carboxylic acids. However, when allyl acetates or allyl groups with strongly electron-withdrawing substituents (such as sulfones, phosphonates, esters, etc.) are used, the reaction leads to the formation of a γ -butyrolactone that now contains a vinyl group at the γ -position as seen on the right side of Figure 4b. For both processes, the presence of the MPATHio ligand (at least 30 mol%) is required to achieve complete conversion of the reactants, as well as a base (Na_2HPO_4) and an oxidant (Ag_2CO_3) to regenerate the catalytic cycle, with hexafluoroisopropanol (HFIP) as the solvent. Under these conditions, γ -butyrolactones (**12**) can be obtained in good yields, though with low diastereoselectivity, whereas the derivatives (**13**) are obtained in moderate to low yields.^[74] The key steps of this mechanism are outlined in Figure 5.

Thus, after the C—H activation step and the formation of the Pd(II) complex with the cyclometalated ligand and the auxiliary ligand MPATHio (**A**), the migratory insertion of the alkene occurs, giving intermediate (**B**). This is followed by β -H-elimination, leading to the formation of the hydride-alkenyl derivative (**C**). The reductive elimination from this hydride-alkenyl species generates Pd(0), which, after oxidation with Ag^+ , re-enters the catalytic cycle. Meanwhile, alcohol (**D**) is formed, which undergoes oxidation to yield ketone (**E**). Finally, this ketone undergoes a 1,4-addition followed by tautomerization to produce the final product (**F**).^[74]

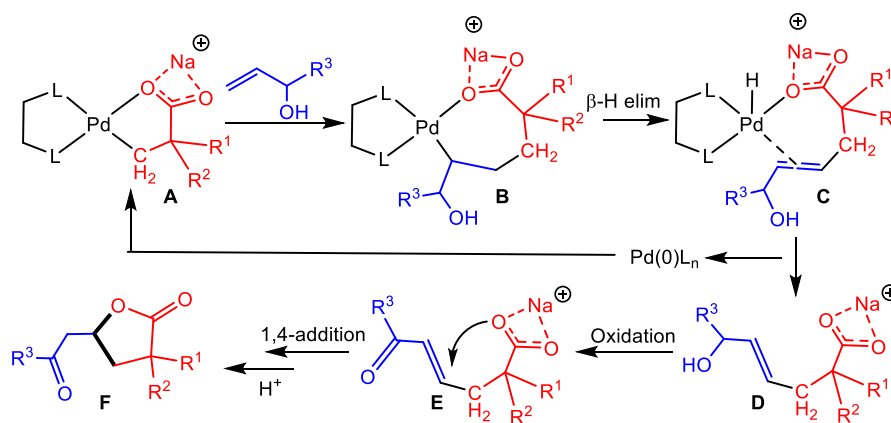


Figure 5. Mechanism of formation of γ -butirolactones 12.

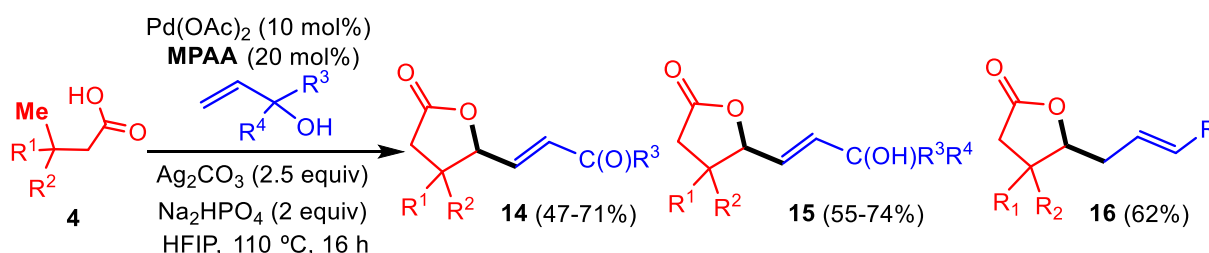


Figure 6. Synthesis of lactones 14–16 by $C(sp^3)$ –H cyclization of carboxylic acids and C–C coupling with allylic alcohols.

The γ -lactones (**14**), (**15**), and (**16**), which feature an α,β -unsaturated group at the γ -position, are structurally closely related to species (**12**) and (**13**) (Figure 4b). These compounds have also been obtained through oxidative coupling between unactivated allylic alcohols and aliphatic carboxylic acids (**4**), which contain an additional carbon in the backbone compared to (**11**).^[75] The process, outlined in Figure 6 is catalyzed by $Pd(OAc)_2$ and assisted by an MPAA-type ligand (*N*-Ac-^tLeu) without which the reaction is completely inhibited. In the presence of other MPAA-type ligands, the reaction proceeds but with significantly lower yields. The reaction requires Ag_2CO_3 as an oxidant, Na_2HPO_4 as a base and HFIP as a solvent and it takes place without the need for moisture or air exclusion. Formally, the reaction involves a double $C(sp^3)$ –H activation of the methyl group present in carboxylic acid (**4**), a previously unprecedented feature until this study. Furthermore, C–H activation is the RDS of the reaction, as evidenced by kinetic isotopic effect (KIE) measurements. The scope of this reaction is remarkably broad, both in terms of carboxylic acids and allylic alcohols, which can be primary (yielding lactones **14** where $R=H$), secondary (lactones **14** with $R=Me$), or tertiary (lactones **15**).

The mechanism proposed for this reaction by Maiti and collaborators in the original study aligns with that shown in Figure 5 up to species **E**, except for differences in the acid structure.^[75] That is, the adduct formed by the doubly deprotonated MPAA coordinated to Pd and the acid salt undergoes a C–H activation process to yield (**A**), which then reacts with the alkene via migratory insertion, β -elimination, and reductive elimination, releasing alcohol (**D**), which is subsequently oxidized to generate ketone (**E**). This ketone then re-coordinates to the catalytically

active $[Pd(MPAA)]$ fragment to initiate a new cycle of allylic C–H activation and reductive elimination, ultimately forming the final lactone. This mechanism has been studied in great detail using DFT computational methods by Li and coworkers.^[76] These authors confirmed that the first $C(sp^3)$ –H activation proceeds via a CMD mechanism and represents the highest energy barrier of the entire process. They also found that the second activation occurs through a CMD mechanism at the allylic position and that the presence of a base is critical for generating the MPAA dianion and the acid anion, which facilitate C–H activation.

A recent study by the same group of Maiti and coworkers on the dehydrogenative lactonization of aliphatic carboxylic acids containing a cycloalkyl group has enabled the synthesis of unsaturated bicyclic lactones.^[77] The starting substrates are the cycloalkyl derivatives (**17**) shown in Figure 7a. A reaction scheme similar to the one described in previous paragraphs would indicate two positions susceptible to intramolecular cyclization and lactonization: the methyl group at the γ -position and a methylene group of the cycloalkyl ring, also at the γ position. This study demonstrates that there is no competition between these two groups and that selective C–H activation toward the methylene group is possible. This selectivity is based on the fact that C–O coupling via reductive elimination from the methyl group is unfavorable (as it would generate a spirobicyclic), whereas methylene activation in (**18**) can readily proceed with the expected β –H elimination to form an alkene, which subsequently undergoes oxypalladation to yield the unsaturated bicyclic lactones (**19**). The intermediate complex (**18**) contains the MPAA ligand *N*-Ac-^tLeu κ^2 -N,O-coordinated as a dianion, which is crucial for the reaction to proceed with high yield. Other

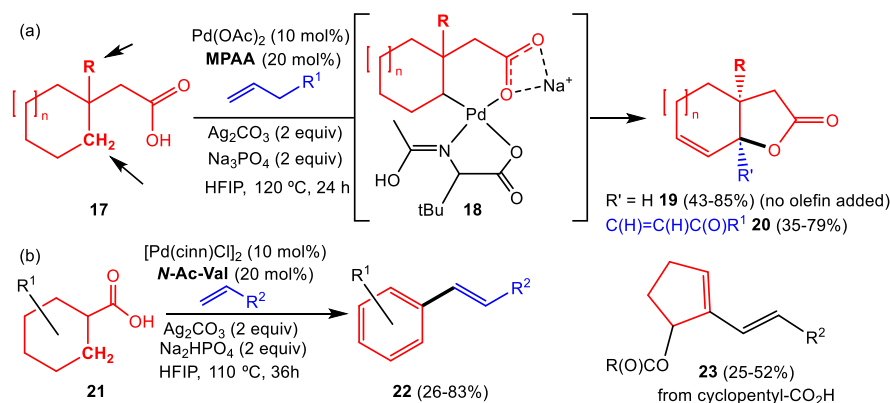


Figure 7. Synthesis of unsaturated bicyclic lactones by dehydrogenative lactonization of cycloalkyl carboxylic acids.

MPAAs result in significantly lower conversions and ligands of a different nature did not lead to any conversion at all. This process is depicted in Figure 7a.^[77] When this reaction is carried out in the presence of an alkene or an allylic alcohol, using the same MPAA, the result is also an unsaturated bicyclic lactone (**20**) but with an α,β -unsaturated substituent at the γ -position of the bicyclic system. In other words, a quaternary carbon is formed through double C–H activation of the initial methylene group, a highly significant achievement from a synthetic perspective.

With this method, a diverse set of bicyclic lactones can be obtained, as it accommodates a wide range of substituents both on the cycloalkyl ring and at the β -position (Me in **17**). Additionally, the size of the cycloalkyl ring can be varied with examples reported for rings of 5, 6, 7, 12, and 15 members without any significant loss in yield. In all the bicyclic lactones obtained, the stereochemistry of the substituents is *syn*, which is both kinetically more accessible and thermodynamically more stable than the *anti* configuration. Both reaction products (**19**) and (**20**) are high-value compounds, serving as precursors to complex natural products or bioactive molecules. In this regard, this method has been applied to the synthesis of sesquiterpenes such as Trichodiene and Seychellene, as well as natural compounds like Capnellene and Mesembrane.^[77]

More recently,^[78] the same group has reported the transformation of cyclohexane-derived carboxylic acids (**21**) into arenes with vinyl substituents (**22**) through a sequence of dehydrogenation – olefination – decarboxylation – aromatization reactions (DODA). These tandem processes are catalyzed by palladium in the presence of the MPAA *N*-Ac-Val. As mentioned earlier, this is another significant example of how a slight change in the substrate (a difference of just one CH₂ group) leads to drastically different reactivity. This unique transformation, which has high synthetic value is illustrated in Figure 7b. It is important to highlight that although both processes described in Figures 7a,b involve dehydrogenation, in the first case, the reaction stops after the initial unsaturation, whereas in this second case, it continues until the complete aromatization of the substrate, requiring successive C–H activations promoted by the same catalyst. In the case of cyclopentyl carboxylic acids, where aromatization is not possible, the reaction instead yields difunc-

tionalized cyclopentenenes (**23**) as shown on the right side of Figure 7b.^[78]

In both cases (cyclohexyl and cyclopentyl acids), the presence of MPAA (here a valine derivative) is essential as the reaction does not take place in its absence. Additionally, while previous examples of olefination of carboxylic acids systematically led to lactonization, here it is overridden by Pd-mediated decarboxylation. Regarding the scope of these processes, they exhibit remarkable structural diversity, as nearly 100 different compounds have been synthesized, some of them derived from natural products or pharmaceuticals, covering a wide range of substituents on both the cyclohexyl ring and the olefin. Interestingly, when the reaction is carried out in the absence of an olefin, the corresponding arene is still obtained through dehydrogenation and decarboxylation, albeit in very low yield. All these findings have been thoroughly detailed in the same study through mechanistic investigations based on control experiments.^[78]

Beyond the lactonization and lactamization processes described, olefins serve as an excellent starting point for the preparation of a wide range of valuable elaborated products, including precursors of pharmaceuticals, agrochemicals, medicines, and more. Figure 8 summarizes a portion of the contributions made during the 2022–2025 period that share common characteristics. In all the cases described, the participation of an MPAA-type auxiliary ligand is essential, either to accelerate the reaction, achieve high selectivity, or even both purposes.^[79–85]

The groups of Yuan and Dong have reported (Figure 8a) the synthesis of substituted indoles via the coupling of olefins with *N*-monosubstituted anilines in the absence of DG.^[79] While the oxidative coupling of anilines with alkynes to form indoles is well known, coupling with olefins is much less developed as the direct reaction typically leads to different types of products. In this contribution, the treatment of monosubstituted anilines (**24**) with olefins bearing a strongly electron-withdrawing group ($R_1 = \text{EWG}$) results in 3-substituted indoles (**25**) through a [3 + 2] cyclization. The process is catalyzed by Pd(OAc)₂ using Ag₂CO₃ and benzoquinone as oxidants and requires MPAA1 (*N*-Ac-Ala) for the reaction to proceed with high yield. Alongside indoles (**25**), variable amounts of benzofurans (**26**) are also obtained,

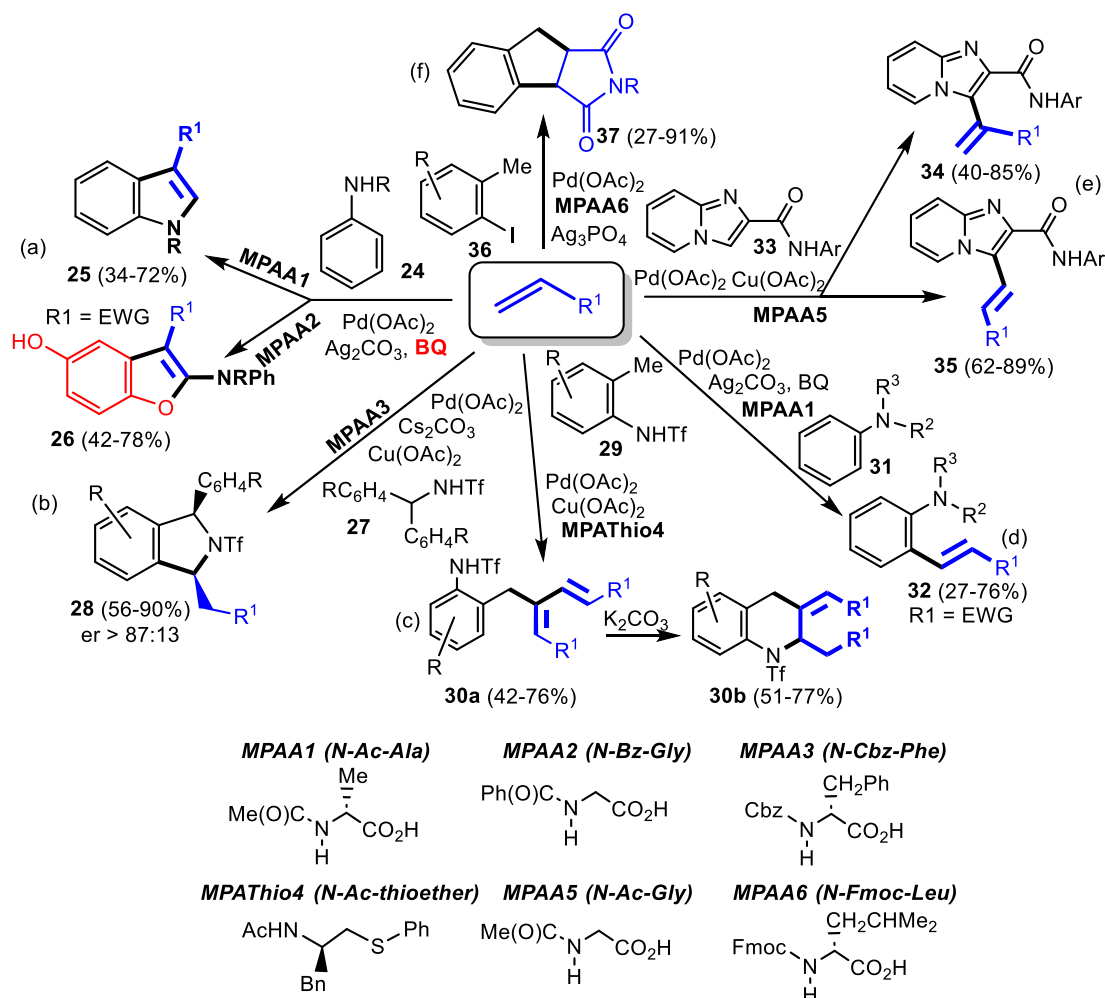


Figure 8. Different C–H functionalizations performed with olefins as starting materials.

resulting from the reaction between aniline (24), the olefin, and benzoquinone (BQ). However, their formation is minimized (<5%) when **MPAA1** is used. The choice of **MPAA** is critical in controlling the reaction orientation due to its steric effect. For instance, when **MPAA2** (hippuric acid, *N*-Bz-Gly) is used, the reaction selectively yields benzofurans (26) with indoles (25) detected in less than 5% yield. The reaction exhibits broad scope for the synthesis of indoles (25), both in terms of aniline and olefin substrates, allowing access to pharmaceutical precursors. However, the method fails when applied to internal olefins.^[79]

When the reacting substrate is a (diaryl)methyltrifluoromethylamide (27), its reaction with electron-poor olefins proceeds via C–H activation of one of the aryl rings followed by a [4 + 1] cyclization with the olefin, leading to the formation of chiral *cis*-1,3-disubstituted isoindolines (28). This process, described by Dethe's group and illustrated in Figure 8b,^[80] results in the desymmetrization of trifluoromethylamides (27), which is controlled and promoted by **MPAA3** (*N*-Cbz-*L*-Phe), generating *cis*-isoindolines (28) with good yields and enantiomeric ratios exceeding 87:13 in all tested cases. The role of the **MPAA** in this reaction exemplifies bifunctionality (Figure 2), as it both promotes and accelerates the reaction while simultaneously creating a chiral environment to induce enantioselectivity. This is illustrated by the coupling of Ph₂CHNTf

with methyl vinyl ketone; in the absence of **MPAA**, racemic isoindoline (28) is obtained with a 45% yield, whereas in the presence of **MPAA** (under otherwise identical reaction conditions), the yield improves to 72%, and the enantiomeric ratio reaches 75:25. Moreover, the selectivity provided by **MPAA** in various aspects of the reaction is remarkable, as it proceeds with exceptionally high chemo-, regio-, and enantio-selectivities. The configuration of isoindoline (28) is directly influenced by that of the **MPAA**. When *N*-Cbz-*L*-Phe is used, the stereoisomer shown in Figure 8b is obtained, whereas employing *N*-Cbz-*D*-Phe leads to the enantiomer *ent*-28 with both configurations inverted.^[80]

Ji and coworkers have described the double olefination of *N*-protected ortho-toluidines (29) with different acrylates, a Pd-catalyzed reaction that requires *N*-acetyl-protected thioether ligands (**MPATHio4**, Figure 8c).^[81] The initial diene formed in the reaction (30a) results from the consecutive double olefination of the methyl group on *o*-toluidine, involving a first C(sp³)–H activation followed by a second C(sp²)–H activation. This dual activation does not occur at all in the absence of the thioether ligand, nor in the presence of other ligands such as pyridines, pyridones or **MPAAs**. Surprisingly, when the starting aniline contains more than one methyl group, olefination occurs exclusively on the methyl group positioned ortho to the NHTf group. Even

if two methyl groups are ortho to the NHTf fragment, only one undergoes functionalization. Moreover, if additional alkyl groups are present alongside the methyl, selective functionalization still occurs at the methyl group. The reaction tolerates a variety of ester substituents on the olefin, but the presence of the proton on the NHTf group is essential—when this position is methylated ($-\text{NMeTf}$), the reaction does not take place. This suggests that ortho-toluidine (**29**) must undergo deprotonation to coordinate with the metal. The dienes (**30a**) thus obtained serve as excellent precursors for the synthesis of 1,2,3,4-tetrahydroisoquinolines (**30b**), compounds of high pharmaceutical interest. These are formed by basic treatment (K_2CO_3) of the dienes, as illustrated in Figure 8c.^[81] This base-mediated transformation exhibits broad tolerance to different substituents, allowing the entire process from (**29**) to (**30b**) to be carried out in a one-pot manner without isolating or purifying the intermediate diene (**30a**).

The nondirected functionalization of tertiary anilines (**31**) remains a challenge since it is not possible to install DG (e.g., imines) on them. Additionally, as mentioned in the previous paragraph, they lack a deprotonable N—H unit, making the approach of the neutral species to the metal less effective and in any case, it would generate a four-membered metallacycle, which is unstable. Recently, Yuan, Dong, Xu and collaborators have described a method for the ortho-alkenylation of tertiary anilines without DG, based on the use of **MPAA** ligands (**MPAA1**, *N*-Ac-Ala) as shown in Figure 8d.^[82] The reaction is catalyzed by $\text{Pd}(\text{OAc})_2$, promoted by Ag_2CO_3 , and benzoquinone and requires the *N*-Ac-Ala ligand to proceed with complete conversion. Under these reaction conditions, selectivity for ortho functionalization in the alkenyl-anilines (**32**) is nearly complete in most cases. In a small set of examples, the formation of the para isomer is not entirely avoided, but in those cases, the ortho/para ratio exceeds 20. This high selectivity is observed for a wide range of substituents, both on the carbon skeleton and the N of the aniline as well as on the olefin. The authors of this study compare this **MPAA**-based ortho alkenylation method, which does not require DG, with previously reported methods finding that other approaches predominantly direct functionalization to the para position. These findings highlight the crucial role of the **MPAA** ligand. Experimental and theoretical mechanistic studies demonstrate that C—H bond activation is the RDS of the process, that in this stage the N of the aniline is not coordinated, and that activation of the ortho C—H bond relative to the N is 4.1 kcal/mol more favorable than para activation due to the presence of hydrogen bonding interactions.^[82]

Sharma and coworkers have recently reported the generation of atropisomerism through Pd-catalyzed alkenylation of biaryls.^[83] Treatment of 1-naphthylisoquinoline *N*-oxide with various acrylates, styrenes, and maleimides leads to the formation of the corresponding olefinated derivatives as a single atropoisomer. The reaction is catalyzed by $\text{Pd}(\text{OAc})_2$ and requires Ag_2CO_3 as an oxidant and *N*-Ac-Phe as the **MPAA** promoter. DFT studies of the reaction indicate that the rate-limiting step is the alkene insertion and that the selectivity arises from the lower distortion of one diastereomer compared to the other, rather than from electronic factors.

Just as varying the **MPAA** ligand can alter the orientation of olefination, as seen in the case of compounds (**25**) and (**26**), changing the substituents in the starting materials can also lead to divergent reactivities. This is especially true for olefins, where the electronic nature of the substituents determines whether a reaction is feasible or not. The research groups of Bera and Karpoomath have reported that the alkenylation of imidazo[1,2-*a*]pyridines can yield two different types of products depending on the nature of the alkene.^[84] This process is outlined in Figure 8e. Specifically, the Pd-catalyzed reaction of imidazo[1,2-*a*]pyridines (**33**) with olefins, promoted by the **MPAA5** ligand (*N*-Ac-Gly) and $\text{Cu}(\text{OAc})_2$ leads to the formation of a branched alkenylation product (**34**) when using an unactivated aliphatic alkene, and a linear alkenylation product (**35**) when using a styrene derivative. As in previous examples, the presence of the **MPAA** ligand is essential for the reaction to proceed successfully. Additionally, in this case, the *N*-substituent (3- FC_6H_4) plays a noninnocent role. Using electron-rich alkenes, a collection of branched derivatives can be obtained by varying the substituents on both the alkene and the substrate (**33**). During the scope determination process, it was observed that the reactivity with styrene and its less electron-rich derivatives selectively yields the linear alkenylation product (**35**). This new alkenylation approach, which diverges from the previous one, exhibits a broad scope in terms of both the heterocycles (**33**) and the styrene derivatives, leading to a diverse range of hetero-stilbenes (**35**).^[84] The reaction mechanism, determined experimentally and corroborated by DFT studies indicates that the C—H activation step is the RDS as supported by the KIE value. Additionally, the barriers associated with the migratory insertion and β -elimination processes are critical in directing the reaction.

The applicability of **MPAA** ligands in Pd catalysis extends even to halogenated substrates, which are typically used with phosphine or NHC ligands to stabilize reaction intermediates in cross-coupling processes. In this context, Zhang and coworkers have reported the synthesis of functionalized dihydroindenes (**37**) through the reaction of iodomethylbenzenes (**36**) with maleimides as depicted in Figure 8f. This [3 + 2] cyclization reaction is catalyzed by $\text{Pd}(\text{OAc})_2$ and promoted by Ag_3PO_4 and the **MPAA6** ligand (*N*-Fmoc-Leu). Depending on the starting iodobenzene, the reaction can also in some cases be promoted by NHC ligands, but with lower yields. A comparative study of **MPAAs** and NHCs demonstrates the superior catalytic performance of **MPAAs** in accelerating and promoting the reaction.^[85] Furthermore, using **MPAAs** under optimized reaction conditions, a broad range of halomethyl arenes and *N*-substituted maleimides can be coupled, generally affording tricyclic products (**37**) with good yields. However, the scope observed by these authors for the same process using NHCs is significantly more limited with lower yields.

2.2. Olefination in Meta and Para Positions

The immense importance of olefination reactions based on C—H bond activation in the construction of molecular frameworks

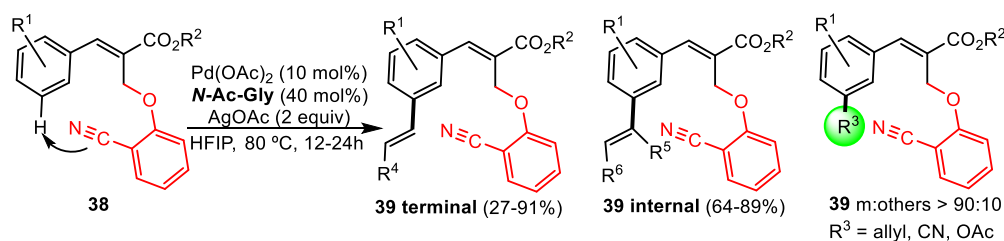


Figure 9. Meta-functionalization of cinnamic derivatives using cyano-templates.

drives the expansion of the current limits of this reaction. In the case of aromatic substrates, ortho functionalization has been much more extensively studied and developed due to the use of DG and the concept of proximity-driven functionalization. However, despite remarkable breakthroughs in specific cases, activation at the meta and para aromatic positions has been less explored and remains a challenge for synthetic chemists. During the period covered by this review, significant advancements have been made in these directions. In most of the analyzed cases, the presence of a more or less sophisticated template that moves the metal away from the ortho position and brings it closer to the meta/para positions is almost a constant.

Cinnamic acid derivatives (such as ferulic, caffeic, or sinapic acids) possess well-documented and highly valuable biological and pharmacological properties. Therefore, developing selective modification methods for these molecules is of great interest. Bakthadoss et al. have designed a simple-structured template to achieve meta-functionalization of cinnamic acid esters and derivatives.^[86] Directed functionalization in these substrates presents a challenge due to the *trans*-configuration of the aryl and ester groups relative to the double bond. This research group designed a substituent at the α -position of the cinnamate containing a 2-cyanophenoxymethyl group and prepared a variety of starting materials (38). The spatial arrangement of this system causes the metal, after coordinating with the cyano group, to selectively activate the meta-C—H bond of the cinnamyl fragment, as illustrated in Figure 9. Precursors (38) react with a broad range of terminal olefins, internal olefins, cyclic olefins, and acetylation, cyanation, or allylation reagents to yield the corresponding meta-substituted cinnamates (39), all under nearly identical reaction conditions (Figure 9). Nearly 150 derivatives have been obtained, demonstrating the robustness and general applicability of this method. Although some side isomers are formed alongside the meta isomer, the meta/other isomer ratio consistently exceeds 90/10. Despite the presence of the template, the reaction strictly requires the MPAA ligand *N*-Ac-Gly to achieve high yields. Regarding the reaction scope, a wide variety of processes have been explored with olefination reactions using terminal and internal olefins to give cinnamates 39terminal and 39internal being the most represented (Figure 9, more than 130 products). This includes cases where the cinnamic fragment contains a heterocycle (such as furan or thiophene) instead of an aryl group and derivatives of bioactive compounds (such as chalcone, paracetamol, estrone, etc.).^[86]

The research groups of Yang, She, Li, and collaborators have developed templates for the meta selective alkenylation of

arenes based on backbones similar to cinnamic acid. One such backbone is the amide derivative of hydrocinnamic acid (40), shown in Figure 10a, a flexible species containing a 2-benzoic group anchored to the nitrogen atom to achieve meta orientation. The alkenylation reaction requires the participation of the MPAA ligand *N*-Ac-Phe and the work of these groups has involved modeling the interaction between the substrate (40) and the MPAA using DFT calculations.^[87] The results indicate that the C—H activation step and the formation of species (41) via the CMD mechanism are responsible for both the reaction rate and the regioselectivity of the process. In species (41), the MPAA ligand acts as a dianionic κ^2 -N,O chelate, assisting in the removal of the hydrogen at the meta position of the phenyl ring through its acyl group while also forming additional hydrogen bonds with the carboxylate group of the template via its own carboxylate group. The flexibility of ligand (40) through its hydrocarbon chain, along with the presence of ortho and para isomers (albeit in lower proportions) in the functionalized product (42), suggests that C—H activation at the ortho and para positions is also feasible. In the calculated minimum-energy conformation, the transition state (TS) activation barriers are 23.0 kcal/mol (meta), 23.1 kcal/mol (para), and 23.4 kcal/mol (ortho) aligning with experimental findings. Both the migratory insertion of the alkene and the β -elimination step exhibit lower barriers. Other energetically accessible conformations exist, in which the energy differences between the various TSs are larger. However, the general trend remains: the meta TS is the lowest in energy, followed by the para TS. The Boltzmann distribution predicts a meta:para:ortho ratio of 78:11:11, which is in perfect agreement with the experimentally observed 88% yield for the meta isomer.^[87]

The substrate (43) has also been studied undergoing desymmetrization via alkenylation or arylation as illustrated in Figure 10b for alkenylation.^[88] This desymmetrization process is a true challenge, as it involves selective, asymmetric, and remote functionalization directed by the MPAA ligand. In this process, the MPAA ligand not only accelerates the reaction and directs C—H activation toward the meta position (regioselectivity) but also discriminates which of the two phenyl rings in the substrate is preferentially activated (enantioselectivity), generating enantiomerically enriched derivatives (44). The optimized alkenylation process is catalyzed by Pd(OAc)₂ (10 mol%) and promoted by AgF₂ (as an oxidant) and the MPAA ligand *N*-Ac-Phe, the latter in substoichiometric amounts (50% mol). DFT studies of this reaction yield conclusions very similar to previous findings^[87]: (i) The C—H activation step is the RDS; (ii) A hydro-

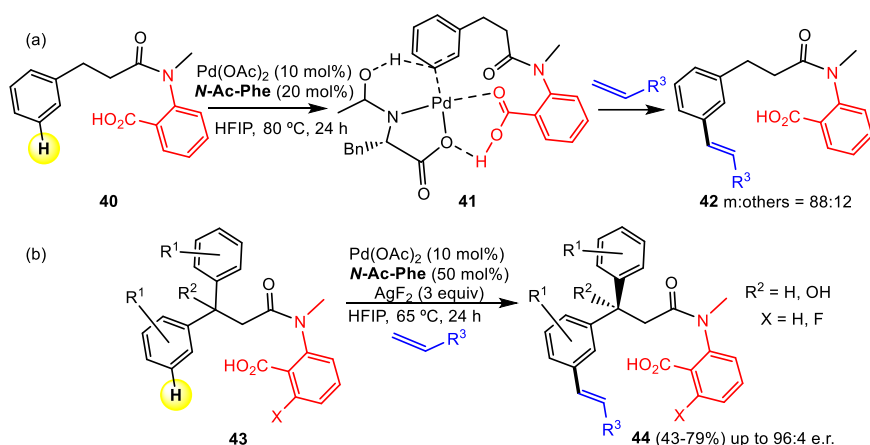


Figure 10. Meta functionalization of different hydrocinnamic derivatives using carboxylate-templates.

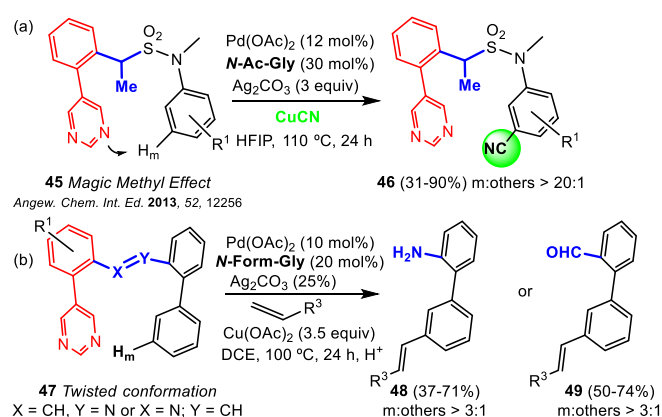


Figure 11. Meta-functionalization of (a) aniline and (b) benzaldehyde derivatives using pyrimidine-based templates.

gen bonding network is established, similar to that observed in derivative (41); (iii) The key difference lies in the relative positioning of the two phenyl rings on the prochiral carbon in the *R*-TS1 and *S*-TS1 intermediates. The energy difference between these transition states is 3.7 kcal/mol in favor of *R*-TS1, which, along with distinct intramolecular interactions in these TSs leads to less distortion in *R*-TS1 compared to *S*-TS1. Ultimately, these factors are responsible for the observed enantioselectivity.^[88]

Maiti and coworkers have designed templates based on pyrimidine fragments that induce meta functionalization in aniline-type substrates. As shown in Figure 11a, both units (pyrimidine and aniline) are connected by a bridge containing a sulfonyl group and a methylene carbon.^[89] The degree of substitution on this methylene carbon is critical for achieving the desired meta orientation. When there are no methyl groups on this carbon, free rotation leads to poor reactivity and selectivity. Conversely, when two methyl groups are present, excessive steric repulsion between the two fragments completely blocks reactivity. In this latter case, the Thorpe-Ingold effect is entirely detrimental to the reaction. Only when there is a single methyl group on this carbon—illustrated in Figure 11a—does the ligand adopt the optimal conformation, resulting in high reactivity and selectivity. These concepts have been applied

to the meta-cyanation of aniline precursors, a particularly challenging reaction to achieve with this orientation, as aniline strongly directs substitutions to the ortho and para positions. Thus, treating compound (45) with CuCN under the optimized conditions shown in Figure 11a—including the essential presence of the MPAA ligand *N*-Ac-Gly—leads to the formation of meta-cyanoanilines (46), regardless of the nature and position of the *R*₁ substituents on the initial aniline fragment. In general, the meta:other isomer ratio is greater than 20:1, though in some cases, this ratio drops to 7:1. Although not depicted in Figure 11a, this study also describes the meta-cyanation of aniline-related substrates such as tetrahydroquinolines, indolines, benzylamines, and phenethylamines.^[89] DFT studies of the reaction mechanism indicate that C–H activation is not the rate-limiting step in this case; instead, either the transmetalation or reductive elimination step becomes rate-limiting, depending on the number of methyl groups in the substrate. Regardless, the calculated energy barriers for the substrate with a single methyl group are the lowest, explaining the observed differences in reactivity among the three substrate variations.

The Maiti group has also designed a template (47) based on phenyl-pyrimidines for the functionalization of 2-phenyl-benzaldehydes and 2-phenyl-anilines as shown in Figure 11b. In this case, the bridge between the directing pyrimidine core and the biphenyl to be functionalized is an imine linkage, which is easily accessible through the condensation of the corresponding aldehydes and amines and constitutes the first step of the reaction.^[90] After forming the templates (47), their treatment with different olefins—catalyzed by Pd and in the presence of *N*-Form-Gly as the MPAA ligand—followed by acidic hydrolysis as the final step, leads to the formation of meta-olefinated 2-phenyl-anilines (48) or meta-alkenylated 2-phenyl-benzaldehydes (49) in moderate to high yields, as represented in Figure 11b. The broad scope of this reaction, with variations in aldehydes, amines, and olefins is remarkable and includes bioactive products. In all cases, the major isomer obtained is the meta product, although the proportion of other isomers varies depending on the substrate, ranging from 3:1 to > 20:1. Subsequently, the Maiti and Gupta groups have experimentally and computationally (DFT) determined the mechanism of this reac-

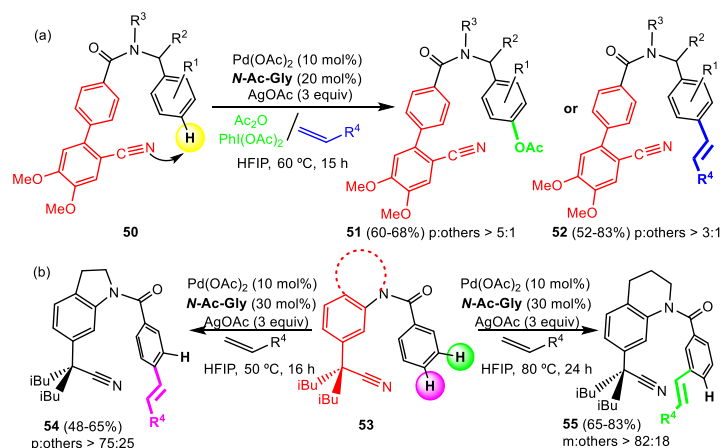


Figure 12. Different templates for (a) para and for switching between (b) meta and para-functionalizations.

tion, providing a detailed explanation of the crucial role of the MPAA ligand and the origin of meta selectivity. In this case, and in the presence of MPAA, the RDS is the migratory insertion, and the energy barrier for the meta position (24.5 kcal/mol) is significantly lower than that of the next lowest barrier (para, 27.5 kcal/mol).^[91] A distortion-interaction energy analysis of the different transition states (TSs) shows that the distortion energy of TS(meta) is notably lower than that of TS(para) and TS(ortho) (2.3 kcal/mol and 9.3 kcal/mol, respectively) demonstrating that these template-induced distortions regulate both reactivity and selectivity.

Jin and collaborators have developed a slightly more sophisticated template (50), shown in Figure 12a designed to selectively direct functionalization to the para position.^[92] This template is based on a DG containing a cyano moiety, similar to the one shown in Figure 9, which coordinates to the metal. Additionally, it features a spatial extension with a phenyl group intercalated between the carbonyl and the DG, positioning the metal further away compared to other templates. This template binds to benzylamines, as illustrated in Figure 12a generating precursors (50). It is important to highlight that benzylamines are highly valuable compounds that typically undergo almost exclusive ortho functionalization due to the strong directing effect of the nitrogen. Achieving alternative regioselectivity in these compounds is particularly challenging. This study successfully enables the para functionalization (acetoxylation, alkenylation) of benzylamines by treating (50) with $\text{PhI}(\text{OAc})_2$ or olefins in a reaction catalyzed by $\text{Pd}(\text{OAc})_2$ and promoted by *N*-Ac-Gly yielding acetoxyated (51) or alkenylated (52) derivatives. In both (51) and (52), ortho-reactivity is almost completely suppressed. Although in some cases the para:other isomer ratio is 3:1—mainly due to the presence of ortho or meta substituents on the benzylamine—most examples described in this study achieve a ratio exceeding 10:1.^[92]

The ability to control reactivity achieved with certain templates has proven to be remarkably high. Even small variations in structure or in the substrate's proximity to the metal can lead to significantly different reactivities. Xu, Jin, and coworkers have developed a template based on cycloalkyl fragments for the functionalization of benzamides (53) shown in Figure 12b.

They found that it is possible to selectively direct functionalization to the meta or para position of benzamides depending on the size of the cycloalkyl group.^[93] A simple modification of the angle formed by the benzamide substituent with the template adjusts the spatial distances between the metal and the C—H bonds, facilitating either meta or para activation. The degree of proximity and the proper alignment significantly influence activation barriers, determining which activation pathway is favored. Experimental determination of the KIE confirms that C—H activation is the RDS for both templates. Computational simulations reveal that for the template containing the cyclopentyl group, the activation barriers for meta and para C—H activations are 24.6 and 26.5 kcal/mol, respectively, which is in perfect agreement with experimental observations. As expected, simulations for the template with the cyclohexyl group yield activation barriers of 27.0 kcal/mol (meta) and 25.4 kcal/mol (para) also in excellent agreement with experimental findings.^[93] Based on this, the authors describe the olefination of benzamides at the para (54) and meta (55) positions, as shown in Figure 12b. This process is catalyzed by $\text{Pd}(\text{OAc})_2$ and promoted by *N*-Ac-Gly and AgOAc. The reaction scope is extensive with meta:other selectivities exceeding 82:18 in all cases, and para:other selectivities always above 75:25.

The use of templates for the selective functionalization of substrates in positions that are not inherently accessible (electronically or sterically biased) or in the absence of pre-installed DG is not limited to meta/para activations in aromatic rings but also extends to more challenging substrates. For example, C—H functionalization of quinolines (57), which contain seven distinct C—H bonds is well developed at the C2 position with known examples at C3, C4, and C8. However, functionalization at the C5, C6, and C7 positions of the carbocycle remains a significant challenge.^[94,95] Tantillo, Maiti, and collaborators have developed a palladium-template complex (56) shown in Figure 13, which enables functionalization of challenging positions like C5 in quinoline substrates.^[96,97] Initially, quinoline (57) displaces the acetonitrile ligand in (56), generating a species in which quinoline is *N*-coordinated. Once coordinated and encapsulated within the template, the catalytic reaction begins. The catalyst $\text{Pd}(\text{OAc})_2$ reacts with the MPAA *N*-Ac-Gly, forming the corresponding κ^2 -

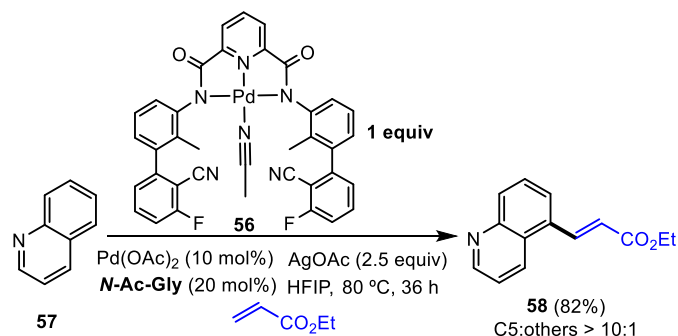


Figure 13. Template for the selective functionalization of quinolines at C5 position.

N,O-chelate, which additionally bonds to the nitrogen of one of the cyano groups in the template, leaving a vacant coordination site. From this position, selective activation of the C5–H bond in quinoline occurs, assisted by the carbonyl of *N*-Ac-Gly, with this C–H activation being the RDS. Subsequent reactivity with alkenes follows the typical pattern of alkene functionalization reactions: migratory insertion, β -elimination, and reductive elimination, ultimately releasing the alkylated quinoline species (**58**), reoxidizing Pd with AgOAc, and coordinating a new substrate (**57**). This mechanism has been determined through DFT calculations,^[96] which validate the experimental data.^[97] The method delivers excellent results not only for quinoline (**57**) but also for substituted quinolines, benzothiazoles, benzoxazoles, and phenylpyridines, as well as across a wide range of olefins.^[97]

In the absence of templates, maintaining selectivity is challenging except for specific substrates. Yamada, Hashimoto, Tamura, and collaborators have described an alkene functionalization protocol for 2,6-dialkoxy-pyridines at the C3(5) positions. This reaction involves treating these pyridines with alkenes in the presence of Pd(OAc)₂ (10 mol%), a thioether-type ligand (30 mol%), Ag₂OCF₃ (1.5 equiv), and Ti(O₂CCF₃)₃ (1 equiv). Under these conditions, monoalkenylation occurs predominantly at the C3 position, with no alkene observed at C4. The same study also describes the dialkenylation of pyridines by treating the monoalkenylated intermediates with an excess of alkene in the presence of the same Ag(I) and Ti(III) salts. This approach enables the synthesis of asymmetric bis-alkenylpyridines, even through a one-pot, two-step process. Furthermore, this method can be extended to other electron-rich *N*-heteroarenes, such as carbazole, pyrrole, and indole.^[98]

2.3. Arylations

MPAA ligands have also been used effectively and recurrently to promote arylation reactions. The groups of Yu and Zhou have described a method based on MPAA and NBE to achieve remote enantioselective arylation of monosubstituted ferrocene derivatives (**59**).^[99] The introduction of an additional substituent in ferrocene (or ruthenocene) derivatives like (**59**), which already contain a functional group, generates planar chirality. This is a type of chirality that is rarely observed when disubstitution occurs at the 1 and 3 positions of the cyclopentadienyl (Cp)

ring in metallocenes. Starting from monosubstituted derivatives (**59**) and using an MPAA (*N*-Boc-Val) and a functionalized NBE, following the Catellani methodology,^[100] the introduction of an aryl group into a remote position relative to the original substituent is achieved enantioselectively (only one side of the Cp is functionalized) generating the ferrocene derivatives (**60**). The process is shown in Figure 14. The scope of aryl groups coupled to ferrocene is very broad (up to 62 examples provided) with generally good to excellent yields and enantiomeric excesses above 96% in all cases. The derivatives (**60**) can be further functionalized in a second step, leading to the formation of 1,2,4-substituted compounds (**61**). This is exemplified in Figure 14 with the Fujiwara-Moritani alkenylation, which selectively occurs at the ortho position.

The formation of (**60**) implies that the initial stage is the enantioselective C–H activation of only one of the two C–H bonds adjacent to the CH₂NMe₂ group (**A**). This is achieved thanks to the action of the chiral *N*-Boc-Val ligand coordinated to Pd as a κ^2 -N,O-chelate, which directs Pd selectively to C2 (Figure 15, species **B**). In other words, the MPAA ligand is ultimately responsible for the enantioselectivity in the first stage of the catalytic cycle. This Pd–C bond is highly reactive and reacts with NBE, resulting in the migration of Pd to the remote C3 position through migratory insertion, generating the alkyl derivative, decoordination of the NMe₂ group, rotation around the C–C bond, and subsequent activation of the C–H bond at position 3 (Figure 15, species **C**). This new palladacycle now reacts with the aryl halide via oxidative addition, after which the arylation product is formed through reductive elimination and C–C coupling (species **D**). The subsequent β -carbon elimination and protodemetalation regenerate the active species and release the reaction products (**60**). Figure 15 outlines the main stages of this process.^[99]

The mechanism of this reaction has been fully elucidated using DFT methods and it confirms the presence of the species shown in Figure 15. Although a completely satisfactory explanation for the origin of the enantioselectivity has not been provided, it appears to be related to the energy difference in the insertion of the NBE into the two different isomers generated after the first C–H activation.^[101]

The enantioselective arylation of ferrocenes with indolizine-type heterocycles has been studied by the group of You et al.^[102] Unlike the arylation shown in Figure 14, which occurs at the remote meta position (position 3) thanks to the involvement of NBE, the present reaction leads to the arylated product at the ortho position (position 2) because it takes place in the absence of NBE. The reaction of ferrocenes (**62**) with indolizines (**63**) results in the formation of oxidative coupling ortho C–H/C–H products (**64**) (Fujiwara-Moritani coupling, Figure 16), a process catalyzed by Pd, where the involvement of the MPAA ligand (*N*-Boc-Val) is critical for achieving good yield and high enantioselectivity. The process tolerates the presence of substituents with different electronic and steric properties at the N atom of the ferrocene, the carbocycle, and the heterocycle, without compromising enantioselectivity. The derivatives (**64**) exhibit pharmacological properties, and some of them have bioactivity.

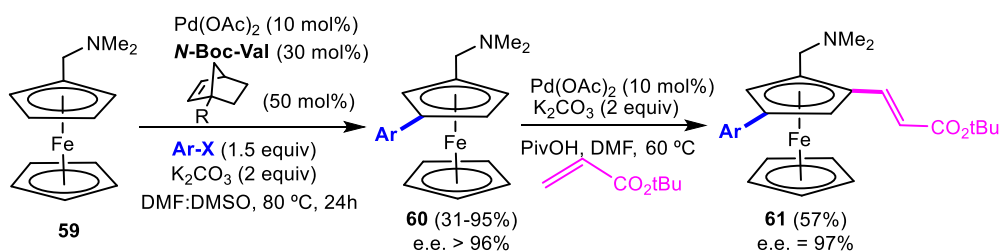


Figure 14. Arylation of monosubstituted ferrocene derivatives following Catellani methodology.

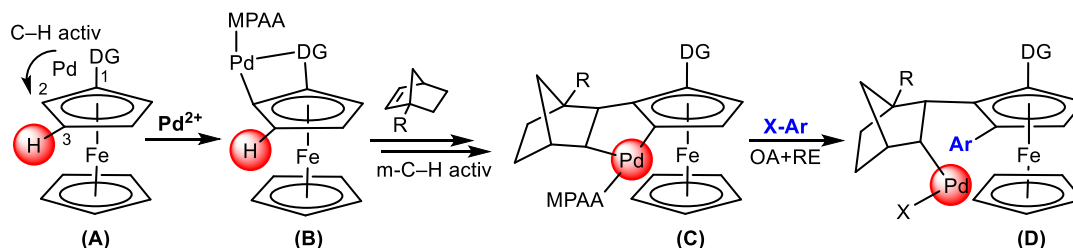


Figure 15. Mechanism of the Catellani arylation of ferrocene derivatives.

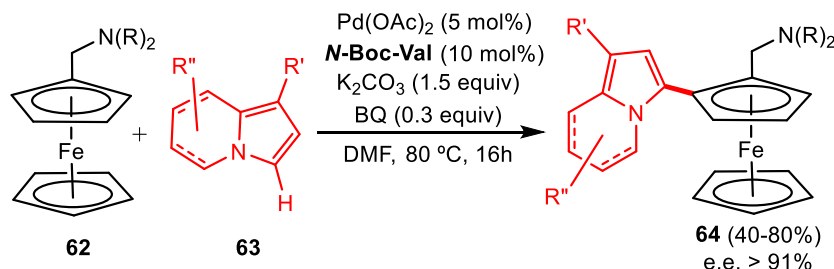


Figure 16. Enantioselective heteroarylation of ferrocenes with indolizine derivatives.

From the mechanistic point of view, the first stage proceeds identically to what is shown in Figure 15 for the formation of species A and B. However, in this case, it is the Pd(MPAA) fragment containing species B that promotes a new C–H activation in the indolizine, followed by reductive elimination via C–C coupling to give the derivatives (64).^[102]

In the previous sections, examples have been presented of how MPAA-type ligands assist the process of C–H activation and functionalization in the presence of weakly coordinating functional groups, such as carboxylic acids. The ability of MPAA ligands to assist enables the functionalization of substrates with even lower coordinating capacity, such as alcohols. Yu and coworkers have developed a procedure for the arylation of alcohols at the δ -C(sp³)–H position, in which the auxiliary ligand is absolutely essential and must meet several requirements.^[103] The first requirement is maintaining charge balance, meaning that the complex must remain neutral throughout the entire catalytic cycle. Therefore, the ligand must be doubly deprotonable. The second requirement is the formation of a secondary coordination sphere through hydrogen bonding, which facilitates and stabilizes the coordination of the alcohol in the transition state involving C–H activation. In other words, the alcohol group must be permanently coordinated to the metal, as this stabilizes the transition state. The third requirement, already mentioned previously is that the ligand must contain a functional group that

assists in proton removal after C–H activation. Based on these premises, the authors determine that the optimal ligand for alcohol arylation shown in Figure 17a is the *bis*-amide displayed in the upper inset, whose mode of action, including all operational conditions for coordination, is depicted in the lower inset. Using this ligand and the optimized reaction conditions, alcohols (65) react with various aryl halides to produce arylated products (66) with a wide range of R¹ and R⁴ substituents. However, when the method is extended to the δ -position of cyclobutyl alcohols (67), the yield of 1,3-cyclobutanes (68) is significantly lower (37%, Figure 17b) requiring a re-optimization of reaction conditions. In this second case, the optimal ligand is a pyridone-type ligand, which will be discussed in Section 3.^[103]

The use of MPAA's and their derivatives can also promote cascade multiarylation processes. In the case of cyclohexyl carboxylic acids (69), coupling occurs with three molecules of aryl halide consecutively, generating dihydrophenanthrenes (70), as demonstrated by Yu's group and coworkers.^[104] The reaction, shown in Figure 18 is catalyzed by Pd(OAc)₂ and promoted by the aminothioether MPATHio depicted in the side box. More interestingly, the reaction proceeds enantioselectively guided by the configuration of the aminothioether. It selectively activates two C(sp³)–H bonds of the cyclohexyl ring (at the β and γ positions) and three C(sp²)–H bonds, forming four new C–C bonds and three chiral centers. The reaction exhibits broad general-

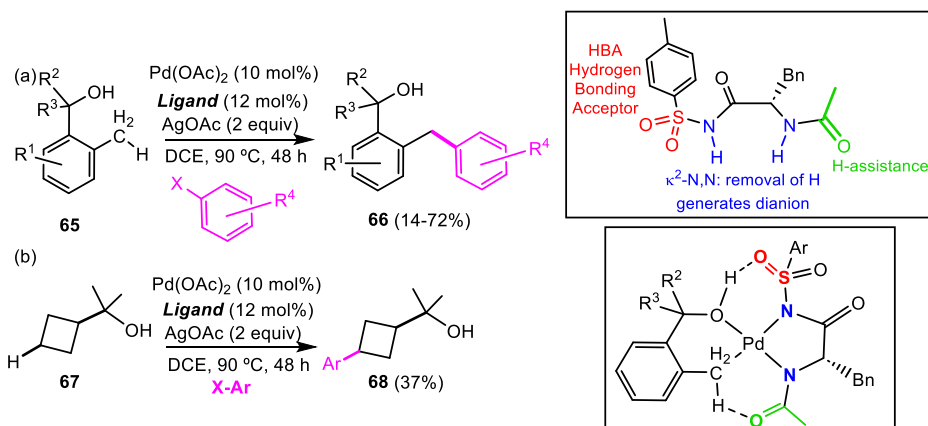


Figure 17. C(sp³)–H arylation of different (a) benzyl and (b) cyclobutyl alcohols.

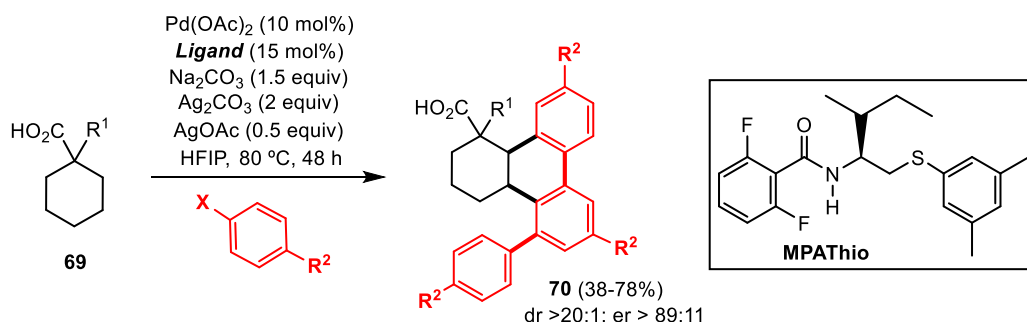


Figure 18. Cascade multiarylation processes undergone by cyclohexyl carboxylic acids.

ity and tolerates various substituents R¹ at the α -carbon of the acid (69) and R² on the aromatic ring, proceeding with very high enantio- and diastereoselectivity. However, neither cyclopentyl nor cycloheptyl carboxylic acids showed any reactivity in this process, presumably due to the lack of reactivity of the β,γ -dehydrogenation products. The mechanism proposed by the authors for this reaction begins with the β,γ -dehydrogenation of the cyclohexyl ring, oxidative addition of an aryl halide to Pd(0), and subsequent migratory insertion of the alkene into the Pd–C bond. This generates a Pd–C σ -alkyl species that undergoes three consecutive processes of C–H activation, oxidative addition, and reductive elimination in a cascade, ultimately yielding the dehydrophenanthrenes (70).^[104]

In certain catalytic processes, the reaction conditions such as temperature, solvent, or the compatibility between different reagents can lead to their degradation and/or reduction. For example, in Pd-catalyzed reactions involving allyl amines, the reduction of Pd to nanoparticles is frequently observed. These nanoparticles do not necessarily exhibit the same catalytic behavior as molecular catalysts leading to different reaction products. Young and collaborators have demonstrated that the use of *N*-Boc-Val in these reactions, in addition to the acceleration and selectivity-promoting effects previously discussed, enables the stabilization of Pd in the homogeneous phase and the preservation of its activity and selectivity under conditions that would otherwise lead to its decomposition.^[105] In the case of cinnamyl amines (71), the arylation reaction in the absence of MPAA follows a Heck-type mechanism, yielding *trans*-products.

However, in the presence of MPAA, arylation is guided by the C–H activation process, leading to *cis*-products as shown in Figure 19a. The treatment of cinnamyl amines (71) usually as a mixture of isomers with boronic acids results in the formation of functionalized amines (72) with an exclusive *cis*-geometry of the allyl group relative to the introduced functional group. This reaction works efficiently with a variety of boronic acids, including diphenyl, naphthyl, carbazole, and triphenylamine. It also accommodates a broad range of substituents on the aryl group of the cinnamylamine and on the nitrogen atom. Additionally, it is highly useful for synthetic applications as it can be performed on a gram scale.^[105]

In catalytic reactions with dialkylpropylamine-type substrates, two competing processes can occur. On one hand, C–H activation promoted at γ -position by the metal can take place, with the nitrogen atom acting as a DG. On the other hand, a β -elimination process can also occur. Gaunt and Rodriguez have recently demonstrated that the use of MPAA can control reactivity in one direction or the other.^[106] Using DFT methods, these authors calculated the activation barriers for C–H bond activation in both processes (β -elimination and γ -activation) in dialkylpropylamines (73) as represented in Figure 19b. In their study, they compared Pd(OAc)₂ alone with the Pd complex formed by coordinating the MPAA *N*-Ac-tLeu to Pd(II), evaluating the role of the acyl group in suppressing β -elimination. The results show that in the absence of MPAA (i.e., using only Pd(OAc)₂), both activation barriers are quite similar, regardless of whether the amine is cyclic or non-

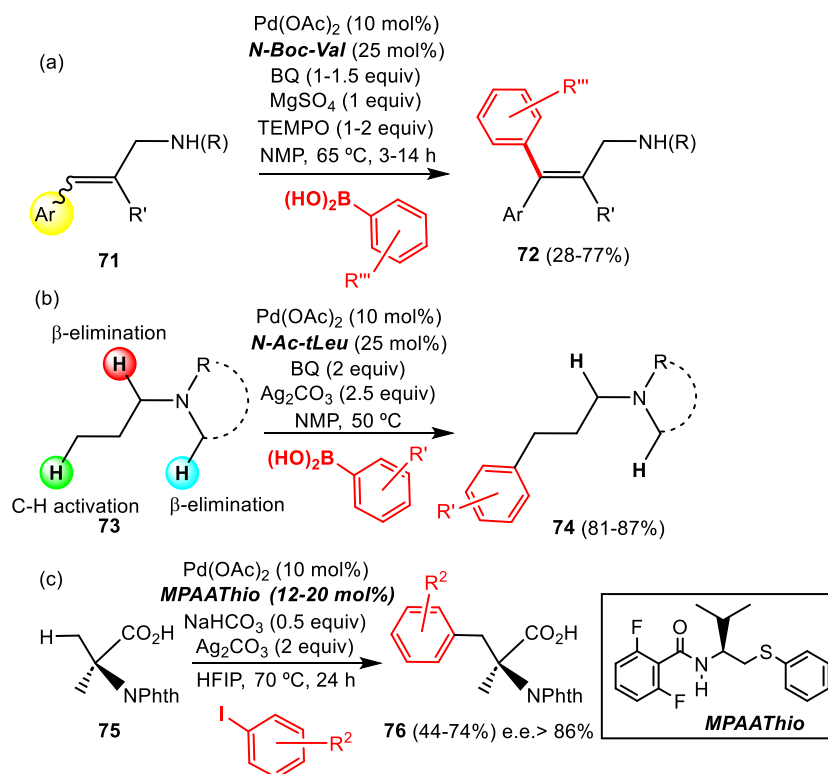


Figure 19. Arylation of (a) cinnamylamines, (b) dialkylpropylamines, and (c) amino acids.

cyclic or whether β -elimination occurs at the propyl group or another *N*-substituent (30.2–31.7 kcal/mol). However, the lowest barrier corresponds to β -elimination. Experimentally, only trace amounts of cyclometalation are observed in all cases, which aligns well with theoretical calculations. In contrast, when *N*-acetyl-tert-leucine acts as a κ^2 -N,O-dianion, the activation barrier for the C–H activation process drops significantly to 26.3 kcal/mol in the cases of dimethylpropylamine or *N*-propylpiperidine, while the β -elimination barriers remain around 32 kcal/mol. Therefore, the presence of the MPA ligand favors C–H bond activation at the propyl group, leading to the corresponding cyclometalated product, while completely inhibiting decomposition via β -elimination in these two cases. However, in the case of *N*-propylpyrrolidines, the activation barriers for both processes are very similar. Theoretical predictions regarding the relative activation barrier values were validated through experimental γ -arylation assays using dimethylpropylamine, *N*-propylpiperidine, and *N*-propylpyrrolidine as substrates. The results showed excellent agreement between the DFT predictions and experimental findings, with arylated derivatives (**74**) obtained for dimethylpropylamine and *N*-propylpiperidine in 81–87% yield, while the γ -arylation yield was below 5% for *N*-propylpyrrolidine.^[106]

Yu and collaborators have described an enantioselective arylation method for α,α -disubstituted α -amino acids via $\text{C}(\text{sp}^3)$ –H activation, with the simplest and most commonly used starting material for further functionalizations being α -aminoisobutyric acid (**75**).^[107] The process, shown in Figure 19c is catalyzed by $\text{Pd}(\text{OAc})_2$ and promoted by the phenyl(aminoethyl)thioether MPAATHio depicted in the right inset of Figure 19c. The scope of

arylated derivatives (**76**) is broad in terms of R^2 substituents, and they are obtained with excellent enantiomeric excesses. These enantiopure amino acids are highly valuable, as they induce the formation of helical structures in the peptides they are incorporated into. Although other methods exist to obtain species similar to (**76**), none achieve this in a single reaction step with the yields and enantiomeric excesses described here, making it a highly effective approach for expanding the chemical space of these species. In addition to the derivatives (**75**), the same study presents an extension to aminocyclopropanecarboxylic acids, which are of high interest in the agro-food sector.^[107]

2.4. Halogenation and Glycosylation

The fluorination of organic molecules is a highly interesting process with applications in medicinal chemistry, agrochemistry, and materials science. Despite its significance, forming the C–F bond remains challenging, particularly when attempting to achieve it catalytically through the activation of $\text{C}(\text{sp}^3)$ –H bonds. This difficulty arises due to the low reactivity of these bonds and the challenges associated with C–F coupling during the reductive elimination step in Pd(II). For this reason, reductive elimination from the more reactive Pd(IV) oxidation state has been extensively studied. To reach Pd(IV), electrophilic fluorination is commonly employed, typically using N–F bond containing compounds that generate the F^+ species. In contrast, there are very few reported cases of nucleophilic fluorination using F^- in the presence of external oxidants. Van Gemmeren and collaborators have described a direct nucleophilic fluorina-

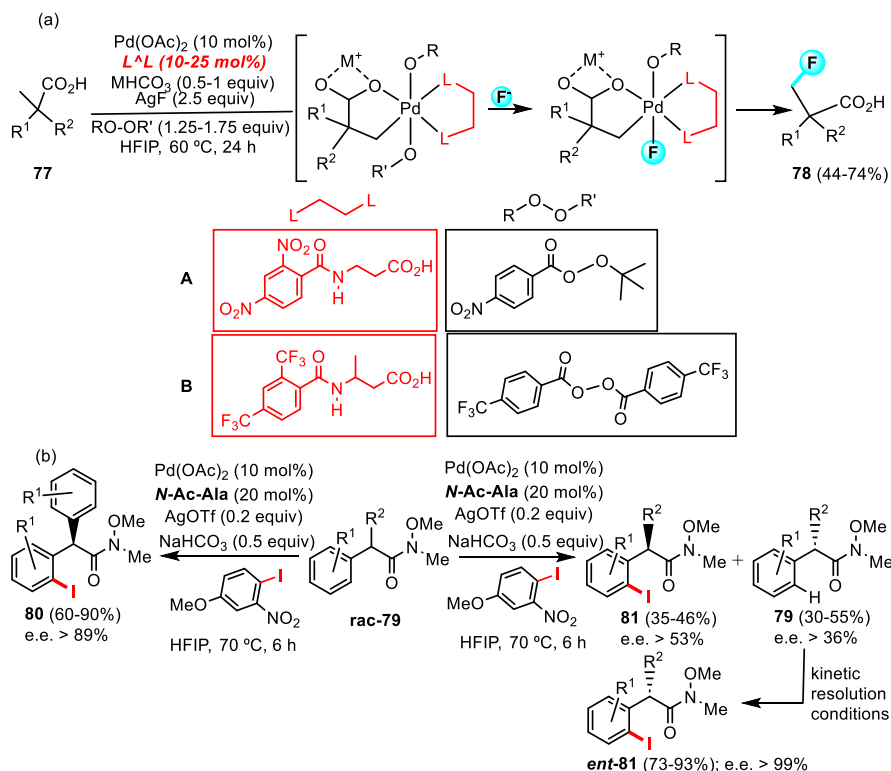


Figure 20. Nucleophilic fluorination of (a) pivalic acids and (b) iodination of Weinreb amides.

tion method for C(sp³)—H bonds in pivalic acid derivatives (**77**) using an external oxidizing agent, as shown in Figure 20a.^[108] The reaction proceeds through the cyclometalation of the starting pivalic acid (a process assisted by MPAA), oxidative addition of the peroxide ROOR', exchange of one OR group for fluoride (F[−]), and reductive elimination via C—F coupling leading to the formation of fluorinated species (**78**). The oxidant design is critical in this study, as it has been demonstrated that the peroxides shown in Figure 20 are optimal for minimizing (or eliminating) reductive elimination through C—O coupling while facilitating ligand exchange and C—F reductive elimination from the Pd(IV) intermediate. When the carboxylic acid is bound to a quaternary carbon, conditions A (shown in Figure 20a) are used, whereas for a tertiary carbon (R² = H), conditions B are optimal. Under these conditions, the scope of substituents R¹ and R² is broad, although reaction yields are only moderate.^[108]

Continuing with halogenation reactions, Li's group and collaborators have described an isodesmic method for the enantioselective iodination of Weinreb amides derived from phenylacetic and 2,2-diphenylacetic acids, *rac*-(**79**) through their reaction with 1-iodo-4-methoxy-2-nitrobenzene.^[109] Two processes are described, as outlined in Figure 20b. The first one involves the desymmetrization of amides derived from 2,2-diphenylacetic acid (**79**) via iodination, yielding compounds (**80**). The second process is the kinetic resolution of phenylacetic acid amides *rac*-(**79**), producing iodinated derivatives (**81**) that are enantiomerically enriched, along with the starting amides (**79**), which become enriched in the enantiomer opposite to the iodinated derivatives (**81**). In both cases, the reaction exhibits broad tolerance to various substituents on the amides, making it highly

general. Moreover, the desymmetrization process typically proceeds with excellent enantiomeric excesses, whereas the kinetic resolution yields slightly lower enantiomeric excesses. Notably, if the recovered derivatives (**79**) from the kinetic resolution iodination are subjected to a second iodination under the same reaction conditions, the enantiomers *ent*-(**81**) are obtained with excellent yields and enantiomeric excesses.^[109]

The research groups of Lei and Yu have achieved the C—glycosylation of phenylacetic acid derivatives in the absence of DG—an uncommon type of reactivity compared to the more prevalent O—glycosylation. This approach yields metabolically stable compounds with potent bioactivity.^[110] The acidic substrates (**82**) react with the sugar in the form of a vinyl borane, resulting in the formation of C—glycosylated coupling products (**83**), as illustrated in Figure 21 (TIPS = triisopropylsilyl). The reaction is catalyzed by PdCl₂(NCPH)₂ in the presence of the MPAA *N*-Ac-Ala, without which the reaction does not proceed. Using optimized conditions, the described method exhibits broad generality (with over 60 reported examples) and has been applied to the functionalization of commercial drugs such as ibuprofen and its derivatives, as well as diclofenac, aiming to facilitate new drug discovery. In this context, the synthesis of a potent new SGLT-2 inhibitor for diabetes treatment is also reported.

2.5. Transformations Performed Under Dual Ligand Conditions

In the previous sections, the improvements achieved in Pd-catalyzed processes have been presented in terms of selectivity

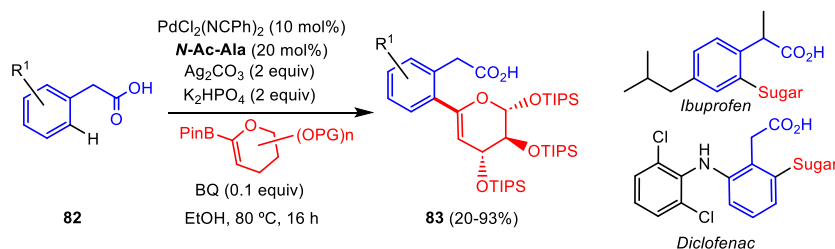


Figure 21. C-glycosylation of phenylacetic acid derivatives.

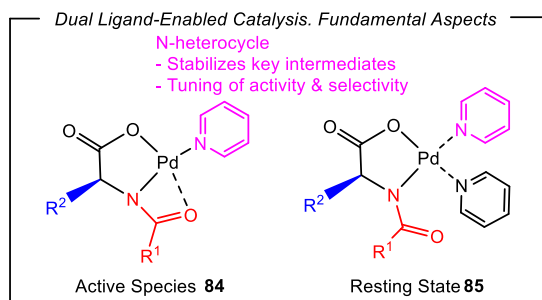


Figure 22. Schematic representation of the proposed active species (84) and the resting state (85) for the dual ligand-enabled catalysis.

and activity when the processes are controlled by the structure of the catalyst rather than that of the substrate. This has been accomplished through the introduction of specific ligands that play very particular roles during the reaction, such as assisting proton transfer, stabilizing transition states in different oxidation states, or creating chiral pockets. In the cases analyzed so far, all the ligands are of the MPAA type, but throughout this review, examples of ligands with different characteristics are also described. Despite their differences, these ligands have a similar effect: they enable the reaction, accelerate it, and improve selectivity. The effects of using ligands such as pyridones (section 3), *N*-heterocycles (section 4), thioether-acids (section 5) or phosphines (section 6) will be discussed later.

Given this situation, several authors have investigated the effect of having two ligands from the previously mentioned categories coexisting in the catalytic mixture, seeking synergies between them. The van Gemmeren group has been a pioneer in this field, working primarily with combinations of MPAA and electron-deficient *N*-heterocyclic ligands such as pyridines or quinolines,^[111–115] as well as the Ritter group.^[116] These authors base their hypothesis on the idea that the *N*-heterocyclic ligand would act as the donor atom of the DG and therefore, its electronic and steric properties could be used to control and modify the activity and selectivity of the catalytic system. Additionally, the presence of this additional ligand in varying amounts would help stabilize the catalyst at different points in the catalytic cycle, as shown in Figure 22. For example, these authors have proposed that the resting state of the catalyst (85) is stabilized in the presence of two equivalents of pyridine, while the active species (84) contains only one coordinated pyridine.^[112] The weak bond between Pd and pyridine facilitates the creation of a coordina-

tion vacancy in the active species from the resting state. These facts have been validated later by DFT.^[117]

The combination of an MPAA ligand and an *N*-heterocyclic ligand has led to excellent contributions in the past two years. The *N*-Ac-Gly/pyridone or quinoxaline combination has enabled the Maiti and van Gemmeren groups to carry out the chalcogenation and iodination, respectively, of aromatic and heteroaromatic systems.^[118,119] Figure 23 outlines the studied processes. In the case of chalcogenation, shown in Figure 23a, the treatment of arenes (87) as limiting reagents with diaryl dichalcogenides Ar_2E_2 ($\text{E}=\text{S}, \text{Se}$) results in the incorporation of the $-\text{EAr}$ fragment into the starting arene (87), generating the chalcogen derivatives (88) with good yields and excellent selectivities. This is due to the additional selectivity control exerted by the pyridine ligand through steric factors in the transition state (86).^[118] For example, in naphthyl precursors, the $\beta:\alpha$ selectivity ratio can exceed 30:1, while in substituted benzenes, the final ortho:meta orientation depends on the size of the substituents: the bulkier they are, the higher the proportion of the meta isomer obtained. In general, chalcogenation is also successfully achieved in heteroarenes such as pyridine, quinoline, thiophene, pyrrole, indole, benzothiophene, benzothiazole, and pyridones. The method is also applicable to the chalcogenation of pharmaceutical compounds and complex molecules, demonstrating remarkable generality with over 70 characterized examples.^[118]

Van Gemmeren and coworkers have described an isodesmic method for the iodination of aryls, similar to the one reported by Li and shown in Figure 20, achieving exceptional selectivity through steric control of the reaction.^[119] The reaction of arenes (87) with 2-iodonitrobenzene under the conditions outlined in Figure 23b leads to the formation of iododerivatives (89). The presence of the MPAA ligand *N*-Ac-Gly along with the auxiliary ligand quinoxaline provides the necessary environment for the derivatives (89) to be obtained as exclusive meta isomers in most of the cases examined. This occurs regardless of the electronic nature of the substituents, as the meta position is sterically favored. Therefore, this method grants access to iodides as complementary isomers to those obtained through other classical methodologies. This distinction is clearly illustrated in Figure 23c, comparing iodination by electrophilic substitution, directed lithiation, and isodesmic iodination.^[119]

The Van Gemmeren group has also developed a method for the nondirected deuteration of arenes (90), using the conditions shown in Figure 24 based on a catalytic system that promotes reversible C–H activation. The hydrogen isotope exchange (HIE) process is catalyzed by Pd and promoted by both an MPAA and

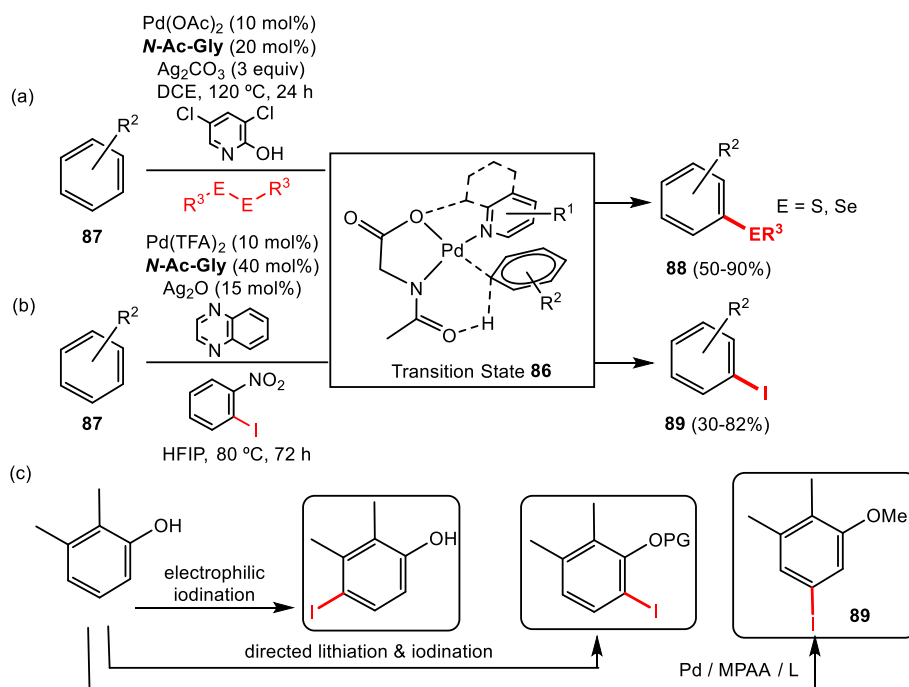


Figure 23. Chalcogenation and iodination of aromatic precursors.

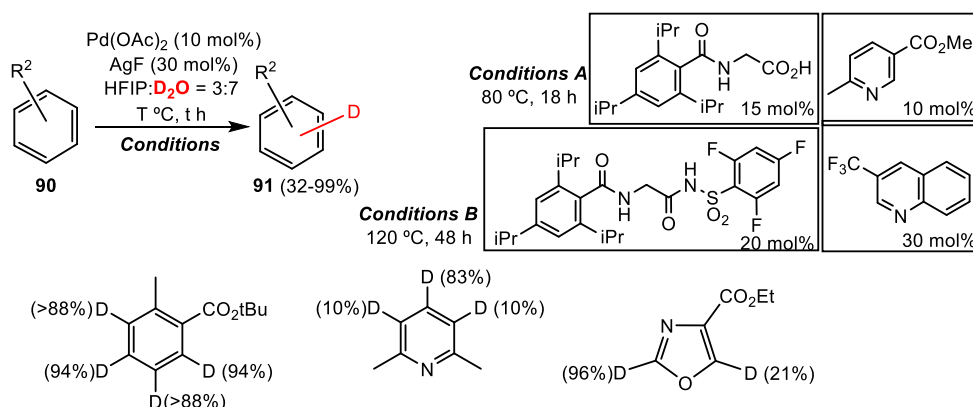


Figure 24. Deuteration of arenes promoted by dual ligand-enabled catalysis.

an *N*-acylsulfonamide, accompanied by pyridine- or quinoline-type ligands, respectively. The choice between conditions A (mild) or B (harsh) depends on the electronic characteristics of the substrate in the sense that electron-rich substrates require milder conditions, while electron-deficient ones need more energy. Under both conditions, total or partial deuteration of all aromatic positions is achieved in molecules (91) with varying degrees of complexity. However, method B enables a higher degree of deuteration, even at the ortho positions to bulky groups, which are the most unfavorable. In contrast, deuteration at the meta and para positions is nearly complete.^[120] The deuteration method described here is robust and general. The concepts involved, spanning experimental and theoretical chemistry as well as characterization techniques, are extensive. The deuteration examples that can be prepared are highly illustrative—so much so that the authors have developed a practical experiment for undergraduate students.^[121]

The synthesis of β -aryl ketones (93) via arene alkylation has been described by Maiti, Lahiri, and Zhang.^[122] The reaction, shown in Figure 25a involves the treatment of arenes and heteroarenes (92) with allylic alcohols, resulting in the hydroarylation of the C=C double bond of the allyl group. This process is catalyzed by Pd and promoted by the combined action of the *N*-Ac-Phe and 2-methyl-quinoxaline ligands. The selectivity of this nondirected functionalization of arenes is controlled by steric effects and is determined by the available space in the transition state once the MPAA and quinoxaline are coordinated, as demonstrated by the reaction mechanism determined through DFT calculations. The results show very high selectivity: in naphthyl-type and disubstituted aryl derivatives, the β : α ratios exceed 5:1, and in monoaryl derivatives, the predominant isomer is the meta with the ortho isomer not observed in many cases. This procedure is also applicable to heterocycles such as thiophenes, benzothiophenes, benzofurans, and thianthrenes

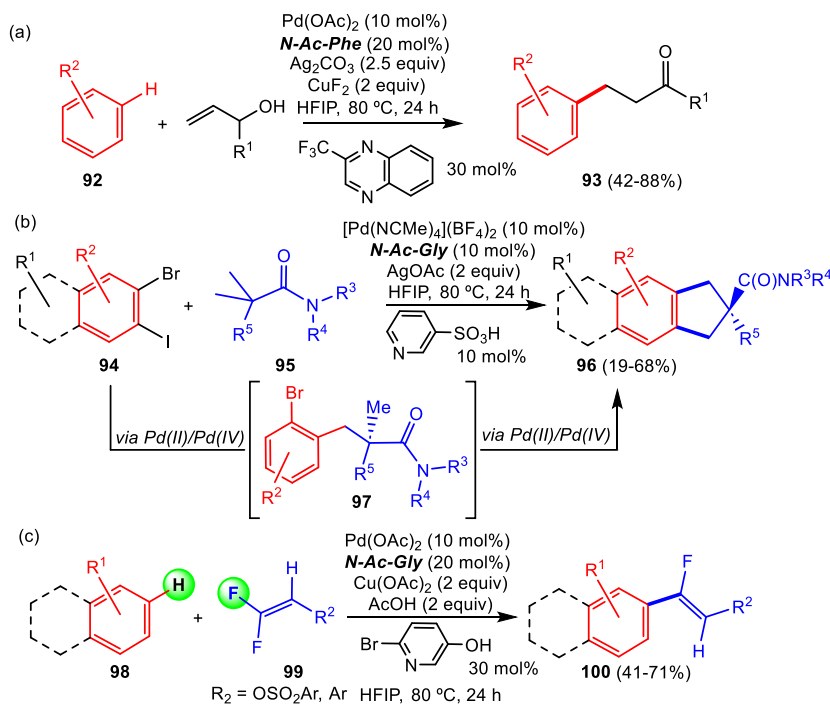


Figure 25. Diverse C–H functionalizations promoted by the dual ligand-enabled methodology.

exhibiting high selectivity as well. This broad applicability successfully extends to the functionalization of biologically relevant molecules such as naproxen and its derivatives, propofol, thymol, cholesterol, and other related substrates.^[122]

On the other hand, Yu has described the synthesis of five-membered carbocycles fused to an arene through the reaction of 1-bromo-2-iodo-arenes (**94**) with *gem*-dimethyl amides (**95**). The process proceeds via $\text{C}(\text{sp}^3)\text{--H}$ activation of both methyl groups of the amide and double alkylation of the $\text{C}(\text{sp}^2)\text{--X}$ bonds ($\text{X}=\text{Br}, \text{I}$) of the arene, generating the carbocycles (**96**) through a double $\text{C}(\text{sp}^3)\text{--C}(\text{sp}^2)$ coupling.^[123] The participation of the auxiliary ligands *N*-Ac-Gly and pyridine-3-sulfonic acid is essential for Pd catalysis to occur. The reaction appears to take place in two stages. The first stage involves a $\beta\text{--C}(\text{sp}^3)\text{--H}$ activation in one of the amide methyl groups, followed by arylation through reaction with the C--I bond via oxidative addition $\text{Pd}(\text{II})/\text{Pd}(\text{IV})$ and reductive elimination via C--C coupling, generating intermediate (**97**). The process is repeated— $\text{C}(\text{sp}^3)\text{--H}$ activation and oxidative addition $\text{Pd}(\text{II})/\text{Pd}(\text{IV})$ at the C--Br bond followed by reductive elimination and C--C coupling—leading to the final species (**96**). However, this second coupling step is more challenging since it involves a C--Br bond, which is less reactive. This stage requires the involvement of both ligands and appears to proceed via Pd--Ag bimetallic catalysis. The reaction has a broad scope, tolerating a wide range of amides and bromo-iodo derivatives with products (**96**) obtained in moderate to good yields. However, other halide combinations including even diiodobenzene or other different leaving groups are not effective in promoting dihalogenation. This synthesis has been applied to the preparation of (\pm)-Echinolactone-D.^[123]

The synthesis of fluorinated compounds has been another area extensively explored by Maiti and collaborators given

the importance of fluoroderivatives in drug discovery.^[124] This group describes the synthesis of α -fluoroolefins (**100**) starting from *gem*-difluoroalkenes (**99**) and their reaction with hydrocarbon substrates (**98**), catalyzed by Pd and promoted by *N*-acetylglutamine (*N*-Ac-Gly) and a hydroxypyridine. The process formally involves the activation of a C--F bond and a C--H bond, followed by oxidative coupling, a reaction illustrated in Figure 25c. The α -fluoroolefins (**100**) are obtained in moderate to good yields with remarkable regioselectivity. In the case of naphthyl or disubstituted aryl derivatives, the $\beta:\alpha$ ratio exceeds 5:1 in most cases. For monosubstituted arenes, the meta orientation prevails when the substituents are bulky, once again demonstrating the steric control of the reaction. However, exceptions to both orientations are discussed in detail. The mechanism reveals that the reaction proceeds through the formation of an aryl derivative via C--H activation, migratory insertion of the *gem*-difluoroalkene, and subsequent $\beta\text{--F}$ elimination, in a manner similar to classical nucleophilic addition-elimination processes in olefins. Finally, it is noteworthy that this protocol has been applied to the synthesis of fluorinated drug derivatives, such as naproxen and tocopherol, as well as in the formation of drug-natural product conjugates (such as propofol and vitamin E), significantly expanding the chemical application space of this methodology.^[124]

2.6. New Directions in Ligand-Enabled Catalysis

It is currently possible to clearly identify two types of innovations in this field. One, more expected, is the development of new ligands and new molecular structures based on the concepts and

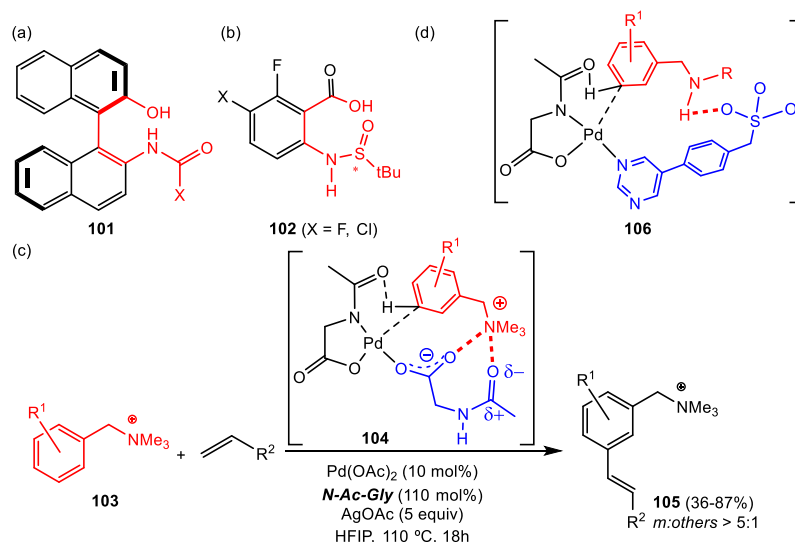


Figure 26. (a,b) New ligands and new concepts. (c) NCI and (d) H-bonds, applied to the dual ligand-enable functionalization.

knowledge acquired over the past few years. For instance, the Mascareñas and Gulías group has designed a new type of ligand that combines the characteristics of MPAAAs with those of BINAP, called NOBINAc (**101**), which is shown in Figure 26a.^[125] This ligand possesses the basic functionalities that allow it to act as a dianion (O—H and N—H groups can be deprotonated), accelerate the reaction via CMD (C=O group), and, in addition, the source of axial chirality comes from the BINAP skeleton. The most notable difference between this ligand and other MPAAAs is that the palladacycle formed by NOBINAc consists of six members, whereas those formed by amino acids consist of five. Therefore, the resulting κ^2 -N,O coordination structure of NOBINAc is less strained. Moreover, the chirality introduced by the binaphthyl fragment is axial rather than point chirality, which should be reflected in its properties. This group has successfully used NOBINAc in the enantioselective synthesis of 2-benzazepines via the [5 + 2] cycloaddition of homobenzylamines with allenes, yielding the corresponding derivatives with up to 92% yields and enantiomeric excesses of up to 97% for a wide variety of amines and allenes.^[125] The reason for this excellent selectivity has been explained through DFT modeling of the transition states, which reveal significant destabilizing intramolecular interactions for one of the TS, leading to severe distortions around the molecular plane of Pd. These distortions do not occur in the other TS, resulting in an energy difference between the two TS of up to 8.2 kcal/mol.

Along the same lines of designing new ligands, the research groups of Zhang, Zhang, and Shi have prepared derivatives of *N*-sulfinyl anthranilic acid, such as species (**102**) shown in Figure 26b, which follow a structural scheme similar to that of NOBINAc and MPAAAs. These derivatives can act as κ^2 -N,O dianionic ligands through deprotonation of the carboxylic acid and NH group. The S=O group can assist in proton removal when the C—H activation step is the RDS and the mechanism follows a CMD pathway, while the sulfur atom itself serves as a stereogenic center capable of inducing enantioselective transformations. The novelty of this ligand lies in the fact that the

chiral information resides in the *N*-protecting group, which is closer to the reactive site. Thus, the direct interaction between the protecting group (the *N*-tert-butylsulfonamide fragment) and the substrate appears to be responsible for the chiral induction of this ligand, due to the large steric bulk of the tBu group and its proximity to the metal center. This ligand has been employed in the desymmetrization of diarylmethanol via alkynylation of one of the two aromatic rings.^[126] After C—H activation and exo-coordination of diarylmethanol in the form of an oxime ether, the steric effect exerted by the tBu group enables stereodifferentiation between the two phenyl groups of the substrate, selectively functionalizing one of them.

The second innovation identified in this field focuses on developing new concepts to achieve the desired activity and selectivity. The research groups of van Gemmeren^[127] and Maiti^[128] have reported charge-controlled catalytic systems based on electrostatic interactions or NCIs (NonCovalent Interactions: H bonding), respectively achieving excellent activity and selectivity.

Thus, Van Gemmeren and coworkers have developed a method for the undirected alkenylation of benzylammoniums (**103**), which proceeds with selective meta orientation to yield the olefinated derivatives (**105**) as shown in Figure 26c.^[127] The starting benzylammonium substrate (**103**) has a formal positive charge on nitrogen, which is crucial since the Pd catalyst, in addition to the participation of the *N*-Ac-Gly MPAA coordinated in an N,O-chelate manner, requires a second ligand that has either a formal negative charge or a permanent dipole. In this case, the second ligand is the same MPAA, which is used in excess (110 mol%) and coordinates to Pd in a monodentate anionic fashion through one of the oxygen atoms of the carboxylate, playing two distinct roles. In the transition state (**104**), shown in the same Figure 26c, an interaction occurs between the positive charge of the substrate and the negative charge of the ligands. The resulting spatial distribution, the extent of stabilization due to these interactions, and the final orientation of all species are responsible for the observed selectivity. Strictly speaking, these

reactions remain catalyst-controlled, though the substrate must meet the requirement of carrying a charge. The reaction has a broad scope, allowing the synthesis of a wide variety of alkenylation products. The diversity of substituents demonstrates that the reaction's *meta* orientation, achieved through charge control, completely surpasses the orientation dictated by electronic control. This orientation is complementary to that achieved through other methods, as demonstrated in this work by preparing all three isomers (*ortho*, *meta*, and *para*) from the reaction between trimethylbenzylammonium and ethyl acrylate. DFT calculations determining the mechanism of this unique reaction confirm that the activation barrier for C–H bond activation at the *meta* position is the lowest, whereas the *ortho* and *para* barriers are higher, in perfect agreement with experimental observations. The reason for this lower barrier lies in the fact that, in *meta* activation, the nitrogen atom of the ammonium group engages in two electrostatic interactions—one with the oxygen of the carboxylate group and another with the carbonyl oxygen, as depicted in TS **104** in Figure 26c. In contrast, the transition states for *ortho* and *para* activations exhibit only a single interaction.^[127]

The work of Maiti et al., which overlaps in time with the study by van Gemmeren that was just discussed, originates from a similar inspiration. However, in this case, it is not electrostatic interactions but rather hydrogen bonds that are the weak interactions responsible for the observed orientation.^[128] They describe the *meta*-alkenylation of *N*-protected benzylamines, a process catalyzed by Pd and assisted by *N*-Ac-Gly and an anionic ligand. This ligand consists of a pyrimidine ring, which coordinates to Pd, a phenyl spacer, and a CH₂SO₃ group in the *para* position relative to the pyrimidine ring. After the coordination of *N*-Ac-Gly to Pd in the usual manner, the anionic ligand coordinates via one of the pyrimidine nitrogen atoms. With this structural arrangement, the approach of the benzylamine enables the formation of a hydrogen bond between the proton of the N–H group and the sulfonyl group. In turn, this H-bond dictates that the most favorable position for *meta*-alkylation in the aromatic ring of the benzylamine is the *meta* position. The transition state (**106**) depicted in Figure 26d summarizes the chain of interactions that explains the observed selectivity. Regarding the reaction scope, it is also quite broad. However, in this case, the variation of substituents allows the conclusion that the electronic nature of the substituents on the benzyl ring significantly influences the reaction's orientation, as it affects the extent to which the hydrogen bond forms. The alkenylated benzylamines are obtained with yields ranging from 25% to 95%, and the *m*:*o*ther isomer ratio is always greater than 3:1. The mechanism has been determined using DFT methods, including the characterization of all noncovalent interactions (H-bonds) through Bader's AIM (Atoms In Molecules) analysis.^[128]

In conclusion, the use of MPAA ligands coordinated to Pd has proven to be an outstanding tool for promoting a wide variety of stereoselective catalytic processes under mild reaction conditions, as these ligands assist in the C–H activation step and control the space around the metal. Their synthesis is straightforward and highly modular and it is possible to design a broad

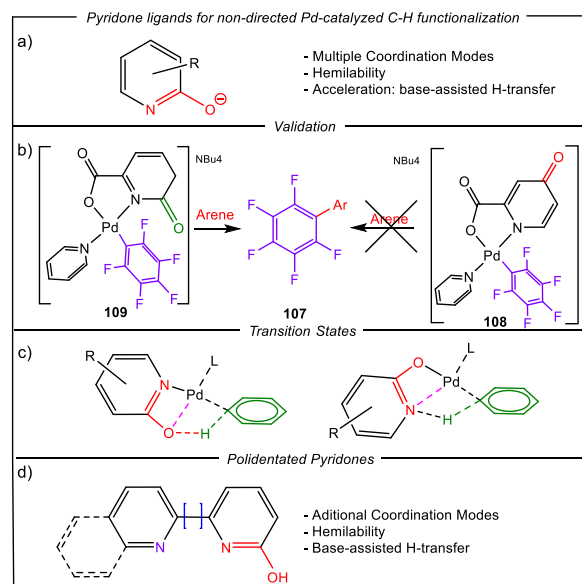


Figure 27. (a) Diagram of pyridones (hydroxypyridines) and their mode of action. (b) Comparison of the reactivity of **108** and **109**, showing the necessity of the carbonyl group in close proximity to the ligand to be activated to promote C–H activation. (c) Proposed transition states involving Pd-bonded pyridones and (d) schematic diagram of multidentated pyridones.

range of MPAA ligands by modifying either the amino acid (chain length, auxiliary functional groups, number of stereogenic centers, absolute configuration of each center) and the *N*-protection. However, in the latter case, it is essential that a carbonyl group is adjacent to the nitrogen. In the development of Pd-catalyzed processes, the paradigm shift brought about by the use of these ligands (from substrate control to catalyst control) is arguably the most significant advancement in recent years, and the field remains in active development, aiming to improve even more both the activity and the selectivity.

3. Pyridones

Pyridone ligands, as shown in Figure 27, are widely used in Pd-catalyzed C–H functionalization processes. Similarly to MPAA, these ligands are able to accelerate the C–H activation step when it occurs via a CMD mechanism by acting as an internal base through the carbonyl oxygen. In fact, the structural basic framework NC(O)C responsible for the capture and proton transfer assistance can be recognized as the same in pyridones and MPAA, as shown in Figure 27a, therefore the role of this unit is similar in both ligands. This behavior was validated by Pinilla and Albéniz (Figure 27b), which isolated complexes **108** and **109**. Complex **108**, which uses 6-hydroxypicolinic acid as a ligand is capable of accelerating the C–H activation of arenes, leading to the formation of **107**. However, complex **108**, which uses 4-hydroxypicolinic acid, is not capable of C–H activation, as the oxygen atom is far from the metal and cannot be involved in the CMD mechanism.^[129] Additionally, pyridones also show a

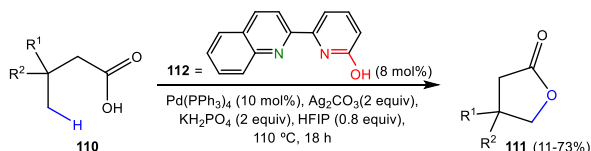


Figure 28. γ -Lactonization of aliphatic carboxylic acids via C(sp³)-H bond functionalization.

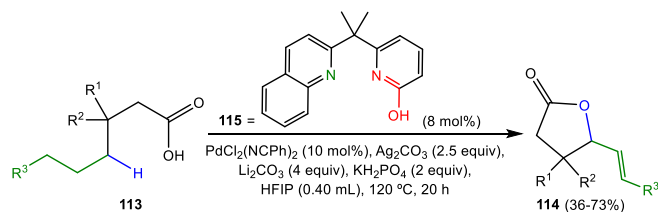


Figure 29. Chemoselective γ -lactonization of aliphatic carboxylic acids.

rich coordination chemistry, because they can coordinate to the metal center via κ^1 -O, κ^1 -N or κ^2 -N,O bonding modes, depending on the metal's environment. Pyridones can also change their bonding mode from κ^2 -N,O to κ^1 -O or κ^1 -N depending on the present ancillary ligands, allowing the formation of a vacant position in the metal center when necessary. This flexibility is very convenient as it allows to accommodate the required ligands at different times of the catalytic cycle (Figure 27c). The pyridone ligands can be accompanied by additional coordinating functional groups, such as pyridines, quinolines, and so on (Figure 27d). This polydentate provides additional bonding modes to the metal center resulting in versatile synthetic tools, as presented in the next paragraphs.^[130]

3.1. Intramolecular Cyclization

Lactones are present in a wide range of natural products and active biomolecules,^[131] which makes developing new more efficient methods for their synthesis desirable. This has led to the development of a palladium-catalyzed γ -C—H functionalization of carboxylic acids (110) by Yu's group. With this methodology they are able to control the chemoselectivity of the reaction by changing the quinoline-pyridone ligand used (112). As shown in Figure 28, using 6-(quinolin-2-yl)pyridin-2-ol (112) led to γ -methyl C—H lactonization exclusively, affording lactones (111).^[132] A wide variety of carboxylic acids (110) were tested, substrates containing γ -methylene, γ -methine or C—H benzylic bonds showed complete selectivity towards γ -methyl lactonization. Meanwhile, substrates liable of β -elimination reactions yielded lower yields due to the competition from a β -elimination process after the C—H activation.^[132]

Previous studies by Yu and collaborators proved that the bite angle of pyridine-pyridone ligand is an important factor in the chemoselectivity between γ -methylene and γ -methine in the C(sp³)-H arylation of aliphatic carboxylic acids (113), directing the C—H activation towards the γ -methylene position (Figure 29).^[133] The use of quinoline-pyridone ligand (115), which possesses a

bigger bite angle compared to (112), resulted in the switch in chemoselectivity from γ -methyl to γ -methylene C—H activation. A wide variety of carboxylic acids (113) were tested and in all cases it led to the formation of the γ -methylene lactonization products (114) with moderate to good yields.^[132]

Benzolactones are present in many bioactive natural products such as stachybotrylactone acetate, 3-Deoxyzinnolide and (+)-Bicuculline.^[134–136] These applications have led Yu's group to develop a new, more efficient strategy, for the preparation of these derivatives via palladium catalyzed C—H lactonization using molecular oxygen as the sole oxidant, following the procedure shown in Figure 30. By using a gas mixture of 5% oxygen in nitrogen, 10 mol% of PdCl₂(NCPh)₂, 30 mol% of 3-trifluoromethyl-2-pyridone (118), 2.5 equivalents of K₂HPO₄, 2 equivalents of acetic anhydride and chlorobenzene as a solvent they were able to exclusively activate the C(sp³)-H bond of the carboxylic acids (116) over the ortho-C(sp²)-H bond present in the aromatic ring, resulting in the formation of the desired benzolactones (117). A wide variety of benzoic acids (116) were tested. Benzoic acids containing electro-donating groups such as methoxy, phenyl or methyl gave the desired lactones with good yields (39%–70%). Benzoic acids with electron-attracting functional groups such as halides, trifluoromethyl, and ketone led to lower yields (34%–59%).^[137]

To shed some light on the palladium catalyzed C—H lactonization mechanism, Musaev and collaborators performed a joint experimental and computational study on the mechanistic pathway of the Pd(II)-catalyzed C(sp³)-H lactonization. They found out that, despite the fact the C(sp³)-H activation (14.2 kcal/mol) is less favored than the C(sp²)-H activation (10.9 kcal/mol), both are reversible and the following C—O bond formation is the RDS. In this step C(benzylic)-O bond formation (35.3 kcal/mol) is favored against C(ortho)-O bond formation (48.2 kcal/mol).^[138]

γ -butyrolactones with a tertiary center adjacent to the oxygen atom (121), shown in Figure 31, are present in many natural products and are useful as synthetic intermediates for bioactive targets.^[131] This led Yu's group to develop a new catalytic pathway for the synthesis of arylated γ -butyrolactones using a wide variety of linear carboxylic acids (119) coupled with a wide range of aryl iodide substrates (120). By using Pd(OAc)₂ (10 mol%) with carboxyl-pyridone (122) (15 mol%) as a ligand they were able to achieve a tandem γ -C(sp³)-H arylation/lactonization of linear carboxylic acids to obtain γ -arylated γ -lactone products (121) as shown in Figure 31. The presence of chloro substituents at the aliphatic chain, branched chain substrates or changing the length of the aliphatic chain in the carboxylic acid (119) led to the formation of the desired products (121) with good yields (up to 83%). However, substrates containing aryl groups in the γ -position resulted in lower yields (28%–38%). Concerning the aryl iodide (120), the presence of electron-donating groups such as aliphatic substituents in the 3 and 4 positions, methoxy or OPh led to the formation of the γ -arylated γ -lactone products with good yields (48%–90%). Electron-withdrawing substituents, such as NHAc, CHO, COOMe or NO₂, are tolerated, but led to a decrease in yields (46%–70%).^[139]

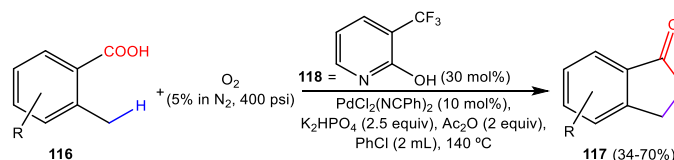


Figure 30. γ -Lactonization of aromatic carboxylic acids using O_2 as the sole oxidant.

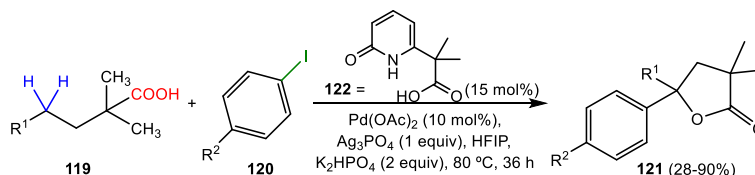


Figure 31. Synthesis of arylated γ -butyrolactones by tandem arylation-lactonization of linear carboxylic acids.

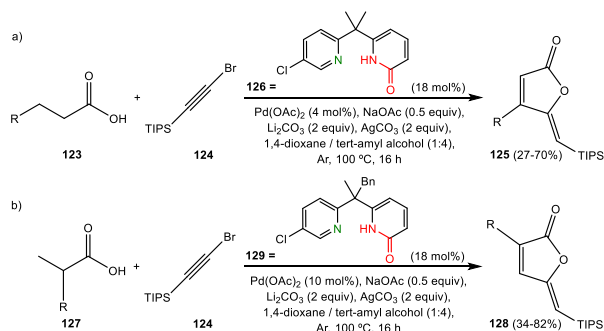


Figure 32. (a) Synthesis of γ -alkylidene butenolides by C–H dehydrogenation-alkynylation-cyclization of linear or (b) of branched carboxylic acids.

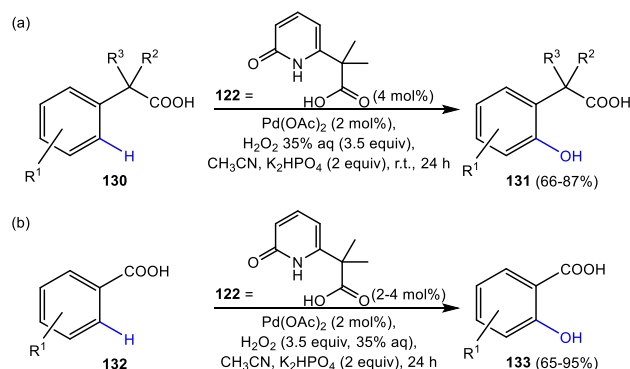


Figure 33. Synthesis of phenols by hydroxylation of aromatic precursors (phenylacetic and benzoic acids).

In 2021, Yu's group developed a new Pd(II)-catalyzed C–H dehydrogenation-alkynylation-cyclization method for the synthesis of γ -alkylidene butenolides using carboxylic acids (**123**, **127**) and bromoalkynes (**124**) as coupling partners. The presence of a bidentate, six membered chelating pyridine-pyridone is crucial as they allow for both the $C(sp^3)$ –H activation for the formation of the α,β -unsaturated acids and the posterior $C(sp^2)$ –H activation for the vinyl functionalization and formation of the γ -alkylidene butenolide (Figure 32).^[140] A wide range of linear carboxylic acids (**123**) were tested using pyridine-pyridone ligand **126** as it gave the best results for this type of substrate (Figure 32a). Aliphatic carboxylic acids substrates provided the desired product (**125**) in moderate yields (27%–70%). Carboxylic acids with ester groups resulted in the formation of the γ -alkylidene butenolide with good yields (47%–67%). Carboxylic acids with ring systems provided the expected fused butenolides with good yields (48%–64%). The use of a α -quaternary substituted carboxylic acid, such as 1-propylcyclohexane-1-carboxylic acid led to the formation of the γ -alkylidene butenolide (**125**), although with lower yields (27%).^[140] In the case of branched carboxylic acids (**127**), pyridine-pyridone ligand (**129**) proved to be the optimal ligand for these kinds of substrates (Figure 32b). Carboxylic acids with alkyl, heteroatoms, aryl, and saturated heterocycles provided the desired product (**128**) in moderate yields (34%–82%). In the cases where the substrate possesses

both β -methylene and β -methyl C–H bonds, the formation of the corresponding butenolide took place at the methyl C–H bond.^[140]

3.2. Hydroxylation

The synthesis of phenolic compounds has attracted the interest of chemists since they are a family of compounds showing interesting biological properties, such as anti-inflammatory, antioxidant, antimicrobial, among others,^[141] but they also behave as versatile building blocks in organic chemistry.^[142,143] This led Yu's group to develop a new synthetic route for the hydroxylation of both phenylacetic acids (**130**) and benzoic acids (**132**) to give hydroxylated compounds (**131**) and (**133**), respectively, as summarized in Figure 33. By using $Pd(OAc)_2$ with carboxylpyridone ligand (**122**) they managed to selectively activate the $C(sp^2)$ –H bond, even in the presence of highly reactive cyclopropyl β - $C(sp^3)$ –H bonds. A wide variety of phenylacetic acids (**130**) were tested, those containing electron-donating, electron-withdrawing or unsubstituted led to the desired phenol (**131**) in high yields (66%–87%). In the case of benzoic acids (**132**), the presence of electron-withdrawing groups such as trifluoromethyl required an increase in temperature to 60 °C to achieve good

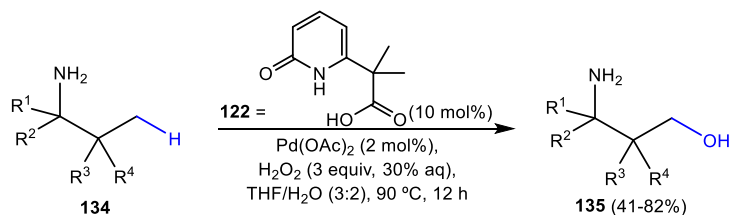


Figure 34. Hydroxylation of primary amines using hydrogen peroxide as the sole oxidant.

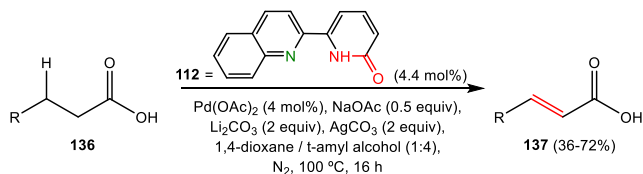


Figure 35. Synthesis of α,β -unsaturated carbonyl compounds by dehydrogenation of aliphatic carboxylic acids.

yields (81%). Meanwhile, using alkyl- or aryl-substituted precursors afforded the corresponding hydroxylated product (**133**) in excellent yields at room temperature (65%–95%).^[144]

In 2023, Yu's group developed a Pd(II)-catalyzed selective γ -C(sp³)-H hydroxylation of primary amines, morpholines and piperidines (**134**) using hydrogen peroxide as the sole oxidant. The presence of the carboxy-pyridone ligand (**122**) is critical for this process, as not only participates in the C–H activation step in a CMD process, but also prevents the formation of the unreactive bis(amine) palladium complex and promotes the oxidation of the alkyl palladium intermediate. A wide variety of amines (**134**) were tested, the presence of alkyl, cycloalkyl, heteroalkyl, aryl or other aromatic substituents led to the γ -hydroxylated amines (**135**) with good yields (41%–82%) as shown in Figure 34.^[145]

3.2.1. Dehydrogenation of Carboxylic Acids

α,β -Unsaturated carbonyl compounds are useful synthetic blocks in organic chemistry, so finding methods that allow their preparation from their saturated precursors is quite desirable.^[146] This led Yu's group to develop a new Pd(II)-catalyzed α,β -dehydrogenation of carboxylic acids (**136**) via a CMD mechanism thanks to the presence of 6-(quinolin-2-yl)pyridin-2-ol (**112**) as a ligand (Figure 35). The formation of a five-membered ring is critical, as the bite angle allows the C(sp³)-H activation of the substrate, but disfavors subsequent C(sp²)-H activation of the olefin product.^[140] A wide scope of carboxylic acids (**136**) was tested. Using linear and branched aliphatic acids such as butyric acid and 4-methyloctanoic acid as substrates led to the formation of the desired α,β -unsaturated acids (**137**) in good yields (76%–82%). Carboxylic acids with ring systems produced the desired product as well with excellent yields (72%–87%). Substrates with protected amines and ethers were tolerated as well, resulting in good yields (67%–79%). Phenylpropanoic acids with a diverse range of substituents produced the α,β -unsaturated acids with moderate yields (42%–85%). The presence of enolizable ketones and esters did not affect

the selectivity of the reaction, as the α,β -dehydrogenation was selective for carboxylic acids, leading to good yields of the desired product (54%–79%). Finally, the dehydrogenation of α -branched carboxylic acids was possible, giving the desired products with good yields (42%–65%).^[140]

Conjugated dienes (**139**) are compounds found in numerous bioactive natural products, such as sorbic acid, Piperine or Trichostatin A.^[147] In addition, they are useful as substrates in various chemical transformations such as cycloadditions, metathesis, ene-reaction, and they are employed as building blocks in polymerization processes as well.^[148] The Yu's group has developed in this area a Pd(II)-catalyzed sequential dehydrogenation of aliphatic acids (**138**) via β -methylene C–H activation (Figure 36). The presence of the quinoline-pyridone (**112**) ligand is crucial for this process, as it allows for the activation of the β - and γ -C–H bonds using a 4:1 mixture of CH₃C(CF₃)₂OH and *tert*-amyl alcohol, leading to the formation of the desired 1,3-dienes (**139**) as shown in Figure 36. A wide scope of aliphatic carboxylic acids (**138**) were evaluated. Linear and branched aliphatic acids, as well as carboxylic acids bearing aliphatic ring systems provided the desired product (**139**) in moderate to good yields (36%–72%). The selectivity of the reaction was not affected by the presence of amines, cyano, ketones or esters, leading to obtain the desired product.^[149]

Seeing the promising results of the catalyzed sequential dehydrogenation of aliphatic acids (**136**) and (**138**), shown in Figures 35 and 36, Yu and coworkers attempted the dehydrogenation of cyclohexyl carboxylic acids (**140**) into benzoic acid derivatives (**141**), as represented in Figure 37. By changing the quinoline-pyridone ligand (**112**), shown previously, to (**115**) (Figure 37) they were able to fully dehydrogenate a variety of substituted cyclohexyl carboxylic acids (**140**).^[149]

In 2023, Yu's group published a new ligand-enabled β,γ -dehydrogenation of free aliphatic acids (**142**), shown in Figure 38. By using the pyridine-pyridone ligand (**126**) or quinuclidine-pyridone ligand (**144**) in presence of the solvent mixture of HFIP/CH₃CN led to the formation of the desired dehydrogenated products (**143**) exclusively. The presence of CH₃CN is critical for the reaction, as in its absence, the β,γ -dehydrogenation did not take place.^[150] A wide variety of cyclic and acyclic carboxylic acids (**142**) were tested. Cyclopentane carboxylic acids α -substituted afforded the β,γ -dehydrogenated products (**143**) with moderated yields (42%–66%). In the cases where additional β,γ -activation sites are available, the β,γ -dehydrogenation took place only in the cyclopentane ring, as this selectivity depends on the ligand's structure. Then, the β,γ -dehydrogenation of biologically and

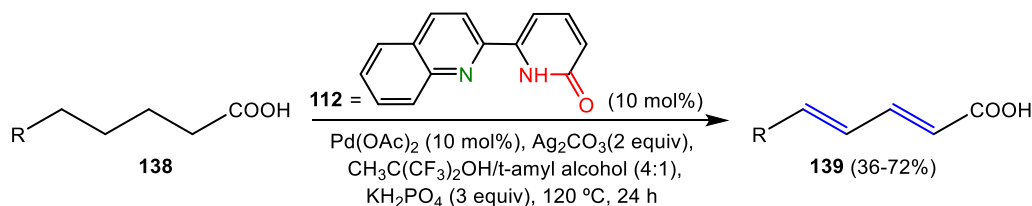


Figure 36. Synthesis of conjugated dienes by dehydrogenation of aliphatic carboxylic acids.

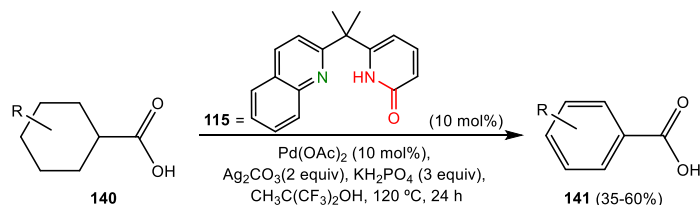


Figure 37. Synthesis of benzoic acids by dehydrogenation of cyclohexyl carboxylic acids.

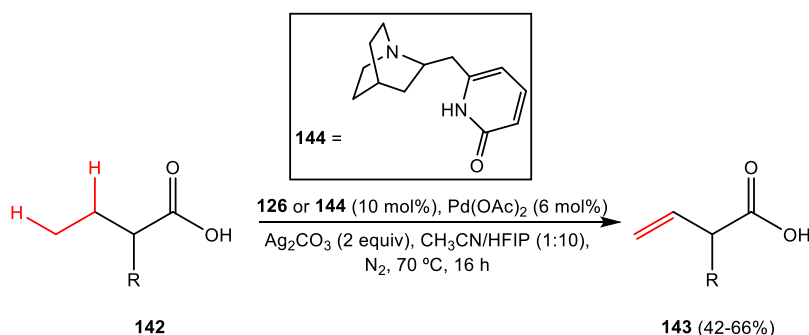


Figure 38. Synthesis of terminal alkenes by β,γ -dehydrogenation of free aliphatic acids.

synthetically significant terpene natural products was tested, resulting in the formation of the desired product with yields up to 99%.^[150]

3.3. Iodination

The presence of amine groups in bioactive compounds is ubiquitous.^[151] Therefore, it is highly desirable to develop new, more efficient methods for their synthesis. In this regard, Li's group developed a new Pd(II) catalyzed meta-C–H iodination of phenethylamines, 2-arylanilines and benzylamines (generally represented as **145**). All amines (**145**) contain two *N*-protecting groups, one of them is the C(O)OEt fragment and the other one is a cyclohexyl-carboxylic acid, which behaves as DG as well. By using Pd(OAc)₂ as a catalyst, 3-nitropyridin-2-ol (**147**) as the ligand, and 1-iodo-4-methoxy-2-nitrobenzene as the iodinating agent, they were able to obtain the desired products (**146**) in high yields, as shown in Figure 39. Moreover, the site-selectivity was excellent, as the competing C–H arylation and para iodination products were found as traces. A wide range of phenethylamines, benzylamines and 2-arylanilines were tested. In the case of phenethylamines, the reaction tolerates the presence of substituents in the ortho and meta positions, affording the desired products in good yields (55%–83%), but the pres-

ence of substituents in the para position led to a decrease in yields (40%–55%). For benzylamines, the scope and yields were generally lower than those from the phenethylamines, as it tolerated only methyl, chloro, bromo and ester substituents. Although the yields and scope were lower, the chemoselectivity was excellent for substituted benzylamines, as only the desired product was formed (42%–63%). Finally, using 2-arylanilines as a substrate led to the meta C–H iodination for substituted 2-arylanilines, however using 2-phenylaniline led to the formation of the di-iodinated product exclusively. The presence of electro-withdrawing groups in the 2-position such as fluoro or chloro were compatible with this method (66%–70%), although electro-donating groups in this position were not tolerated. Meanwhile, substrates with both electro-withdrawing and electro-donating groups in the 3 position were tolerated, leading to the formation of the desired product (64%–67%). Finally, 4-substituted substrates were not tolerated except the methyl group, which led to the desired product with moderate yield (47%).^[152]

3.4. Alkenylation

Heteroarenes are prevalent in many pharmaceutical, agricultural, and natural products, such as *Vismodegib*, *Atazanavir*, or

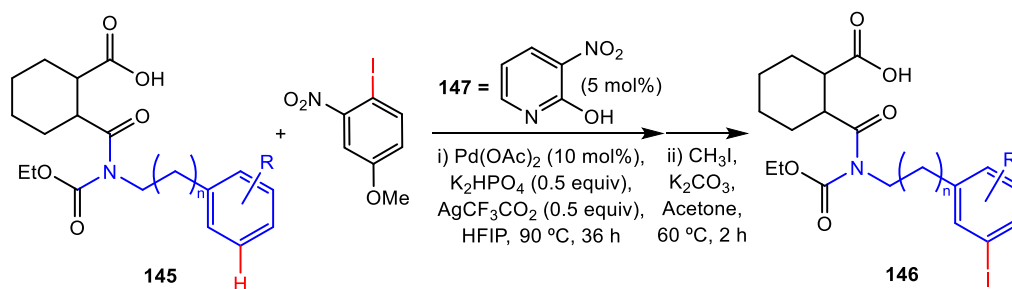


Figure 39. Meta-C–H iodination of a variety of amines promoted by 3-nitropyridin-2-ol.

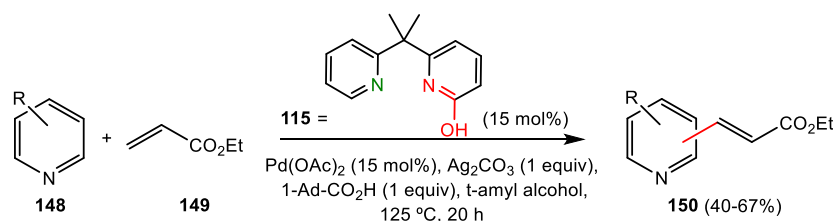


Figure 40. Synthesis of alkenylated pyridines promoted by a pyridin-pyridone ligand.

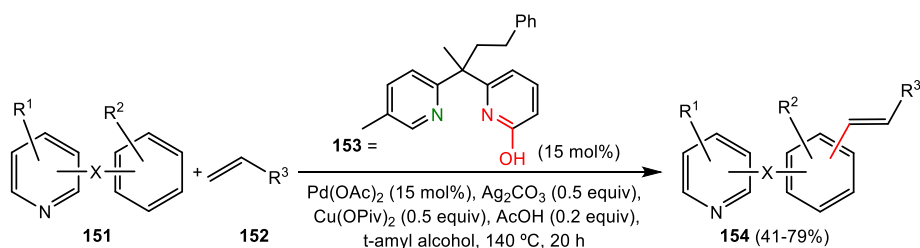


Figure 41. Alkenylation of aryl-heterocycles promoted by a pyridin-pyridone ligand.

Tropicamide.^[153] As such, the development of new, more efficient pathways to their synthesis is desirable. In this regard, Yu's group developed a dual-ligand catalyst for Pd(II)-catalyzed nondirected C–H activation of heteroarenes and heterocyclic biaryls (Figure 40). The use of a six membered chelating pyridine-pyridone ligand (**115**) allowed the C–H activation of the heterocycle via a CMD mechanism and subsequent deprotonation of the pyridine-pyridone ligand by the 3,5-dimethylpyridine or the substrate itself, allowing the olefination of the heterocycle (Figure 40).^[154] A wide range of *N*-containing heterocycles were tested (**148**). Pyridines with both electron-donating and electron-withdrawing groups in the 2- and 3-positions were tolerated, resulting in the formation of the C-3 olefinated product (**150**) as the mayor product in moderate yields (40%–67%). The presence of a substituent on the C-4 position led to a decrease in yields, due to the increased steric hindrance. Using quinolines, pyrimidine or quinoxaline as substrates led to the C-3 olefinated product in moderate yields (42%–57%).^[154]

Seeing the promising results of the C–H olefination of heterocycles, Yu's group decided to expand the scope of the method to biaryls. Using a different pyridine-pyridone ligand (**153**) they were able to olefinate the aryl-pyridines (**151**) to give the alkenylated derivatives (**154**) (Figure 41). Surprisingly, the regioselectivity changes substantially, as the olefination mainly occurs in the aryl group instead of the heterocycle. This can be

explained by the higher electron-density of the aryl group compared to the heterocycle as the catalyst is highly electrophilic.^[154] A wide range of aryl-heterocycles (**151**) were examined. The use of 4-phenylpyridines as substrates afforded the desired product (**154**) in moderate yields (41%–71%). Substituents in the 2- and 6-positions in the heterocycle led to lower yields due to the steric hindrance to the coordinative N-atom. In such cases, adding 3,5-dimethylpyridine led to an increase in yields. The presence of a fluoro group led to the preferential olefination of the C–H bonds in the ortho position relative to the fluoro group. Other aryl-heterocycles, such as isoquinoline-, quinoxaline-, benzo[*c*][1,2,5]-thiadiazole and functionalized quinoline-containing substrates led to the olefinated products (**154**) in moderate to good yields (48%–73%). Substrates containing two pyridine rings, pyrimidines or pyrazoles led to the desired products in moderate yields (56%–67%). Pyridine-containing arenes without an aryl-aryl bond were tested as well, giving the desired product in the cases where the linkage between the pyridine and arene are ester, ether, amine or an alkyl chain (51%–79%).^[154] Finally, the scope of the olefin coupling partners (**152**) was tested. A range of acrylates, acrylamide, vinyl phosphate, and pentafluorostyrene were compatible with this method, leading to the desired products in moderate to good yields (41%–74%). Less reactive olefines, such as styrenes and aliphatic alkenes only produced the desired products in trace amounts.^[154]

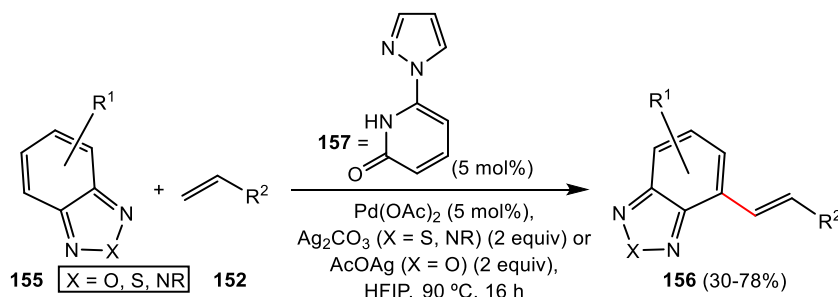


Figure 42. Selective alkenylation of benzofused heterodiazoles promoted by a pyrazole-pyridone ligand.

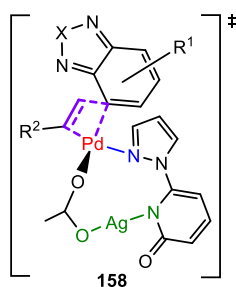


Figure 43. Proposed bimetallic Pd-Ag transition state responsible of the reactivity observed in Figure 42.

In 2024, Joo's group developed a new bimetallic Pd(II)–Ag(I) catalytic system that allows the C–H alkenylation of benzofused 2,1,3-heterodiazoles (**155**) to give the functionalized compounds (**156**) (Figure 42). The presence of the pyrazole-pyridone ligand (**157**) is crucial for the reaction, as it facilitates both the C–H activation through a CMD mechanism and the subsequent migratory insertion due to the coordination of the nitrogen of the pyrazole group to the palladium atom, the coordination of the pyridone nitrogen atom to the silver atom and a π – π stacking interaction between the substrate and the pyridone, as shown in the transition state **158** (Figure 43) proposed by Joo et al.^[155] A range of 2,1,3-benzofused heterodiazoles was tested (**155**). Substrates containing methyl or halogen groups produced the desired product (**156**) in moderate to good yields (30%–78%). When a phenyl group was present in the 2,1,3-benzofused heterodiazoles, both the phenyl and benzofused rings were alkenylated, with preference for the benzofused ring.^[155] Finally, the scope of alkenes (**152**) was tested. Substrates containing acrylates, acryl amides, acrolein, and vinyl phosphonate afforded the expected products in moderate to good yields (37%–76%). Moreover, even though 1,2,3,4,5-pentafluoro-6-vinylbenzene provided the desired product in moderate yields (31%–39%), unsubstituted styrene was not suitable for this process.^[155]

Also in 2024, Yu and collaborators designed a new palladium-catalyzed meta and para C–H olefination of silyl-protected phenols (**159**), process shown in Figure 44. The use of 2-nitro-5-trifluoromethylpyridone (**160**) allowed para-olefination with high selectivity. Meanwhile, using pyridine-pyridone ligand (**115**) combined with 3,5-dimethylpyridine, they were able to selectively olefinate the meta position with high selectivity. The presence of 3,5-dimethylpyridine is crucial for the meta-olefination process, as in its absence the reaction does not take place.^[156] A

wide variety of alkenes (**152**) were tested for the para-olefination reaction. Alkenes with electron-withdrawing groups, such as acrylates, amides, ketones, sulfone, sulfonamide, phosphonate, or 1,2,3,4,5-pentafluoro-6-vinylbenzene led to the desired para olefinated products (**161**) with excellent selectivity in moderate to good yields (39%–80%). However, using tert-butyl acrylate as a substrate did not afford the desired product. The scope of protected phenols (**159**) was evaluated as well. Ortho substituted phenols provided the para olefinated products with excellent para selectivity in moderate to good yields (37%–80%). 1,3-disubstituted substrates afforded the desired para olefinated products instead of the less hindered meta position in moderate yields (38%–50%) and good selectivity.^[156] Concerning the alkenes (**152**) tested for the meta-olefination reaction, acrylates, vinyl amides, vinyl ketones, and vinyl phosphonates afforded the desired meta-olefinated products (**162**) with good meta-selectivity in good yields (43–74%). Meanwhile, using alkenes containing sulfonamide, sulfone substituents and 1,2,3,4,5-pentafluoro-6-vinylbenzene as substrates resulted in low yields for meta-olefination. Phenols (**159**) with substituents in the meta positions were all tolerated, affording the meta-olefinated products in moderate yields (39%–62%). The presence of various substituents in the ortho position led to a decrease in selectivity. Finally, the presence of bulky substituents in the para position dramatically reduced the reactivity.^[156]

3.5. Arylation

As noted earlier, the functionalization of carboxylic acids is an area of great interest, since they are very common, accessible and generally inexpensive raw materials. In this regard, Yu's group developed a Pd(II)-catalyzed β -C(sp³)–H arylation of free aliphatic acids (**163**) (Figure 45). The use of a five-membered chelate quinoline-pyridone ligand (**112**) promoted the β -methylene C–H cleavage.^[157] The scope of the aryl iodides (**120**) was tested, showing that the presence of substituents in either the ortho-, meta- or para- positions afforded the desired β -methylene arylation product (**164**) in moderate yields with both electron-donor and electron-withdrawing groups (40%–63%). Disubstituted phenyl iodides and heteroaryl iodides were tolerated as well, providing the desired products in moderate yields (37%–56%). The scope of carboxylic acids (**163**) shows that aliphatic carboxylic acids, both linear and branched, as well as those containing cycloalkyl groups, afforded the desired

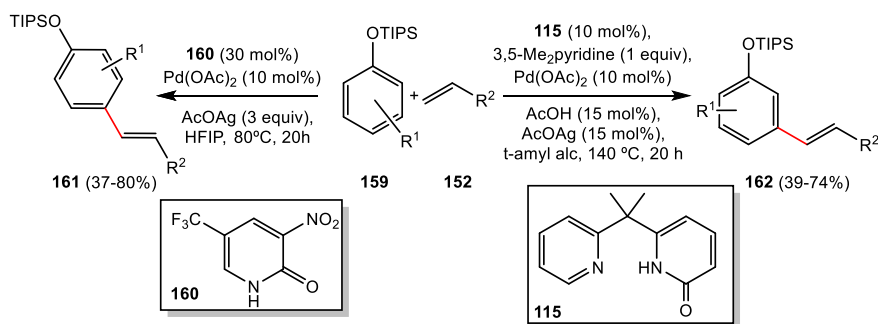


Figure 44. Orthogonal synthesis of *meta*-/para alkenylated silyl-protected phenols depending of the pyridone ligand.

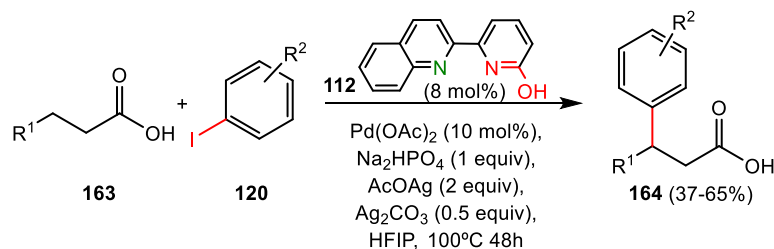


Figure 45. Arylation of linear aliphatic carboxylic acids.

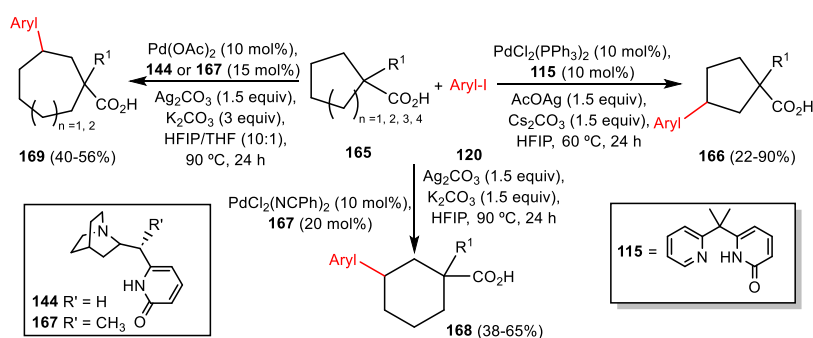


Figure 46. Selective γ -transannular arylation of different cycloalkane carboxylic acids.

β -methylene arylation product (**164**) in moderate yields (40%–65%). Phenylpropanoic acids, both unsubstituted or bearing chloro or trifluoromethyl substituents provided the desired product with moderate yields (40%–44%). Finally, the presence of enolizable ester and ketones was tolerated, leading to the β -methylene arylation product in moderate yields (42%–55%).^[157]

In 2022, Yu's group developed a new methodology for γ -selective transannular C–H arylation of cycloalkane carboxylic acids (Figure 46). The combination of a Pd(II) catalyst with a pyridone ligand, such as **115**, **144**, or **167** allows the transannular γ -arylation of cyclopentane, cyclohexane, cycloheptane, and cyclooctane rings (**165**) containing carboxylic acids by treatment with aryl iodide (**120**), as shown in Figure 46. The α -aryl and α -alkyl substituted cyclopentane carboxylic acids (**165**) afforded the desired transannular γ -arylation product (**166**) in good to excellent yields (45%–90%). The presence of functional groups such as ether, ester or chloride in α -alkyl substituted substrates was well tolerated. However, bicyclic carboxylic acids afforded the desired product in moderate yields (22%–34%). Moreover, carboxylic acids containing an heteroatom in the α -position were

poor substrates for the reaction. Next, a wide range of cyclohexene carboxylic acids (**165**) were tested, which required using quinuclidine-pyridone ligand (**167**) to increase the yields. The α -methyl, α -ethyl and α -aryl substituted cyclohexane acids provided the desired product (**168**) in moderate to good yields (47%–65%). The presence of two methyl groups in the γ -position afforded the desired γ -arylation product in modest yields (38%). Moreover, using 4-propyltetrahydro-2H-pyran-4-carboxylic acid as a substrate led to the desired product in 39% yield, proving that this methodology is a viable pathway for the functionalization of some heterocyclic carboxylic acids. A variety of 7- and 8-membered cycloalkane carboxylic (**165**) acids containing α -alkyl chains with functional groups such as ether, ester or chloride provided the expected γ -arylation product (**169**) in moderate yields (40%–56%) as shown in Figure 46.^[158] The scope of aryl iodides (**120**) shows that para substituted aryl iodides with both electron-donor and electron withdrawing substituents were tolerated affording the γ -arylation product in good yields (55%–85%). Ortho and meta-substituted substrates were compatible as well, providing the desired product in good

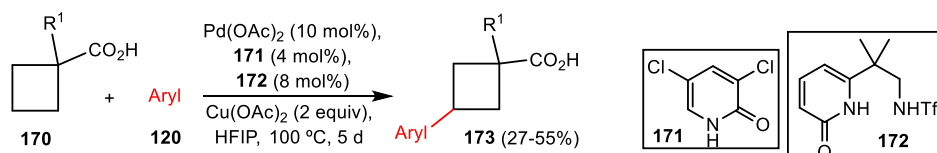


Figure 47. Synthesis of γ -arylated cyclobutane carboxylic acids.

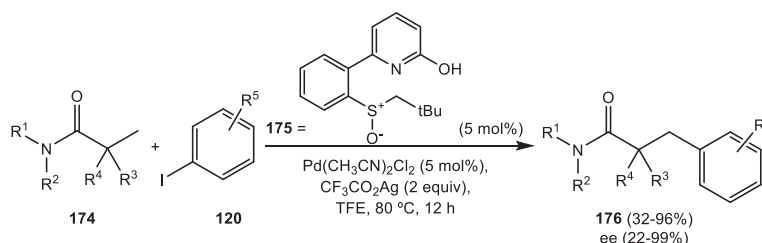


Figure 48. Enantioselective β -C(sp^3)-H arylation of aliphatic tertiary amides.

yields (67%–84%). Next, a variety of 2- and 2,3- substituted 4-iodopyridines were tested, which resulted in the formation of the γ -arylation product in moderate to excellent yields (51%–87%). Other heterocycles, such as pyrimidine, quinoline, quinoxaline, thiophene and benzothiazole led to the formation of the expected product in moderate to good yields (38%–78%). Unfortunately, substrates containing phenols, carboxylic acids or anilines were not tolerated.^[158]

Seeing the promising results of the γ -selective transannular C–H arylation afforded for cyclopentane carboxylic acids, Yu and collaborators decided to expand this methodology to cyclobutane carboxylic acids (**170**). However, using the conditions developed for cyclopentane carboxylic acids resulted in the β -arylation product exclusively. This led them to change the aryl iodide (**120**) with an in situ generated aryl palladium species, resulting in the net cross-coupling of two C–H bonds and affording the 1,3-cyclobutane (**173**) (see Figure 47).^[159] The intermediate aryl-Pd species is generated via a non-directed C(sp^2)-H bond activation thanks to the presence of 3,5-dichloropyridin-2(1H)-one (**171**). Meanwhile, pyridone ligand (**172**) accelerates the C(sp^3)-H bond activation of the carboxylic acid substrate. The presence of both pyridone ligands (**171**) and (**172**) is critical for the reaction to take place. With the new conditions in mind, the scope of cyclobutane carboxylic acids (**170**) was tested, showing that α -alkyl substituted cyclobutane carboxylic acids afforded the desired γ -arylated products (**173**) in poor moderate yields (27%–39%). The scope of arenes (**120**) showed that arenes with electron-donating groups provided the desired product (**173**) in moderate yields (48%–55%). Meanwhile, using arenes with electron-withdrawing groups as coupling partners resulted in lower yields (39%–40%). The selectivity of the reaction was modest, biasing towards the meta- and para- positions of the arene. The ortho position was not favored except with electronically biased arenes.^[159]

In 2023, Jiao's group developed a new Pd(II)-catalyzed enantioselective β -C(sp^3)-H arylation of aliphatic tertiary amides (Figure 48).^[160] The use of a sulfoxide-2-hydroxypyridine (**175**) accelerates the C–H activation step, which is responsible for the enantioselectivity of the reaction. A wide range of amide sub-

strates (**174**) were tested and the results strongly depend of the substituents in the substrates. *N*-alkyl disubstituted amides provided the desired β -arylation products (**176**) in good to excellent yields (68%–86%) with high enantioselectivity (ee = 90%–96%). However, primary and secondary amides resulted in low yields (11%–25%) and low ee. Using α -substituted amides afforded the desired products in good to excellent yields (40%–96%), however, the β -arylation products of propionamide and pivalamide were obtained with low enantiomeric excess (22%). Moreover, amides without a methyl β -C(sp^3)-H bond showed no reactivity. The use of cyclobutanecarboxamide and cyclopropanecarboxamide as substrates afforded the expected β -arylation products in excellent yields (40%–95%) with good enantioselectivity (85%–95%). The analysis of the scope of the aryl iodide (**158**) showed that aryl iodides containing electron-donor groups afforded the desired products in good yields (56%–72%) with excellent enantiomeric excess (82%–99%). Electron deficient aryl iodides provided the expected products with excellent enantioselectivity (93%–99%) but reduced yields (42%–75%). The use of ortho-substituted aryl iodides afforded the desired β -arylation products with excellent enantiomeric excess (94%) but diminished yields (32%).^[160]

In a later study, Jiao's group proposed a γ -C(sp^3)-H arylation of free primary aliphatic amines (**177**) by using the same sulfoxide-2-hydroxypyridine ligand (**175**) used for the β -C(sp^3)-H arylation of aliphatic tertiary amides (Figure 49).^[161] The scope of amines (**177**) showed a general reaction, where α -alkyl substituted amines gave the γ -arylation products (**178**) in good yields (67%–82%). However, even though the 2,6-difluorophenyl group was tolerated (64% yield), α -phenyl substituted amines were not compatible. Substrates with two equivalent methyl γ -C(sp^3)-H bond provided a mixture of both mono- and diarylated products with the former as the major product in good yields (79%–88%). Moreover, cycloalkylamines provided the desired γ -arylation products with good yields (68%). Using amino acid esters resulted in the formation of the γ -arylation products with good yields (65%–85%) and good chirality retention. Expanding the scope to secondary and tertiary amines did not provide the expected arylation. The scope of aryl iodides (**158**) shows that

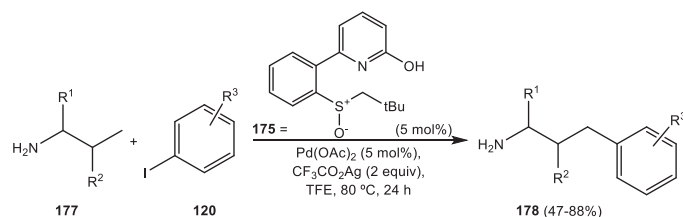


Figure 49. Selective γ -C(sp³)-H arylation of free primary aliphatic amines.

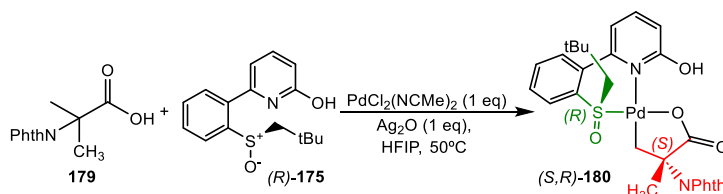


Figure 50. Isolation of the the key palladacycle responsible for the enantioselectivity of the Pd(II)/sulfoxide-2-hydroxypyridine catalytic system shown in Figure 49.

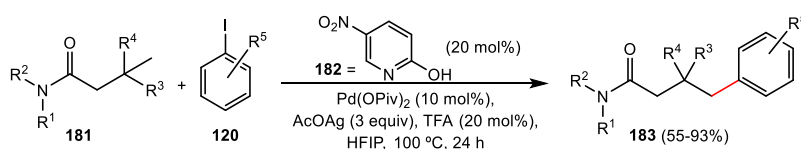


Figure 51. Selective γ -arylation of aliphatic tertiary amides.

substrates containing halogen, sulfonate, ester, trifluoromethyl, and nitro afforded the desired γ -arylation products in moderate to good yields (47%–82%). Moreover, heteroaryl iodides were tolerated as well, providing the expected product in good yields (63%–71%).^[161]

In 2024, Jiao's group isolated the key palladacycle intermediate responsible for the enantioselectivity of the Pd(II)/sulfoxide-2-hydroxypyridine (**175**) catalytic system for asymmetric C(sp³)-H functionalization reactions, which is shown in Figure 50. Using 2-amino-isobutyric acid derivative (**179**), (*R*)-sulfoxide-2-hydroxypyridine, and PdCl₂(NCMe)₂ (*(R)*-**175**) in stoichiometric quantities they obtained palladacycle (*S,R*)-(**180**) in excellent diastereomeric ratio (90:10) (Figure 50). The C(sp³)-H activation via CMD is the enantioselectivity-determining step as the subsequent steps occurred with nearly complete retention of stereochemistry.^[162]

In a later study, Maiti's group developed a Pd-catalyzed distal γ -arylation of aliphatic tertiary amides (Figure 51). Using pyridone ligand with electron-withdrawing groups, such as 2-hydroxy-5-nitro pyridine (**182**), promoted the cleavage of the γ -C—H bond in the amide substrate (**181**) via a CMD mechanism. The presence of silver acetate lowers the required energy for the C—H activation, which is the RDS, by forming a [Pd—Ag] species where the Pd—Ag bonding provides additional stability through the reaction.^[163] The scope of the aryl iodides (**120**) showed that precursors containing ester, aldehyde, ketone, cyano or SO₂NEt₂ groups in the para-position afforded the desired γ -arylation product (**183**) in good yields (55%–91%). Moreover, meta-substituted aryl iodides containing fluor or ketone groups also produced the desired product in

good yields (75%–83%), although using 1-(2-iodophenyl)ethan-1-one resulted in the formation of the homocoupled biaryl product. Additionally, heteroaryl iodides, such as substituted furans, thiophenes, and quinolines provided the γ -arylation product in good yields (70%–75%). Next, a wide variety of *N,N*-disubstituted amides (**181**) were tested. Symmetrical and unsymmetrical *N,N*-dialkyl substituted amides with both linear and branched aliphatic chains afforded the expected products in good to excellent yields (65%–91%). Amides with *N,N*-cyclohexyl, cyclopentyl, and cyclobutyl substituents afforded the γ -arylation products in excellent yields (75%–93%). Moreover, using pyrrolidine, piperidine, and azepane-derived amides as substrates resulted in the expected γ -arylation products in excellent yields (85%–92%). However, indolyne-amide did not produce the desired γ -arylation product. Finally, a wide range of β -substituted amides were tested (**181**). Substrates containing alkyl groups, such as ethyl, iso-butyl, and 2-butane were tolerated affording the monoarylated product from the methyl C(sp³)-H bond functionalization.^[163]

Peptides-based drug development has experienced great progress during the last decades, as they have revolutionized the treatment of various diseases, such as type-1 diabetes.^[164,165] Yao's group has contributed to this field developing a new ligand-enabled, cysteine-directed, alanine β -C(sp³)-H arylation for linear, and cyclic peptides (**184**) as shown in Figure 52. The use of a pyridone ligand with electron-withdrawing groups for linear peptides or with an electron-donating group for cyclic peptides, as well as a *S*-alkyl cysteine residue as a DG was crucial for the reaction to take place.^[166] As in previous cases, the scope of aryl iodides (**120**) was screened using 5-(trifluoromethyl)-

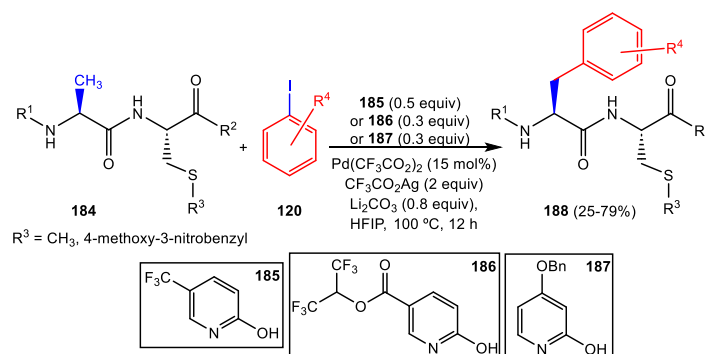


Figure 52. Selective β -C(sp³)-H arylation of the alanine fragment in linear and cyclic peptides using aryl iodides.

2-hydroxy-pyridine (**185**) as a ligand. Aryl iodides containing either electron-withdrawing or electron-donating substituents in the meta- or para- positions afforded the alanine β -arylation products (**188**) in moderate yields (42%–60%). However, ortho-substituted aryl iodides were not reactive, due to the steric hindrance afforded by the substituent. Moreover, bicyclic aryl groups, such as 5-indolyl and 2-naphthyl provided the expected β -arylation products in moderate yields (43%–50%). Using another peptide derivative, such as a 4-iodobenzamide tethered dipeptide, afforded the expected product in good yields (66%).

Other alanine-S-methyl-cysteine containing tripeptides (**184**) were successfully β -arylated in moderate to good yields (36%–58%).^[166] Next, a wide range of complex linear peptides containing up to 9 residues (**184**) were attempted. For these types of peptides, 1,1,1,3,3,3-hexafluoropropan-2-yl 6-hydroxynicotinate (**186**) was used as the ligand, as it provided better yields. Amino acids containing nonpolar side chains, such as glycine, valine, leucine, isoleucine, *tert*-leucine, alanine, phenylalanine, proline, tyrosine, threonine, and methionine were tolerated, affording the desired β -arylated products in moderate yields (25%–63%). However, amino acids with strongly coordinating chains, such as tryptophan or 4-benzyl aspartic acid required the use of a suitable protecting group to achieve acceptable yields (56%–59%).^[166] Additionally, the scope of cyclic peptides (**184**) was examined. These peptides required the use of cysteine with a 4-methoxy-3-nitrobenzyl protecting group as the DG and 4-(benzyloxy)pyridin-2-ol (**187**), an electron-rich pyridone as a ligand for optimal results. Residues containing up to nine peptides were β -arylated in the alanine-cysteine with moderate yields (35%–79%). Cyclic peptides containing unnatural β , γ , δ , and ϵ -amino acid residues exhibited similar reactivities, affording the desired product in moderate yields (45%–64%).^[166]

In 2024, Maiti and collaborators proposed a new approach for the thioarylation of long-chain alkyl picolinamides orthogonally between γ and δ positions (see Figure 53). The selectivity between the distal δ and γ C–H bond comes from the pyridone ligand used. Pyridones with electron-withdrawing groups, such as 5-methyl-3-nitropyridin-2-ol (**160**) or 5-nitropyridin-2-ol (**190**), make the palladium center more electron deficient, skewing the selectivity towards γ -functionalization. However, using a pyridone with electron-donating substituents, such as 4-(benzyloxy)pyridin-2-ol (**187**) changes the selectivity, leading to the δ -functionalization product.^[167] A wide range of picol-

inamides (**189**) and disulfides were tested. Using 5-methyl-3-nitropyridin-2-ol (**160**) or 5-nitropyridin-2-ol (**190**) as ligands they were able to obtain the γ -thioarylation product (**191**) in moderate yields (30%–70%) with moderate γ -selectivity (δ : γ from 1:1.5 to 1:8.5). However, using 4-(benzyloxy)pyridin-2-ol (**187**) led to the δ -thioarylation product (**193**) in lower overall yields (30–50) and moderate γ selectivity (δ : γ from 1:1 to 2.8:1)^[167] (Figure 54).

Hydroxylamines (**194**) derived from benzyl and phenylethyl alcohols are found in common bioactive molecules, such as Tolvaptan, Tramadol, Siponimod, and so on.^[168–170] This led Yu's group to develop a Pd-catalyzed meta-arylation of alcohol-derived oxime ethers. The presence of 3-trifluoromethyl pyridone (**155**) as a ligand is crucial for accelerating this reaction. First, the scope of aryl iodides (**120**) was screened and it showed that para substituted substrates (**120**) containing either electron-donor or electron-withdrawing substituents afforded the desired meta arylation products (**195**) in good yields (40%–84%), as shown in Figure 54. Moreover, meta substituted aryl iodides were tolerated resulting in the formation of the arylated product in good yields (64%–69%). Next, a wide range of phenylethyl alcohol-derived oxime ethers (**194**) were tested. Substrates containing electron-donor and electron-withdrawing groups resulted in the desired meta-arylated products (**195**) in good yields (43%–76%). Moreover, the thiophene ring was able to be arylated, but it resulted in lower yields (52%) due to the stability of the substrate under the reaction conditions. Substrates containing α - and β -substituents provided the meta arylation products in good to excellent yields (50%–87%). The scope of benzyl alcohols was also screened, showing that substituted substrates afforded the meta products in good yields (57%–83%).^[171]

Aminophosphonic acids exhibit biological activity^[172] as well as possessing an outstanding coordination chemistry as ligands, which finds them useful in organometallic catalysis.^[173] This led Yang's group to develop a new TDG-directed methodology for the Pd-catalyzed γ -C(sp³)-H arylation of tetrasubstituted α -aminophosphonates.^[174] However, they found out that this methodology is not applicable to trisubstituted α -aminophosphonates, due to the strong coordination of the amino group to the palladium, as well as due to the Thorpe-Ingold effect.^[175] To overcome this limitation, the reaction was carried using Pd(OAc)₂ with pyridine-2-ol (**197**) as an additive. With these conditions, the γ -C(sp³)-H arylation of trisubstituted α -aminophosphonates (**196**) became feasible (Figure 55).^[174] A

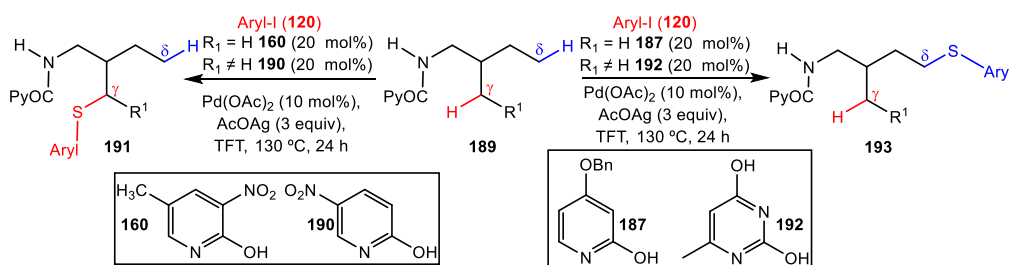


Figure 53. Orthogonal γ - or δ -thioarylation of alkyl picolinamides depending of the combination of ancillary ligands.

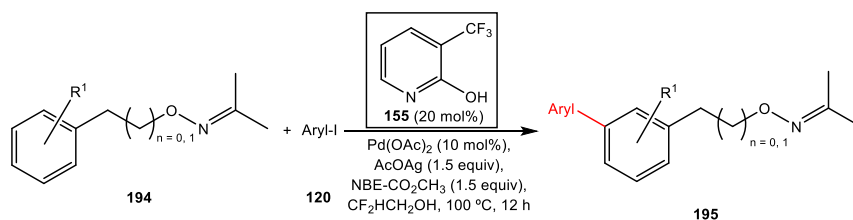


Figure 54. Selective Pd-catalyzed meta arylation of alcohol-derived oxime ethers.

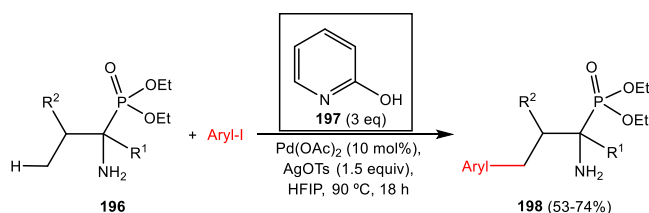


Figure 55. γ -C(sp³)-H arylation of tetrasubstituted α -aminophosphonates.

wide range of aryl iodides (**120**) were tested. Para-iodobiphenyl substrates containing alkyl, aryl or bromide substituents afforded the desired γ -arylation products (**198**) in good yields (76%). Moreover, substrates containing bulky substituents were tolerated, resulting in the formation of the desired products in moderate to good yields (53%–74%). However, aza-aromatic iodides were not compatible with the reaction conditions.^[174]

In 2024, Ge's group developed a new strategy for the β -arylation of tertiary aldehydes. Using Pd(OAc)₂ as a catalyst in the presence of 2-nitro-5-trifluoromethylpyridone (**160**) as a ligand and 2-amino-2-phenylacetic acid as a transient DG they were able to selectively activate the β -C(sp³)-H bond via a CMD mechanism (Figure 56).^[176] First, the scope of aryl iodides (**120**) was tested. Aryl iodides containing electron-withdrawing groups in the meta- or para- positions afforded the desired mono- (**200**) and di- β -arylated products (**201**) in good yields (mono-arylated (**200**): 46%–75%, di-arylated (**201**): 10%–32%). Moreover, aryl iodides containing natural products derivatives, such as menthol and fenchol provided the β -arylation products in moderate yields (mono-arylated: 38%–50%, di-arylated: 24%–30%). However, aryl iodides with electron-donor substituents required the use of a different pyridone ligand and transient DG. Using 5-trifluoromethylpyridone as a ligand and 2-aminoacetic acid as the transient DG led to the desired β -arylation products in moderate to good yields (mono-arylated: 30%–66%, di-arylated: 22%–51%). Next, a wide range of aliphatic aldehydes (**199**) were

tested. Aldehydes bearing a cyclohexyl group and α -methyl- α,α -dialkyl acetaldehydes afforded the β -mono-arylated products (**200**) in good yields (55%–67%). Moreover, using α -aryl- α,α -dimethyl acetaldehydes as substrates resulted in the formation of β -mono-arylated products exclusively in moderate yields (50%–61%). Furthermore, acetaldehydes containing an α -ether substituent were tolerated as well, providing the desired mono- and di- β -arylation products in moderate yields (mono-arylated: 53%–57%, di-arylated: 12%–18%). Finally, non- α -quaternary aldehydes were not tolerated.^[176]

In a recent study, Albéniz's group proposed a new strategy for functionalization of simple arenes using Pd(OAc)₂ with a mixture of a bipyridone ligand (**204**) and a phosphine (PCy₃) (Figure 57). The mixture of both ligands has a beneficial effect on the reaction, as it is accelerated compared to the Pd(OAc)₂-bipyridone system. They proposed that this acceleration comes from a synergistic Pd–Pd mechanism, where two catalytic cycles operate. In the first one, a Pd/phosphine system where the oxidative addition of the aryl halide (**203**) and the reductive elimination of the product take place. In the second one, the C–H activation of the arene (**202**) catalysed by the Pd/bipyridone (**204**) via a CMD mechanism occurs. Both cycles are connected via transmetalation of the aryl group from the Pd/bipyridine system to the Pd/phosphine system.^[177] The scope of aryl halides (**203**) coupling partners was screened. Aryl bromides and aryl chlorides containing either electron-donating or electron-withdrawing groups in the para- position were tolerated, affording a mixture of ortho, meta and para arylation products (**205**) in excellent yields (X=Br: 69%–84%, X=Cl: 71%–76%). Using ortho substituted substrates, such as 1-bromo-2-(trifluoromethyl)-benzene resulted in a reduction in yields (25%). Moreover, para bromobenzoic acid and para bromobenzonitrile were not tolerated due to their coordinating ability. Next, the scope of arenes (**202**) was tested. *N,N*-dimethylaniline, ethyl benzoate, and trifluoro-toluene afforded the desired arylation products in good yields (X=Br: 59%–75%) with preference for

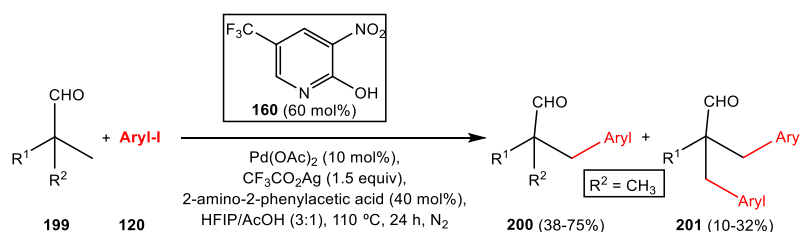


Figure 56. Synthesis of mono- and di- β -arylated tertiary aldehydes.

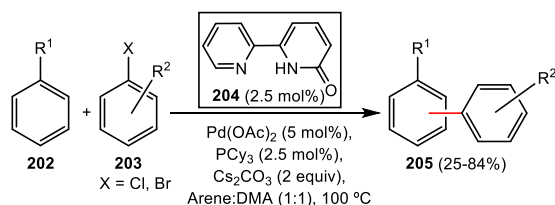


Figure 57. C–H arylation of simple arenes.

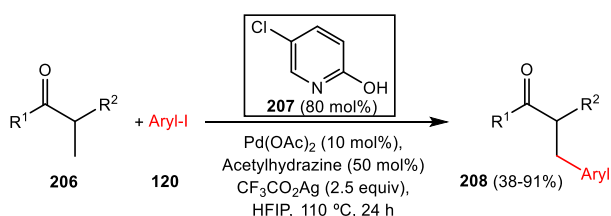


Figure 58. Synthesis of β -arylated aliphatic ketones by Pd-catalyzed C(sp³)–H functionalization.

the *meta*- isomer. However, fluorobenzene and anisole provided the *ortho*-arylation product as the major isomer in good yields (X=Br: 75%–81%). Using pyridine as substrate afforded the *meta*-arylation product exclusively with 63% yield. Finally, using aniline as substrate resulted in the formation of the C–N arylation product as the only product.^[177]

In 2025, Jiang's group developed a palladium-catalyzed β -C(sp³)–H arylation of aliphatic ketones (**206**) using acetylhydrazine as a transient director group and 5-chloropyridin-2-ol (**207**) as ligand, which is shown in Figure 58. Ethylalkylketones (**206**) afforded the desired β -arylation products (**208**) in moderate to good yields (43%–91%). However, ketones (**206**) containing various β -methyl groups promoted the formation of both mono- and di- β -arylation products in moderate yields (mono-arylated: 53%–55%, di-arylated: 14%–24%). Cyclic ketones with an α -methyl group afforded the β -arylated products in excellent yields (84%). Furthermore, ketones with α -cyclobutyl or cyclohexyl substituents led to the formation of the desired products in moderate yields (56%–72%). The scope of aryl iodides (**120**) was also evaluated. Precursors containing electron-withdrawing groups afforded the β -arylated products (**208**) in moderate yields (38%–66%). Moreover, iodides (**120**) containing methoxy- or methoxycarbonyl- substituents in the *ortho*-position led to the formation of the β -arylated products in moderate to good yields (45%–78%).^[178]

The use of pyridone-type ligands in Pd-catalyzed C–H functionalization processes, either alone or in dual combination with

other ligands has led to a parallel development to that described for MPAA ligands, although it has not yet been as extensive as that seen with amino acids. This parallelism is largely due to the fact that the molecular fragment responsible for reaction acceleration is closely related (a carbonyl group bonded to a nitrogen) and that pyridone ligands can also be equipped with chiral auxiliaries to render the reaction stereoselective. Therefore, in principle, the same processes described for MPAA ligands should be achievable. However, they are less commonly used, perhaps due to the greater difficulty in their synthesis. The task for the immediate future is clear: to improve access to this type of ligand and to expand the range of processes in which enhanced activity and selectivity are observed.

4. Pyridines and Related N-Heterocycles

4.1. Macrocyclization

Spirocyclic scaffolds, composed of two or more rings connected through an sp³-hybridized carbon atom, display unique molecular features such as three-dimensionality, rigidity, and restricted rotation around the spiro center. These characteristics make them privileged structures in medicinal and synthetic chemistry. Among the various spiro motifs, nitrogen-containing heterocycles—commonly referred to as spirodiamines—have attracted significant attention over the years. Despite their promising structural properties, the inertness and conformational flexibility of C(sp³)–H bonds present major challenges for selective functionalization, often leading to undesired side reactions such as (n + 2) heterocycle formation. In this context, Pd-catalyzed C(sp³)–H functionalization emerges as a powerful and suitable strategy to overcome these limitations and achieve efficient modification of spirocyclic frameworks.

In 2023, Dutta and Jeganmohan reported an efficient method for synthesizing bicyclic spirodiamine compounds (**212**) via a Pd-catalyzed β -C(sp³)–H functionalization of maleimides.^[179] A broad range of alkyl amides (**209**) were reacted with maleimides (**210**) in the presence of Pd(OAc)₂ (10 mol%), quinoline (**211**) (30 mol%), and Cu(OAc)₂·H₂O (Figure 59). During reaction optimization, it was observed that both the nature of the substituent on the quinoline ligand and the directing group (DG) attached to the nitrogen donor atom significantly influenced the reaction's efficiency. Notably, *N*-aryl and *N*-alkyl maleimides (**210**) as electron-deficient olefins promoted the migratory insertion step by enhancing the maleimide's role as a Michael acceptor. Among

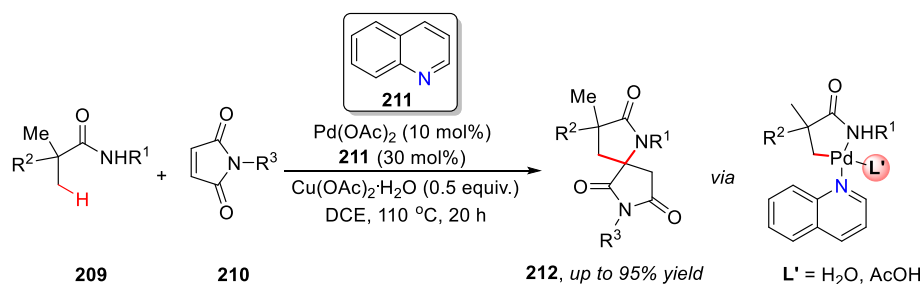


Figure 59. Synthesis of bicyclic spirodiamines and proposed key reaction intermediate.

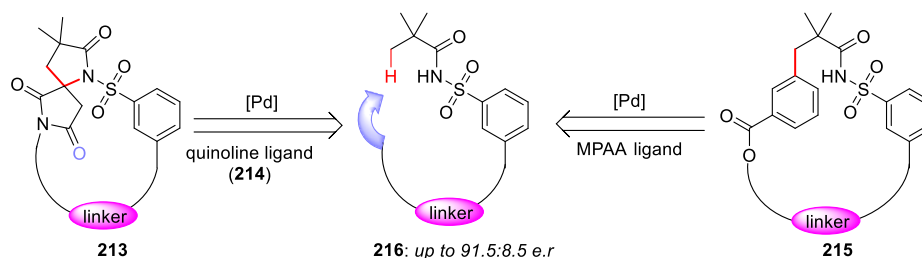


Figure 60. Synthesis of pseudo-natural macrocyclic sulfonamides.

these, *N*-phenyl maleimides provided higher yields than *N*-alkyl variants, owing to their greater electrophilicity, which facilitated a more rapid and efficient insertion. Initially, the quinoline ligand (211) coordinates with the palladium center to form an active Pd(II) species. This species then interacts with the substrate, enabling β -C(sp³)-H activation directed by the sulfonylamide group, generating the key intermediate shown on the right side of Figure 59. Subsequently, the maleimide (210) acts as an electrophile and undergoes migratory insertion into the Pd-C bond, forming a seven-membered palladacycle. This intermediate then undergoes β -hydride elimination, followed by reductive elimination, completing the catalytic cycle, and regenerating the Pd(II) catalyst.^[179]

Building on the previously described mechanistic framework, Yang and co-workers reported in 2024 a Pd(II)-catalyzed C(sp³)-H macrocyclization of substrate (216) to access pseudo-natural macrocyclic sulfonamides (213) as shown in Figure 60.^[180] These macrocyclic structures exhibit promising therapeutic potential, particularly for the treatment of Parkinson's disease. The use of quinoline derivatives bearing electron-donating groups, such as 4-methylquinoline (214), played a key role in stabilizing the Pd(II) catalytic species via an *N*-monodentate coordination mode. This stabilization enhanced catalytic reactivity, enabled enantioselective macrocyclization and helped overcome the inherent inertness of C(sp³)-H bonds—a major challenge in such transformations. A variety of macrocyclic scaffolds (213) were successfully synthesized, including peptide-based macrocycles and complex architectures reminiscent of natural products like Rapamycin.

4.2. Isomerizations

In 2024, Kuo et al. developed innovative “shapeshifting” ligands designed to modulate the Lewis acidity of dicationic Pd(II) species.^[181] These ligands dynamically stabilize the posi-

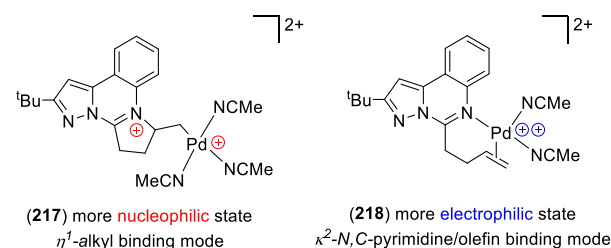


Figure 61. Application of “shapeshifting” ligands, based on a pyrimidine fragment and an alkene group.

tive charge through a reversible coordination mechanism, owing to their unique structure that incorporates both a pyrimidine fragment and an alkene moiety. As illustrated in Figure 61, the ligands can adopt two distinct coordination modes that exist in dynamic equilibrium. In one coordination mode (218), the ligand binds through the pyrimidine nitrogen and the alkene via a κ^2 -N,C pyrimidine/olefin bonding mode. This arrangement does not fully neutralize the Pd center's positive charge, leaving it highly electrophilic (Figure 61, right side). In the alternative coordination mode (217), the pyrimidine nitrogen intramolecularly attacks the alkene, forming a C-N bond and generating an ammonium-type nitrogen center. This results in a positively charged nitrogen and a neutral alkyl group that binds to the metal in a κ^1 -alkyl fashion (Figure 61, left side). In this mode, part of the Pd(II) positive charge is effectively shifted to the nitrogen atom, rendering the Pd center less electrophilic—or more nucleophilic. This dynamic charge redistribution enables the Pd catalyst to switch reversibly between a nucleophilic, charge-separated state, (217) and an electrophilic, charge-localized state (218). These ligands effectively mask the electrophilicity of Pd(II) without compromising its catalytic activity, by reversibly forming and cleaving C-N bonds to modulate the electronic environment. DFT calculations supported this mechanism, demonstrating that the ligand inter-

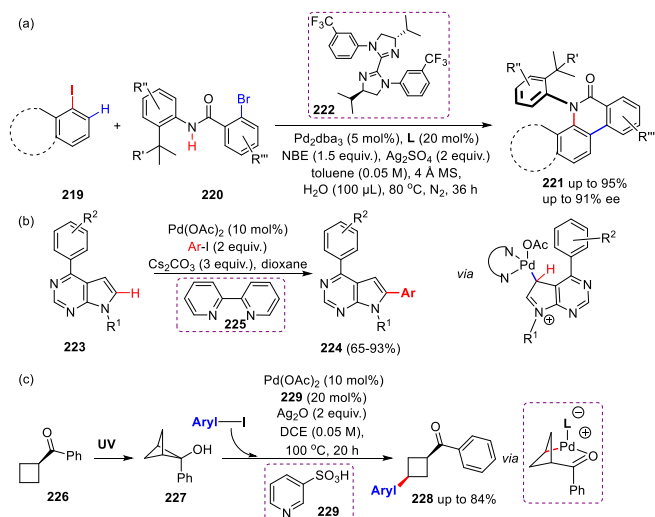


Figure 62. Synthesis of enantiomerically enriched phenanthridinones by (a) chiral Catellani reaction; (b) arylation of pyrrolo[2,3-*d*]pyrimidines, and of bicyclo[1.1.1]pentan-2-ol formed photochemically.

conversion significantly alters the electronic properties around the Pd center. Kuo and coworkers successfully applied these shapeshifting ligands to several Pd-catalyzed Lewis acid-type transformations, including the *cis-trans* isomerization of stilbene and the isomerization of 1-hexene to 2-hexene.^[181]

4.3. Arylations and Allylic Substitutions

Palladium/NBE cooperative catalysis (*Catellani reaction*) has emerged as an indispensable and highly effective strategy for the synthesis of complex, highly functionalized molecules, as discussed earlier (Section 2.3: Arylations, Figure 14). However, the widespread application of this methodology has been limited by the need for high NBE loadings and the requirement for sterically bulky 2,6-disubstituted aryl bromides as coupling partners, which reduces its synthetic utility. To address these limitations, the design and application of novel chiral ligands represent a promising strategy. In 2024, Shi et al. demonstrated the critical role of ligand tuning in enhancing both site- and stereoselectivity in Pd/NBE cooperative catalysis (Figure 62a).^[182] They introduced a chiral dinitrogen ligand (222), based on an *N,N'*-aryl-substituted biimidazoline (BiIM) scaffold, which served as the chiral source for an asymmetric Catellani reaction. Using this ligand in combination with less sterically demanding mono-ortho-substituted aryl bromides (220), a simple NBE mediator, Pd₂(dba)₃ (dba = dibenzylideneacetone), Ag₂SO₄, water, and molecular sieves, the authors carried out the transformation of 1-iodonaphthalene (219) into the desired axially chiral product (221), achieving a remarkable 95% yield and 91% enantiomeric excess (ee). The study highlighted the crucial role of water, which was proposed to enhance enantioselectivity through hydrogen bonding interactions that influence the geometry of key intermediates. Meanwhile, silver salts acted as halide scavengers, improving catalyst reactivity. Notably, the reaction displayed broad substrate scope, tolerating both electron-donating and

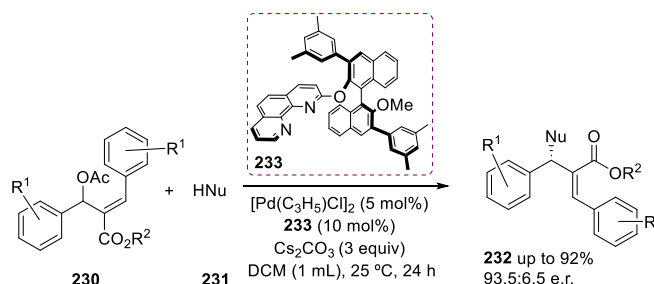


Figure 63. Enantioselective allylic substitution of aryl-substituted Morita-Baylis-Hillman adducts.

electron-withdrawing groups as well as heteroarenes such as thiophene, pyridine, and furan. This method stands out for its high reactivity, excellent enantioselectivity, and scalability, marking a significant advancement in asymmetric Pd/NBE cooperative catalysis.^[182]

In 2024, Zhang et al. reported a C6-selective arylation of pyrrolo[2,3-*d*]pyrimidines (223) using a catalyst generated in situ from Pd(OAc)₂ and 2,2'-bipyridine bidentate ligands (225) and focusing on the compatibility of various heterocyclic substrates and aryl iodides (Figure 62b).^[183] The optimized reaction proceeded under mild conditions, employing air- and moisture-stable reagents, and accommodated a broad range of heterocyclic derivatives and aryl iodides. The desired C6-arylated bioactive products (224) were obtained in good yields (65%–93%) with complete regioselectivity. Notably, the methodology demonstrated broad functional group tolerance, enabling efficient transformations of both electron-rich and electron-poor substrates. However, reduced yields were observed with substrates bearing bulky or strongly electron-withdrawing groups, likely due to steric hindrance or electronic effects.^[183] In 2023, Yu et al. developed an optimized Norrish–Yang photochemical strategy for the arylation of cyclobutanes, establishing an efficient synthetic route to *cis*-1,3-disubstituted cyclobutane building blocks (228) via formal γ -C–H functionalization of cyclobutyl ketones (226), as illustrated in Figure 62c.^[184] A key step involved the photochemical formation of bicyclo[1.1.1]pentan-2-ol intermediates (227) from ketones (226) through Norrish–Yang cyclization, which enabled subsequent C–C bond cleavage and functionalization via strain-relief mechanisms. The catalytic system, comprising Pd and pyridine-3-sulfonic acid (229), showed optimal performance with electron-deficient cyclobutyl aryl ketones. While electron-rich aryl ketones were less effective in the photochemical step, a variety of aryl and heteroaryl iodides were successfully coupled with high stereocontrol. This synergistic approach, combining photochemistry and palladium catalysis, offers a selective and efficient route to bioactive cyclobutane scaffolds with promising pharmaceutical relevance.

Another approach toward the synthesis of chiral molecules bearing a carbon–carbon double bond was reported by Zhang et al. in 2024.^[185] They developed a Pd-catalyzed enantioselective allylic substitution of aryl-substituted Morita–Baylis–Hillman (MBH) adducts (230) to afford the corresponding products (232), utilizing a bidentate phenanthroline ligand featuring axial chirality (233), as shown in Figure 63. A wide range of both cyclic and

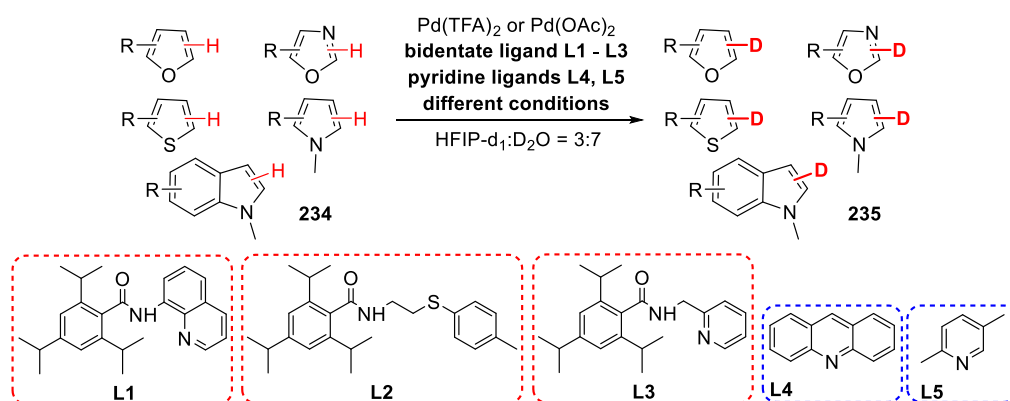


Figure 64. Deuteration of a family of heterocycles and combinations of ligands employed.

acyclic secondary amines and carbon-based nucleophiles (**231**) were found to be compatible with this transformation. However, pyrrolidine substrates exhibited very low enantioselectivity under the optimized conditions. This methodology also demonstrated good tolerance for sterically hindered MBH acetates bearing para substituents such as methoxy, methyl, fluoro, or chloro groups on the phenyl ring.

4.4. Deuteration

Careful tuning of reaction conditions to optimize stereoselectivity in asymmetric catalysis is often achieved through a multisubstrate screening approach, which has become a widely adopted methodology. In this context, van Gemmeren and co-workers applied this strategy not for stereocontrol optimization, but rather to enhance the efficiency of deuteration reactions across a broad range of heteroarenes. As discussed previously (Section 2.5, Figure 24), the van Gemmeren group developed two methods for arene deuteration based on the concept of dual-ligand-enabled catalysis, employing a combination of MPAA-type ligands and pyridines.^[120] The extent and regioselectivity of deuteration were found to depend strongly on the reaction conditions. In 2024, the same group introduced a new Pd(II)-catalyzed method for nondirected, late-stage C(sp²)-H deuteration of *heteroarenes* (**234**), yielding the corresponding deuterated compounds (**235**). This method offers promising applications in isotope labeling for drug discovery and mechanistic investigations.^[186] The primary challenge was achieving broad substrate scope through efficient condition optimization, as illustrated in Figure 64. Through extensive screening, four distinct sets of reaction conditions were identified, varying in the choice of *N*-based ligands (**L1–L5**), temperature, and Pd source, each tailored to specific classes of heterocycles (**234**). In all cases, D₂O served as the deuterium source and HFIP was used as a co-solvent to improve organic substrate solubility and facilitate C–H activation. Bidentate ligands **L1–L3**, incorporating a bulky 2,4,6-triisopropylbenzamide moiety (Figure 64), delivered the best results—consistent with observations from the MPAA-based ligands shown in Figure 24. Catalyst structure significantly influenced the site selectivity of deuteration with electron-rich positions being preferentially labeled over electron-

deficient ones. Steric hindrance negatively affected deuteration efficiency at crowded positions, while certain Lewis-basic moieties acted as DGs, enhancing deuterium incorporation in their vicinity. This study demonstrated excellent functional group tolerance and extended the methodology's applicability to the late-stage modification of bioactive molecules, highlighting its potential for both synthetic and pharmaceutical applications.

In 2024, Dey and van Gemmeren reviewed several protocols for Pd-catalyzed β -C(sp³)-H deuteration of carboxylic acids, as well as nondirected deuteration of arenes and heterocycles.^[187] Among the systems examined, the sterically bulky and finely tuned TRIP ligand (2,4,6-tri-isopropylbenzamide) in HFIP-d₁ emerged as the most effective. The pronounced steric bulk of the ligand enhanced both the catalytic activity and regioselectivity of the transformations. Common challenges such as undesired ligand activation, formation of side products, and sensitivity to air and moisture were effectively addressed by employing milder reaction conditions.

4.5. Oxidations

In all the examples discussed earlier in this review, the catalysts operate in a homogeneous phase. Numerous cases have highlighted the solvent's essential role in solubilizing reactants and facilitating catalysis. However, even in heterogeneous catalysis, the ligands coordinated to the metal center play a critical role in modulating reactivity. This influence is evident in the examples presented in this section. *N,N*-chelating or *N,N,N*-tridentate ligands—such as 1,10-phenanthroline and terpyridine—can stabilize Pd nanoparticles while contributing extensive π -conjugation, thereby enhancing the material's electrical conductivity. Such heterogeneous systems have been applied in combination with oxidants like molecular O₂ or H₂O₂ for transformations including the selective oxidation of alcohols^[188] and cyclization reactions to construct polycyclic aromatic compounds.^[189] Building on these concepts, in 2024, Zheng et al. developed a novel Pd-based heterogeneous catalyst composed of carbon quantum dots (CQDs) functionalized with terpyridine (Tpy) ligands to coordinate palladium nanoparticles (Pd-NPs).^[188] The resulting Pd-NPs/CQD-Tpy nanocomposite was employed in the selective aerobic oxidation of primary and

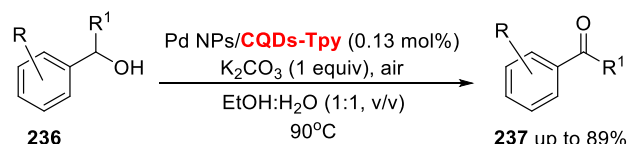


Figure 65. Alcohol to ketone oxidation promoted by carbon quantum dots decorated with terpyridine.

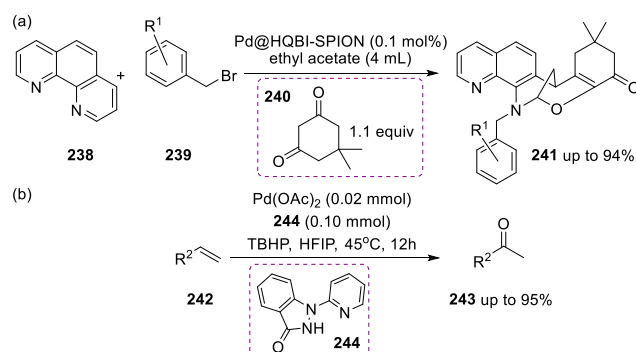


Figure 66. (a) Coupling of phenanthroline with benzyl bromide and dimesone promoted by a Pd catalyst anchored to an iron nanoparticle; (b) Wacker-type selective oxidation of terminal alkenes to ketones.

secondary alcohols (**236**) to the corresponding aldehydes and ketones (**237**) in the presence of K_2CO_3 , using a 1:1 ethanol–water mixture as solvent (Figure 65). The system demonstrated excellent activity, particularly for benzyl alcohols (**236**) bearing electron-donating substituents, which yielded higher conversions and required shorter reaction times compared to their electron-deficient counterparts. This reactivity trend can be rationalized by the stabilization of carbocationic intermediates in the presence of electron-donating groups. However, a limitation of this methodology is its ineffectiveness toward aliphatic alcohols, which were not oxidized under the applied conditions.^[188]

Similarly, in 2024, Mahdavi et al. reported a novel Pd-based heterogeneous catalyst functionalized with 2-(5-hydroxyquinolin-8-yl)-1*H*-benzo[d]imidazole-5-carboxylic acid ligands (HQBI). The palladium catalyst was immobilized on superparamagnetic iron oxide nanoparticles (SPIONs), enabling easy magnetic recovery (Figure 66a).^[189] This catalyst was successfully applied in C–C bond-forming reactions, particularly in the one-pot synthesis of phenanthroline–dimesone polycyclic derivatives (**241**) as depicted in Figure 66a. The reaction involves phenanthroline (**238**), benzyl bromide (**239**), and dimesone (**240**) in ethyl acetate, proceeding through sequential C-alkylation followed by O-alkylation to yield the target compounds (**241**). This tandem sequence forms the core of the methodology. The inclusion of dimesone is especially noteworthy, as this moiety contributes significantly to the biological activity and physicochemical properties of a wide range of natural and synthetic molecules. The catalytic system showed good tolerance toward various benzyl bromides (**239**) bearing electron-withdrawing substituents such as $-Cl$, $-Br$, $-F$ (in ortho, meta, or para positions), and $-NO_2$. However, benzyl chlorides and benzyl iodides were found to be unsuitable under the reaction conditions, limiting the substrate scope.

Another noteworthy advancement in Wacker-type oxidation was reported by Meng et al. in 2024.^[190] The authors developed a novel TBHP-mediated, Pd(II)-catalyzed Wacker-type selective oxidation of terminal alkenes (**242**) to ketones (**243**), facilitated by the *N,N*-bidentate ligand (**244**), as illustrated in Figure 66b. The study emphasized that conventional oxidants such as molecular O_2 or H_2O_2 were found to deliver lower yields and promote side reactions, thereby limiting the scope of the transformation. In this protocol, the $Pd(OAc)_2$ /TBHP catalytic system was applied to styrene derivatives in the presence of the ligand 1-(pyridin-2-yl)-1,2-dihydro-3*H*-indazol-3-one (**244**). The key feature of ligand (**244**) lies in its dual electronic nature, capable of exhibiting both electron-donating and electron-withdrawing characteristics. This unique combination enhances the stability and efficiency of the Pd(II) catalytic system.^[190] Mechanistic investigations revealed that the reaction begins with coordination of the free ligand to the palladium center, forming a dimeric Pd(II) intermediate. In the presence of acetonitrile, this species dissociates into a monomeric active Pd complex. The active catalyst then reacts with TBHP, generating a $Pd-OOTBu$ intermediate, which facilitates olefin activation. The coordinated olefin undergoes regioselective oxygen insertion at the Markovnikov position, forming an alkylperoxide intermediate. This intermediate then undergoes β -hydride elimination and O–O bond cleavage, yielding a Pd–enolate species. Final protonolysis of this intermediate releases the desired methyl ketone product.^[190]

4.6. Alkenylation and Bromination

Besset et al. reported in 2024 a Pd(II)-catalyzed ortho-selective C–H olefination of chlorobenzene derivatives (**245**) using a commercially available quinoline ligand (**211**), as shown in Figure 67.^[191] By fine-tuning the reaction conditions and carefully selecting the substitution pattern on the substrate (**245**), the authors achieved high regioselectivity—favoring ortho-functionalization—and excellent yields of the alkenylated products (**247**), reaching up to 93%. The crucial role of ligand (**211**) was highlighted through control experiments: in its absence, the olefinated product (**247**) was obtained in only 45% yield and as an equimolar mixture of *o:m:p* regioisomers. In contrast, the use of ligand (**211**) promoted selective ortho-functionalization with significantly improved efficiency. Further demonstrating the versatility of this method for late-stage functionalization of complex molecules, the olefination was successfully applied to bio-relevant acrylates (**246**) derived from natural and synthetic molecules such as testosterone, cholesterol, borneol, and menthol. Mechanistic studies suggested that the reaction proceeds via a CMD pathway. The Pd/quinoline (**211**) catalytic system activates the aryl C–H bond, facilitated by reduced distortion energy, partially attributed to favorable $Cl\cdots\pi$ interactions between the chlorine atom and the catalytic species and by increased C–H acidity due to the inductive electron-withdrawing effect of the chloro substituent. The acrylate inserts into the Pd–C bond via carbopalladation, followed by β -hydride elimination to release the olefinated product. A Pd(II)–hydride species is then formed, which undergoes reductive elimination. The cat-

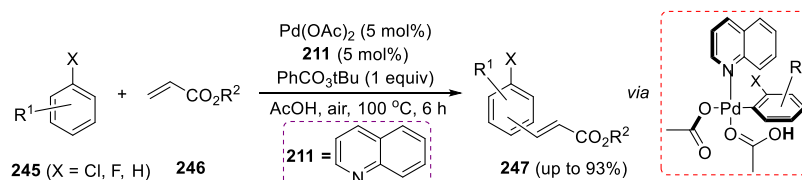


Figure 67. Alkenylation of halobenzenes promoted by quinolines and proposed active key intermediate.

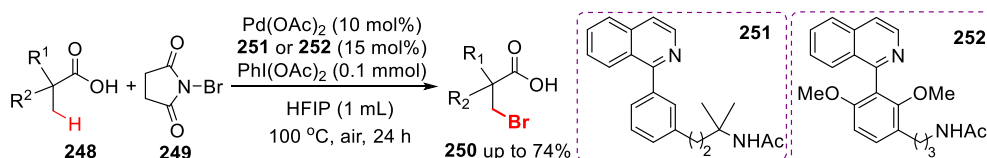


Figure 68. β -C(sp³)-H bromination of free carboxylic acids with NBS promoted by isoquinolines.

alytic cycle is completed by oxidation of Pd(0) back to Pd(II) using tert-butyl peroxybenzoate as the oxidant.^[191]

As previously discussed, H-bond interactions significantly influence the enantioselectivity of catalytic processes.^[182] In a study published by Yu et al. in 2023, this principle was harnessed in the development of a Pd(II)-catalyzed β -C(sp³)-H bromination of free carboxylic acids (**248**), where substrate–catalyst affinity via H-bonding played a central role.^[192] The reaction employed NBS (**249**) as the brominating agent and was promoted by tailored ligands (**251**) or (**252**), shown in Figure 68. To facilitate H-bond formation, the authors incorporated a remote amide (NHAc) group into isoquinoline-based ligands, which works analogously to the NAc fragment in MPAA ligands (Section 2). These weak, yet strategically positioned interactions between the substrate and the catalyst enabled highly selective mono- β -halogenation, furnishing brominated products (**250**) with excellent regioselectivity. Mechanistic studies, supported by X-ray crystallography and DFT calculations confirmed that the H-bonding interaction stabilizes the catalytic complex via a meta-macrocyclophane geometry and contributes to a reduction in activation energy. The methodology demonstrated broad applicability across a diverse set of α -tertiary and α -quaternary aliphatic carboxylic acids.

In summary, the use of *N*-donor ligands such as amines, diamines, pyridines, and related species is a classic approach in Pd catalysis and C–H functionalization reactions are no exception. Whether used as sole ligands or synergistically with MPAA or pyridones, their use is well established as they provide stability to transition states and are compatible with the metal in various oxidation states, making a single ligand useful across a wide range of processes. The variety of available ligands, their easy accessibility, and the possibility of introducing substituents that modulate both electronic density and steric demands make them highly versatile tools.

5. S,O-Thioethercarboxylic Acids

The development of carefully designed ligands that incorporate both a soft donor atom (sulfur) and a hard donor atom (oxygen) within their molecular framework, along with the strategic

selection of the metal center are essential factors for achieving enhanced catalytic efficiency. Pioneering contributions in this area were made by Fernández-Ibáñez et al., who introduced a novel family of *thioethercarboxylic acid* ligands, as illustrated in Figure 1d of the Introduction. This new generation of ligands was specifically designed to overcome the key limitations associated with the earlier ligand systems previously reported by the same research group.^[193]

5.1. Alkenylations

The combination of S,O-ligands with Pd(OAc)₂ exhibits a synergistic effect that enables nondirected Pd-catalyzed C–H alkenylation of both electron-rich and electron-poor arenes (**253**) with olefins, delivering high yields of functionalized derivatives (**254**) (Figure 69). This efficiency arises from two key factors: (a) the presence of a carboxylic acid functional group, which facilitates C–H bond cleavage via a CMD mechanism as discussed in previous sections and (b) the enhanced stability of the catalytic species due to the bidentate S,O-coordination to the Pd center. The ligand's effectiveness was shown to depend significantly on its structural features—specifically, the presence of aliphatic substituents at the α -position and aromatic groups directly attached to the sulfur atom. These modifications influence both catalyst performance and selectivity. Importantly, the S,O-ligand plays a critical role in governing site selectivity, favoring activation at the most electron-rich position of the arene.^[194] One of the notable advantages of this ligand class is its scalability, as the ligands can be synthesized from readily available carboxylic acids. KIE measurements and kinetic studies indicated that C–H activation is the RDS.^[195] This step is facilitated by the formation of a cationic monomeric palladium species as depicted on the right side of Figure 69.

In 2019, Fernández-Ibáñez et al. demonstrated that a Pd/S,O-ligand-based catalytic system is uniquely effective for the para-selective olefination of a wide range of anilines (**257**), as illustrated in Figure 70.^[196] Through extensive investigation of mono, di, and tri substituted tertiary, secondary, and primary anilines, the study confirmed that these substrates are well tolerated under the Pd/S,O-ligand (**256**) catalysis. The reaction

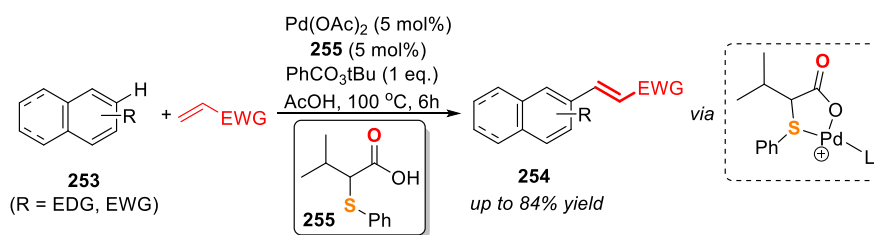


Figure 69. Alkenylation of different arenes promoted by thioethercarboxylates bonded to Pd.

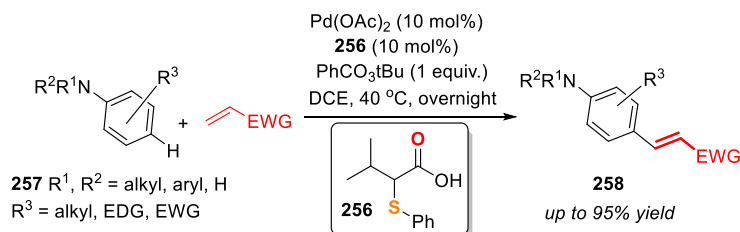


Figure 70. Selective para alkenylation of anilines promoted by Pd(thioethercarboxylates) complexes.

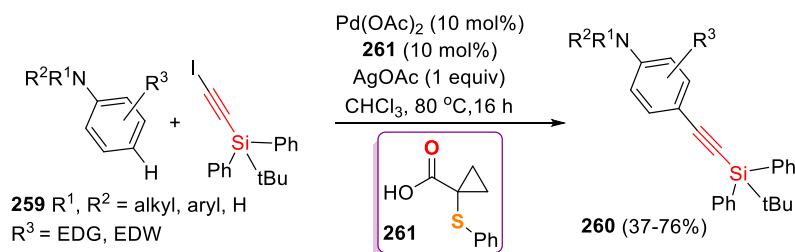


Figure 71. Selective para alkynylation of anilines promoted by Pd(thioethercarboxylates) complexes.

showed broad functional group tolerance, accommodating both electron-donating and electron-withdrawing substituents on the aniline ring. Notably, in the case of primary and secondary anilines, the para-olefinated products (**258**) were obtained almost exclusively and in very good yields. However, a lack of reactivity was observed with ortho-substituted *N,N*-dimethylanilines. DFT calculations revealed that this behavior is due to the steric bulk of the methyl groups on the nitrogen atom, which forces the N-substituent to twist out of the plane of the aromatic ring. This distortion disrupts conjugation between the nitrogen lone pair and the aromatic system, thereby deactivating the ring toward electrophilic aromatic substitution.

5.2. Alkynylation

The electronic and steric environment around the palladium center can be finely tuned by modifying the structure of thioethercarboxylic acid ligands. These adjustments play a crucial role in controlling regioselectivity and minimizing the formation of side products. In 2022, Fernández-Ibáñez and co-workers explored the para selective C–H alkynylation of aniline derivatives (**259**), focusing on the compatibility of meta-substituted anilines with the Pd/S,O-ligand-based catalytic system (**261**) to produce alkynylated products (**260**), as illustrated in Figure 71.^[197] Their findings revealed that meta-substituted anilines exhibited

reactivity comparable to that of unsubstituted tertiary anilines. The study further demonstrated that anilines bearing electron-withdrawing groups yielded even better outcomes. Additionally, both ortho-substituted and disubstituted *N*-benzylanilines were shown to be suitable substrates under the optimized conditions. Building on these promising results, the authors extended their investigation to a broader range of *N*-containing substrates, including pyrrolidine- and morpholine-derived anilines, as well as bioactive spiro-tetrahydroquinoline frameworks.^[197]

5.3. Arylations

While numerous strategies have been developed for the ortho and para functionalization of anilines, selective modification at the less reactive meta position remains a significant challenge. Given the proven compatibility of the Pd/S,O-ligand catalytic system with C–H olefination across a broad range of aromatic amines (as shown in Figure 70), it was reasonable to hypothesize that this system could also be adapted for use in NBE-mediated transformations, such as the Catellani reaction. In 2024, Fernández-Ibáñez et al. reported a general and efficient method for nondirected meta-C–H arylation of aniline derivatives (**262**) with aryl iodides (**263**) via Pd/S,O-ligand/NBE cooperative catalysis (Figure 72).^[198] The reaction proceeds under mild conditions and demonstrates broad substrate scope, accom-

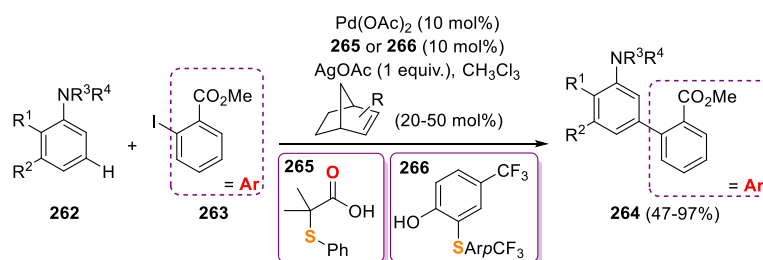


Figure 72. Selective meta Catellani arylation of anilines promoted by Pd(thioethercarboxylates)/NBE complexes.

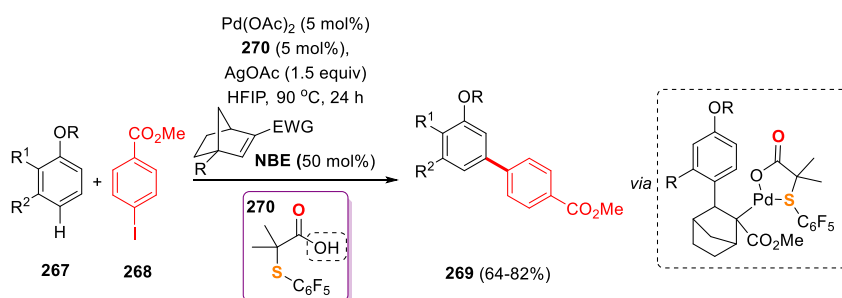


Figure 73. Selective arylation of anisoles promoted by Pd(thioethercarboxylates)/NBE complexes.

modating a wide range of aniline derivatives—including meta-substituted *N,N*-dibenzylanilines and both ortho and meta substituted *N*-benzylanilines—delivering the desired meta arylated products (**264**) in good to excellent yields (62%–88% and 47%–97%, respectively) with complete regioselectivity. Remarkably, through careful selection of S,O-ligands (**265** or **266**) and the NBE mediator, the system was shown to tolerate more challenging substrates, such as ortho-substituted anilines and aryl iodides lacking ortho-electron-withdrawing groups. Preliminary mechanistic studies suggest that both the structural features of the NBE mediator and the meta-substituent on the aniline substrate play key roles in facilitating meta C–H activation.^[198]

This study reinforces emerging synthetic trends previously reported by the same research group in 2022.^[199] In that earlier work, Fernández-Ibáñez et al. employed a Pd/S,O-ligand/NBE cooperative catalytic system for the meta C–H arylation of anisole derivatives, successfully overcoming the classical ortho constraint, that is, the need for an ortho-substituent to enable efficient meta functionalization. This limitation was addressed through the introduction of sterically demanding, bridgehead-substituted NBEs and careful optimization of the reaction conditions. In 2024, the authors extended this methodology to the arylation of anisoles (**267**) with aryl iodides (**268**) to form bis-aryl products (**269**), using a HFIP:H₂O solvent system under milder and more practical conditions (Figure 73).^[200] The new conditions significantly improved both reaction efficiency and selectivity. HFIP played a critical role as solvent, as its strong hydrogen-bond-donating ability stabilizes cationic Pd intermediates, thereby facilitating C–H activation. Moreover, HFIP enhances the solubility of silver salts such as AgOAc, which is essential for the oxidation step. Mechanistic studies confirmed that C–H activation is the RDS. Additionally, the reaction exhibited broad functional group tolerance, accommodating both electron-donating and electron-withdrawing substituents on the

alkoxyarene substrates. The methodology also proved applicable to the late-stage functionalization of bioactive molecules, further demonstrating its synthetic utility.^[200]

To date, the development of thioethercarboxylate ligands for palladium-catalyzed C–C bond formation via C–H functionalization remains in its early stages, with only a limited number of studies reported all originating from the same research group. Nevertheless, these “young” ligands show significant promise having demonstrated the ability to optimize transformations that are less efficient or inaccessible with traditional ligand systems, thereby underscoring their unique potential. Looking ahead, key challenges include broadening their applicability to a wider range of C–C couplings—particularly those involving C(sp³)–H bonds—as well as expanding into other types of bond-forming reactions, such as C–X couplings. The continued exploration and structural refinement of thioethercarboxylate ligands could unlock new reactivity paradigms in Pd-catalyzed functionalization chemistry.

6. Phosphines and NHC Ligands

Phosphine-based ligands and *N*-heterocyclic carbenes (NHCs) have been extensively and effectively utilized in palladium catalysis, owing to their strong metal–ligand cooperation. Both monodentate and bidentate phosphines, as well as NHC ligands, serve as tools for fine-tuning the reactivity and selectivity of Pd-catalyzed reactions.^[201–204] Precise control over the coordination environment at the palladium center—shaped by the steric and electronic properties of the ligand donor atoms is critical for modulating catalytic performance. To achieve optimal reactivity and selectivity, a wide variety of ligand frameworks must be designed and systematically explored. Examples supporting this principle include simple monodentate phosphines (e.g.,

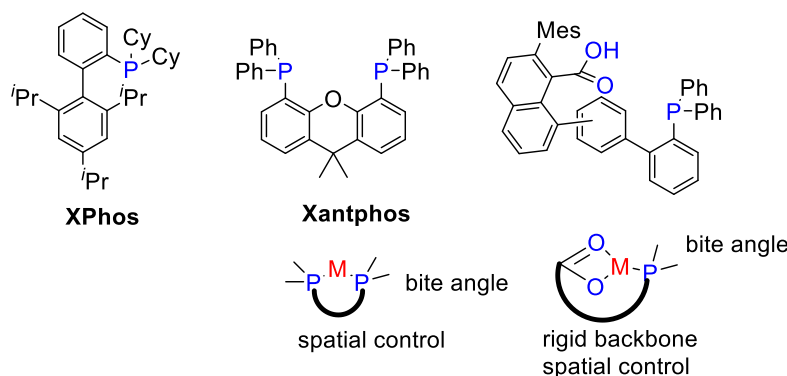


Figure 74. Representative examples of multidentate phosphines and main bonding modes to Pd(II).

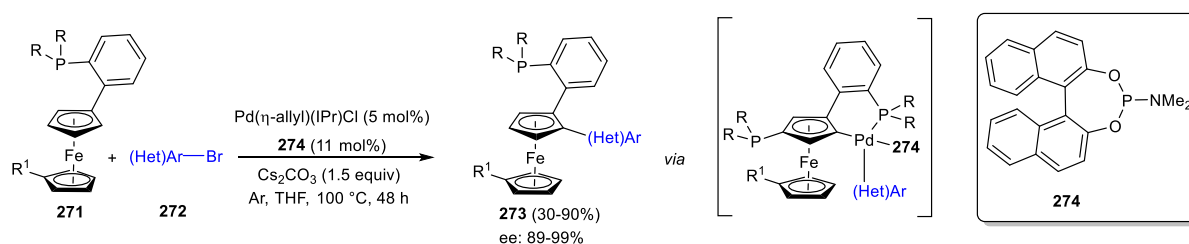


Figure 75. Enantioselective arylation of ferrocene derivatives using a Pd-NHC catalyst and a phosphoramidite.

XPhos), bidentate ligands (e.g., Xantphos) and more complex phosphine-containing systems (see Figure 74), which are tailored to stabilize low-valent Pd complexes. These ligand designs enable predictable coordination modes around the metal center such as κ^2 -, *cis*- κ^1 , and *trans*- κ^1 —which are essential for directing catalytic outcomes. In this section, we will further discuss how the number of phosphine ligands coordinated to the metal, as well as the bite angle in chelating systems influences catalytic behavior.

6.1. Arylations

Shi and co-workers successfully synthesized planar chiral metallocene compounds—specifically chiral ligands—via enantioselective C–H activation using a P(III) directing group. In this approach, the use of a chiral ligand with palladium transferred chirality to a planar chiral phosphapalladacycle, enabling the formation of products with high atom economy. To achieve both high reactivity and enantioselectivity in the synthesis of planar chiral ferrocenyl phosphines (**273**), a Pd catalyst bearing an *N*-heterocyclic carbene (NHC) ligand was employed in combination with a chiral phosphoramidite additive (**274**) and ferrocenyl phosphine substrates (**271**). Several palladium catalysts—including Pd(OAc)₂, Pd₂(dba)₃, [Pd(η^3 -allyl)Cl]₂, and Pd(η^3 -allyl)(IPr)Cl were evaluated. Optimal results, in terms of full conversion and high enantioselectivity were obtained using the NHC complex [Pd(η^3 -allyl)(IPr)Cl] in conjunction with ligand (**274**). Under the reaction conditions outlined in Figure 75, the desired planar chiral products (**273**) were isolated in yields ranging from 30% to 90%.^[205]

The reaction demonstrated a broad substrate scope, accommodating aryl bromides (**272**) bearing electron-neutral and

electron-rich substituents such as alkoxy, thioether, and trimethylsilyl groups. These substrates afforded the desired products (**273**) with excellent enantioselectivity, ranging from 89% to 99%. Similarly, aryl bromides containing electron-withdrawing groups—such as F, CF₃, OCF₃, CO₂Me, COMe, and SO₂Me also provided high enantioselectivities of 90% to 98%. The methodology was further extended to more complex aryl bromides incorporating polycyclic aromatic systems (e.g., naphthalenyl, phenanthren-9-yl, pyren-2-yl) as well as heteroaryl bromides, including quinoline, pyridine, and indazole derivatives. These substrates also yielded products with high levels of enantioselectivity.^[205]

C–H arylation of heteroarenes has proven to be a powerful strategy for the synthesis of pharmaceutically relevant molecules. So and Gu addressed the long-standing challenge of achieving chemoselective C–Cl activation over C–OTf and α,β -regioselectivity in the arylation of heterocycles by employing a novel pyrazole-alkylphosphine ligand (**280**), shown in Figure 76. Initial attempts using conventional phosphine ligands such as PPh₃ and P(*o*-tolyl)₃ favored C–OTf activation, but the newly designed ligand enabled selective C–Cl activation. Guided by DFT calculations, the optimized steric and electronic properties of ligand (**280**) enhanced catalytic activity and selectivity. Using this system, α -arylation products (**277**) were obtained in good yields (41%–92%) from a variety of chloroaryl triflate substrates (**275**), in which the –Cl and –OTf groups were positioned ortho, meta, or para to each other. These substrates reacted chemo- and regioselectively with benzo[*b*]thiophene (**276**). For example, 4-chlorophenyl triflate (**275**) underwent α -selective arylation with both benzo[*b*]thiophene and thiophenes (**278**) bearing electron-donating (e.g., Me, *n*-Bu, *n*-Hex, OMe) or electron-withdrawing (e.g., ester, ketone, pyridyl) groups. The resulting

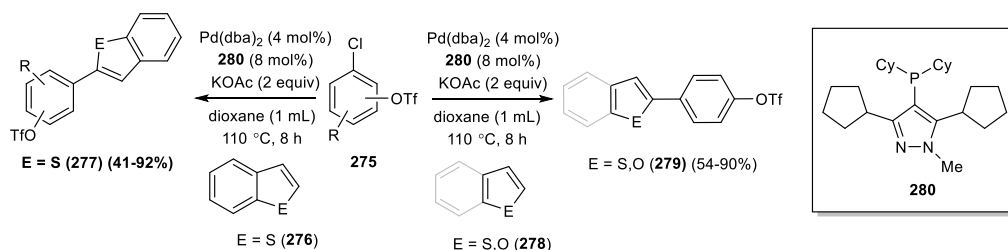


Figure 76. Arylation of heteroarenes using a phosphino-pyrazol ligand.

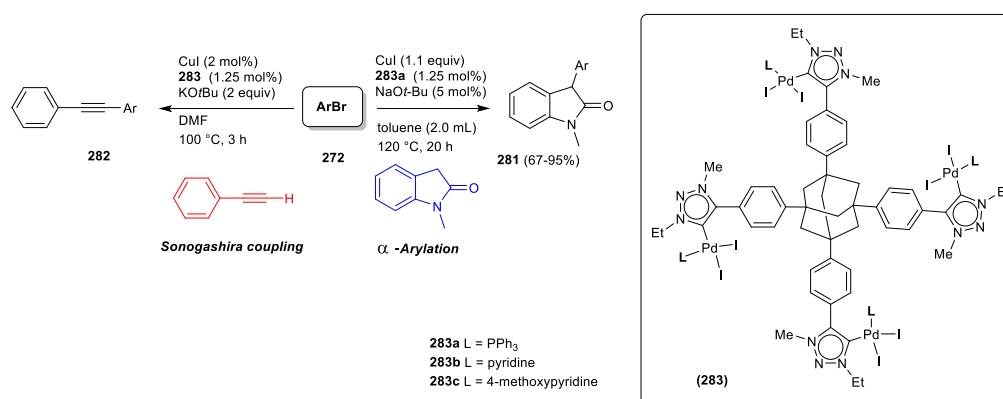


Figure 77. Diverse C—C couplings promoted by a tetranuclear mesoionic carbene MIC-Pd complex.

α -regioselective products (**279**) were isolated in yields ranging from 54% to 90% (Figure 76).^[206]

Maity and co-workers developed a series of novel tetranuclear Pd(II) complexes (**283**) incorporating a mesoionic carbene (MIC) ligand along with various ancillary ligands: triphenylphosphine (PPh₃, **283a**), pyridine (**283b**), and 4-methoxypyridine (**283c**). Among these, complex (**283a**) was successfully applied in the α -arylation of 1-methyl-2-oxindole with aryl bromides (**272**), including 2,4,6-triisopropylbromobenzene, 2,3,5,6-tetramethylbromobenzene, 2-bromomesitylene, and 1-bromonaphthalene. The corresponding arylated products (**281**) were obtained in excellent yields ranging from 67% to 95% (Figure 77). In contrast, replacing the PPh₃ ligand in complex (**283**) with pyridine (**283b**) or 4-methoxypyridine (**283c**) resulted in a dramatic loss of catalytic activity, highlighting the critical role of the ancillary ligand in the reactivity of these complexes. Additionally, the catalytic activity of complexes (**283**) in Sonogashira coupling reactions between phenylacetylene and various aryl bromides (**272**) was evaluated. Among the three complexes, (**283a**) again delivered the best performance, affording the C—C coupling products (**282**) in high yields (Figure 77).^[207]

6.2. Phosphorylation Reactions

Xu, Cao, and co-workers achieved P—Heck reactions, C—H phosphinylation of heteroarenes, and carbon–phosphorus difunctionalization of alkenes using photoinduced palladium catalysis. This strategy, shown in Figure 78, enabled the regiospecific radical incorporation of phosphinyl and phosphonyl groups into

both alkenes (**286**) and heteroarenes (**288**), as well as the C—P difunctionalization of alkenes to afford phosphorylated oxindoles (**290**).^[208] Following optimization of the reaction conditions, **Xantphos** was identified as the optimal ligand. The substrate scope of the formal P—Heck reaction was then explored. A range of mono-substituted aryl alkenes (**285**) bearing electron-donating or electron-withdrawing groups (e.g., Me, MeO, CF₃, F, Cl), along with naphthalene, pyridine, and ferrocene derivatives, provided the desired products (**286**) in yields ranging from 41% to 92%. Alkenes bearing trimethylsilyl and ester groups also underwent the transformation, albeit in lower yields (21%–41%). Using diphenylphosphinic chloride (**284**), a direct C—H phosphinylation of common heteroaromatic compounds (**287**) was achieved under the same photoinduced Pd-catalyzed conditions. A variety of P-substituted heteroarenes (**288**), including functionalized indoles, benzofuran, benzothiophene, benzothiazole, thiophene, and quinoline derivatives, were obtained in moderate yields (24%–60%). Furthermore, carbon–phosphorus difunctionalization of alkenes was accomplished using [(4-MeOC₆H₄)₃P] as the ligand. Starting from substituted anilines (**289**) bearing groups such as MeO, CF₃, F, Cl, and Br, the phosphorylated oxindoles (**290**) were isolated in yields ranging from 43% to 90% (Figure 78).^[208]

6.3. Nondirected Alkenylation

Aryl alkenes remain a valuable class of compounds in organic synthesis and the development of efficient methods for their preparation continues to attract significant interest. Wang and

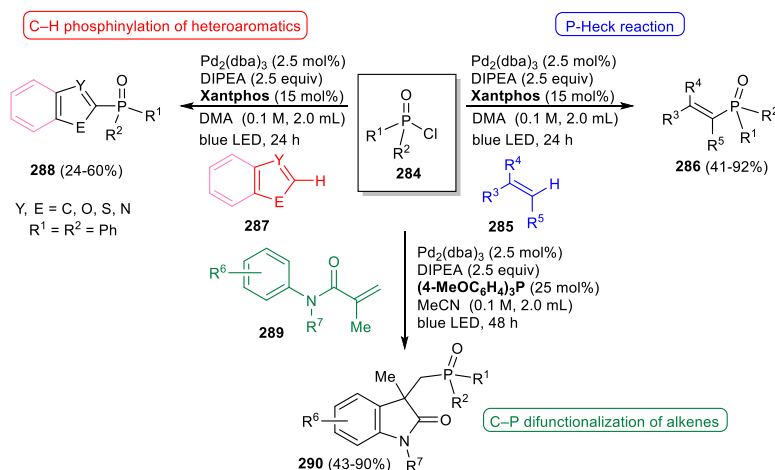


Figure 78. Different phosphorilation reactions promoted photochemically by Pd and diverse phosphines.

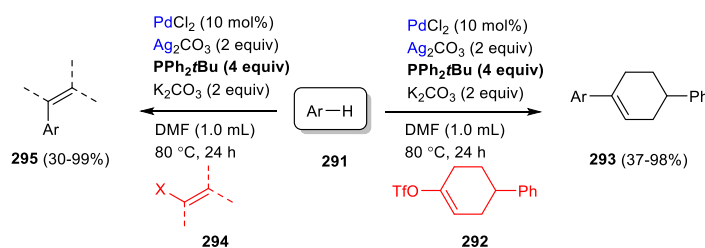


Figure 79. Fujiwara-Moritani coupling of alkenes and arenes promoted by P-stabilized Pd/Ag bimetallic catalysts.

co-workers reported a silver/palladium bimetallic cooperative system for the nondirected C–H olefination of arenes, offering a complementary approach to the classical Fujiwara–Moritani reaction, which typically employs vinyl pseudohalides.^[209] In this methodology, shown in Figure 79, arenes (291) including fluoroarenes and heteroarenes such as furan, thiophene, thiazole, oxazole, and pyrazole were successfully olefinated with cyclic alkenes (292) to afford the corresponding alkenylated products (293) in good yields (37%–98%) and with excellent regioselectivity. Optimal results were achieved using a large excess (4 equivalents) of Ag(I)/PPh₂tBu. In the case of 1-bromo-4-chlorobenzene, a mixture of regioisomers was observed, indicating a less selective transformation under these conditions. The scope of the reaction was further extended to linear alkenes (294), which reacted with difluorobenzene derivatives (291) to furnish the corresponding aryl alkenes (295) in yields ranging from 30% to 99% demonstrating the versatility and efficiency of the system for constructing aryl olefins from simple arenes (Figure 79). Mechanistic studies suggest the transformation proceeds via two key intermediates: an aryl–silver species and a vinyl–palladium species, highlighting the cooperative roles of silver and palladium in facilitating C–H activation and olefination.^[209]

6.4. Transformations Performed Under Dual-Ligand Conditions

To access complex organic molecules and natural products whether for synthetic utility or medicinal applications numerous

dual-ligand-enabled Pd-catalyzed transformations have been developed, as discussed in Section 2.5. In their comprehensive review, Gandhi and co-workers clearly highlighted the significance of synergistic catalysis through the cooperation of *N*-heterocyclic carbene ligands with Pd complexes in organic synthesis.^[210] The combination of NHC and Pd catalysis has emerged as a powerful platform for a variety of synthetic transformations, including the activation of aldehydes and α,β -unsaturated carbonyl compounds. This dual activation—where NHCs engage with electrophilic carbonyls and Pd complexes activate other substrates enables reactions that surpass the capabilities of either catalyst alone. The scope of these systems has further expanded with advancements such as photoredox catalysis, alkylation of alkenes, and C(sp³)–H bond activation, all of which showcase their versatility in tackling challenging substrates.^[210] In the pursuit of innovative methodologies, several additional dual-ligand catalytic systems have been developed. Notable examples include Pd/olefin catalysis promoted by bulky phosphine ligands for the ortho alkylation of iodoarenes,^[211] and a dynamic ligand exchange mechanism involving Dt-BPF and XPhos on the palladium center, which enables synergistic reactivity in Larock/Buchwald–Hartwig annulation and cyclization sequences.^[212]

Jiao and Wang developed an ortho-alkylation protocol (Figure 80) for a broad range of iodoarene substrates using a dual-ligand Pd catalytic system. Iodoarenes (296) bearing either electron-donating or electron-withdrawing groups in the ortho-position afforded the desired alkylated products (298) in high yields (up to 85%). However, substrates with strongly

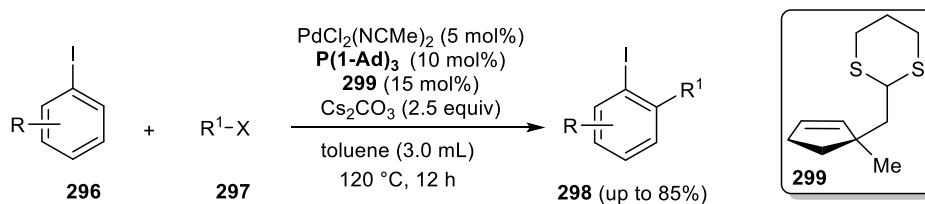


Figure 80. Alkylation of iodoarenes using dual ligand-enabled catalysis.

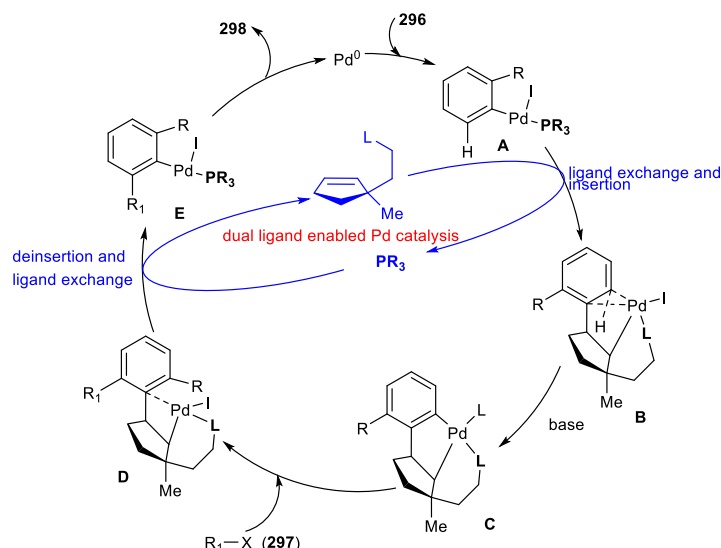


Figure 81. Mechanism of the process shown in Figure 80.

electron-donating or strongly electron-withdrawing substituents tended to give lower yields. The methodology also proved tolerant of various alkyl electrophiles bearing functional groups such as phenyl, acetoxyl, ether, acetal, *N*-phthaloyl, ethyl ester, trifluoromethyl, cyclopropyl, and protected alcohol moieties. Additionally, more complex aryl iodides such as iodonaphthalene, iodobenzothiophene, and iododibenzothiophene were successfully alkylated under the same conditions (Figure 80). The catalytic system, which combines tri(1-adamantyl)phosphine [$\text{P}(\mathbf{1-Ad})_3$], a thio-cycloolefin ligand (**299**), and palladium, effectively expands the scope of these Catellani-type reactions, enabling efficient ortho alkylation across a wide substrate range.^[21]

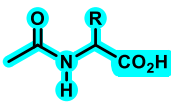
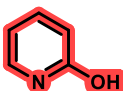
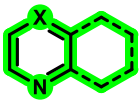
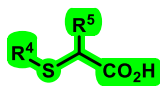
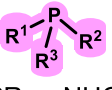
The proposed mechanism for the dual-ligand-enabled Pd catalysis, supported by experimental evidence is shown in Figure 81. The catalytic cycle begins with the oxidative addition of iodoarene (**296**) to Pd^0 , forming intermediate **A**. Subsequent ligand exchange with the thio-cycloolefin ligand (**299**) and insertion into the alkene generates intermediate **B**. Next, base-assisted C–H activation occurs at **B**, producing intermediate **C**. Ortho-alkylation of **C** in the presence of the alkyl iodide (**297**) leads to **D**. This is followed by retro-insertion and ligand exchange, where the cycloolefin ligand is released and the phosphine ligand re-coordinates. Finally, reductive elimination of intermediate **E** yields the ortho-alkylated product (**298**) and regenerates the Pd^0 catalyst (Figure 81).^[21]

7. Summary and Outlook

Although the methodology based on C–H bond activation applied to the synthesis of organic molecules is now firmly established as a fundamental tool in organic and organometallic chemistry, achieving fast and highly selective reactions under sustainable conditions remains a challenge requiring more refined solutions. Substrate modification-based methods have led to significant progress in the field but they are not the most desirable solution. The paradigm shift from substrate-based reaction design to catalyst-based reaction design has brought about a true revolution in this field as highlighted in this review. This catalyst design approach requires a precise understanding of the role played by ligands and how their design can enhance the reaction making it faster and more selective.

The review conducted on palladium-catalyzed processes and the role of various ligands such as mono-*N*-protected amino acids, pyridones, *N*-heterocycles, thioacids, and phosphines demonstrates that, over the period 2022–2025 a series of milestones have been achieved that were unthinkable at the beginning of the 21st century in terms of reaction efficiency and selectivity. The main characteristics of these ligands are summarized in Table 1. This progress applies not only to benchmark substrate functionalization but more importantly to natural product-based substrates, pharmaceutical drugs, and biologically active compounds, where only late-stage functionalization methods can be used. The ability to promote a selective func-

Table 1. Main bonding characteristics, reactivity, strengths, and limitations of the ligands analyzed in this review.

Ligand	Bonding Mode	Reactions Promoted	Strengths	Limitations
 MPAAs	N,O-chelate, N-monodentate O-monodentate	C–C and C–X coupling (Csp ³ /Csp ²) - Olefination - Arylation - Halogenation - Glycosylation - Deuteration - Lactonization - Alkylation	Tailored synthesis Easily tunable Available in grams Air and moisture stable (in general) Sustainable Various bonding modes, can be adopted as needed Control of regio- & stereoselectivity	Mostly restricted to palladium Low enantioselection in some cases Each substrate needs a particular MPAA (long optimizations) Not valid for alkanes High cost, depending of the MPAA Deactivation under harsh conditions
 Pyridones	N,O-chelate, N-monodentate O-monodentate	C–C and C–X coupling (Csp ³ /Csp ²) - Lactonization - Hydroxylation - Dehydrogenation - Olefination - Arylation - Halogenation	Tailored synthesis Easily tunable Available in grams Air and moisture stable Various bonding modes Control of regio- & stereoselectivity	Synthesis could be difficult High cost, depending of the ligand Not sustainable Strong N-bonding could poisoning the catalyst
 N-ligands	N,N-chelate N-monodentate	C–C and C–X coupling (Csp ³ /Csp ²) - Cyclization - Isomerization - Arylation - Deuteration - Oxidations - Olefination - Halogenation	Tailored synthesis Available in grams Air and moisture stable Various bonding modes Control of regio- & stereoselectivity	Synthesis could be difficult High cost, depending of the ligand Not sustainable Strong N-bonding could poisoning the catalyst
 S,O-thioethers	S,O-chelate	Mostly C–C coupling - Olefination - Alkynylation - Arylation	Tailored synthesis Available in grams Air- and moisture stable	Not very developed
 PR ₃ + NHC	Phosphines: P-monodentate P,P-chelate NHC: C-monodentate C,C-/C,X-chelate	Mostly C–C coupling - Arylation - Phosphorylation - Olefination - Alkylation	Tailored synthesis Available in grams (in general) Stabilization of various oxidation states Very general for many metals	Synthesis could be difficult Low stability towards oxidation Limited compatibility with oxidants Not very adequate for high oxidation states

tionalization reaction of a high-value industrial drug by slightly modifying the ligand is a breakthrough that has only recently emerged. Its full implications remain to be determined and further research is needed.

Perhaps the most fascinating aspect of the near future of this methodology lies in the vast amount of experimental data being accumulated in recent years. The introduction of emerging techniques such as artificial intelligence, machine learning, and data-driven reactivity prediction in chemistry is expected to further accelerate the discovery of new catalysts by virtually testing millions of ligands without the need for their experimental synthesis.

Acknowledgments

Esteban P. Urriolabeitia and Jesús Moradell thank Gobierno de Aragón (Spain, research group Química Inorgánica y de los Compuestos Organometálicos E17_23R) for funding.

Conflict of Interests

The authors declare no conflicts of interest.

Keywords: Catalysis · C–H bond activation · Ligand-accelerated reaction · Palladium · Selectivity

- [1] P. T. Anastas, J. C. Warner, *Green Chemistry: Theory and Practice*, Oxford University Press: New York **1998**, p. 30.
- [2] L. Yang, D. Fan, Z. Li, Y. Cheng, X. Yang, T. Zhang, *Adv. Sustainable Syst.* **2022**, *6*, 2100477.
- [3] N. Holmberg-Douglas, D. A. Nicewicz, *Chem. Rev.* **2022**, *122*, 1925–2016.
- [4] P. Bellotti, H.-M. Huang, T. Faber, F. Glorius, *Chem. Rev.* **2023**, *123*, 4237–4352.
- [5] Y. Wang, S. Dana, H. Long, Y. Xu, Y. Li, N. Kaplaneris, L. Ackermann, *Chem. Rev.* **2023**, *123*, 11269–11335.
- [6] C. Zhu, N. W. J. Ang, T. H. Meyer, Y. Qiu, L. Ackermann, *ACS Cent. Sci.* **2021**, *7*, 415–431.
- [7] S. Hwang, S. Grätz, L. Borchardt, *Chem. Commun.* **2022**, *58*, 1661–1671.
- [8] J. G. Hernández, *Chem. -Eur. J.* **2017**, *23*, 17157–17165.
- [9] R. Laskar, T. Pal, T. Bhattacharya, S. Maiti, M. Akita, D. Maiti, *Green Chem.* **2022**, *24*, 2296–2320.

- [10] A. de Meijere, F. Diederich, *Metal-catalyzed Cross-Coupling Reactions*, 2nd ed., Wiley-VCH, Weinheim 2004.
- [11] J. Tsuji, *Palladium Reagents and Catalysts, New Perspectives For the 21st Century*, Wiley, West Sussex 2004.
- [12] Science of Synthesis: Catalytic Transformations via C–H Activation, (Ed: J. Yu), Thieme Chemistry, Stuttgart, Germany 2016, Vol. 1&2.
- [13] X. Chen, K. M. Engle, D.-H. Wang, J.-Q. Yu, *Angew. Chem., Int. Ed.* 2009, 48, 5094–5115.
- [14] T. W. Lyons, M. S. Sanford, *Chem. Rev.* 2010, 110, 1147–1169.
- [15] J. Wencel-Delord, T. Dröge, F. Liu, F. Glorius, *Chem. Soc. Rev.* 2011, 40, 4740.
- [16] L. Ackermann, *Chem. Rev.* 2011, 111, 1315–1345.
- [17] J. J. Topczewski, M. S. Sanford, *Chem. Sci.* 2015, 6, 70–76.
- [18] T. Gensch, M. N. Hopkinson, F. Glorius, J. Wencel-Delord, *Chem. Soc. Rev.* 2016, 45, 2900–2936.
- [19] S. Rej, Y. Ano, N. Chatani, *Chem. Rev.* 2020, 120, 1788–1887.
- [20] T. Dalton, T. Faber, F. Glorius, *ACS Cent. Sci.* 2021, 7, 245–261.
- [21] C. Sambaglio, D. Schönbauer, R. Blicek, T. Dao-Huy, G. Pototschnig, P. Schaaf, T. Wiesinger, M. F. Zia, J. Wencel-Delord, T. Besset, B. U. W. Maes, M. Schnürch, *Chem. Soc. Rev.* 2018, 47, 6603–6743.
- [22] J. Dupont, C. S. Consorti, J. Spencer, *Chem. Rev.* 2005, 105, 2527–2572.
- [23] J. Spencer, *Palladacycles, Synthesis, Characterization and Applications*, (Eds: M. Pfeifer, J. Dupont) Wiley-VCH, Weinheim, Germany 2008.
- [24] J. H. Docherty, T. M. Lister, G. McArthur, M. T. Findlay, P. Domingo-Legarda, J. Kenyon, S. Choudhary, I. Larrosa, *Chem. Rev.* 2023, 123, 7692–7760.
- [25] R. Li, F. Liu, G. Dong, *Chem* 2019, 5, 929–939.
- [26] D. Dupommier, T. Besset, *Chem* 2024, 10, 2651–2665.
- [27] A. F. M. Noisier, M. A. Brimble, *Chem. Rev.* 2014, 114, 8775–8806.
- [28] T. Brandhofer, O. García Mancheño, *Eur. J. Org. Chem.* 2018, 2018, 6050–6067.
- [29] A. Correa, *Eur. J. Inorg. Chem.* 2021, 2928–2941.
- [30] A. S. Barahdia, K. L. Thakare, L. Kaur, R. Jain, *Adv. Synth. Catal.* 2024, 366, 2844–2858.
- [31] G. Rani, V. Luxami, K. Paul, *Chem. Commun.* 2020, 56, 12479–12521.
- [32] F. Zhang, D. R. Spring, *Chem. Soc. Rev.* 2014, 43, 6906–6919.
- [33] A. Zarkadoulas, I. Zgouleta, N. V. Tzouras, G. C. Vougioukalakis, *Catalysts* 2021, 11, 554.
- [34] P. S. Marqués, C. Kammerer, *ChemPlusChem* 2024, 89, e202300728.
- [35] M. Sadeghi, *ACS Catal.* 2024, 14, 15356–15373.
- [36] M. Font, J. M. Quibell, G. J. P. Perry, I. Larrosa, *Chem. Commun.* 2017, 53, 5584–5597.
- [37] F.-L. Zhang, K. Hong, T.-J. Li, H. Park, J.-Q. Yu, *Science* 2016, 351, 252–256.
- [38] P. Gandeepan, L. Ackermann, *Chem* 2018, 4, 199–222.
- [39] Q. Zhao, T. Poisson, X. Pannecoucke, T. Besset, *Synthesis* 2017, 49, 4808–4826.
- [40] J. I. Higham, J. A. Bull, *Org. Biomol. Chem.* 2020, 18, 7291–7315.
- [41] T. Bhattacharya, S. Pimparkar, D. Maiti, *RSC Adv.* 2018, 8, 19456–19464.
- [42] C. Jacob, B. U. W. Maes, G. Evano, *Chem. -Eur. J.* 2021, 27, 13899–13952.
- [43] N. Goswami, T. Bhattacharya, D. Maiti, *Nat. Rev. Chem.* 2021, 5, 646–659.
- [44] M. I. Lapuh, S. Mazeh, T. Besset, *ACS Catal.* 2020, 10, 12898–12919.
- [45] S. St John-Campbell, J. A. Bull, *Org. Biomol. Chem.* 2018, 16, 4582–4595.
- [46] J. I. Higham, T.-K. Ma, J. A. Bull, *Chem. -Eur. J.* 2024, 30, e202400345.
- [47] B. Niu, K. Yang, B. Lawrence, H. Ge, *ChemSusChem* 2019, 12, 2955–2969.
- [48] T. Brückl, R. D. Baxter, Y. Ishihara, P. S. Baran, *Acc. Chem. Res.* 2012, 45, 826–839.
- [49] Y. Fujiwara, J. A. Dixon, F. O'Hara, E. D. Funder, D. D. Dixon, R. A. Rodriguez, R. D. Baxter, B. Herlé, N. Sach, M. R. Collins, Y. Ishihara, P. S. Baran, *Nature* 2012, 492, 95–99.
- [50] Y. Ji, T. Brueckl, R. D. Baxter, Y. Fujiwara, I. B. Seiple, S. Su, D. G. Blackmond, P. S. Baran, *Proc. Natl. Acad. Sci. USA* 2011, 108, 14411–14415.
- [51] H. Choi, M. Min, Q. Peng, D. Kang, R. S. Paton, S. Hong, *Chem. Sci.* 2016, 7, 3900–3909.
- [52] K. Wu, N. Lam, D. A. Strassfeld, Z. Fan, J. X. Qiao, T. Liu, D. Stamos, J.-Q. Yu, *Angew. Chem., Int. Ed.* 2024, 63, e202400509.
- [53] W. Li, J. Zhang, *Acc. Chem. Res.* 2024, 57, 489–513.
- [54] C. A. Salazar, J. J. Gair, K. N. Flesch, I. A. Guzei, J. C. Lewis, S. S. Stahl, *Angew. Chem., Int. Ed.* 2020, 59, 10873–10877.
- [55] S. B. Mohite, Y. K. Mirza, P. S. Bera, S. Nadigar, S. Yugendhar, R. Karpoomath, M. Bera, *Chem. -Eur. J.* 2025, 31, e202403032.
- [56] W. Ali, G. A. Oliver, D. B. Werz, D. Maiti, *Chem. Soc. Rev.* 2024, 53, 9904–9953.
- [57] Y. Wang, J. Feng, E.-Q. Li, Z. Jia, T.-P. Loh, *Org. Biomol. Chem.* 2024, 22, 37–54.
- [58] J. Dey, M. van Gemmeren, *Synlett* 2024, 35, 2191–2200.
- [59] D. Li, X.-B. He, L. Jin, X. Yu, Q. Zhang, *Tetrahedron Lett.* 2024, 138, 154951.
- [60] S. Dutta, T. Bhattacharya, F. J. Geffers, M. Bürger, D. Maiti, D. B. Werz, *Chem. Sci.* 2022, 13, 2551–2573.
- [61] A. Das, B. Maji, *Chem. Asian J.* 2021, 16, 397–408.
- [62] N. Y. S. Lam, K. Wu, J.-Q. Yu, *Angew. Chem., Int. Ed.* 2021, 60, 15767–15790.
- [63] L. Zhang, T. Ritter, *J. Am. Chem. Soc.* 2022, 144, 2399–2414.
- [64] L. Guillemard, N. Kaplaneris, L. Ackermann, M. J. Johansson, *Nat. Chem. Rev.* 2021, 5, 522–545.
- [65] T. Rogge, N. Kaplaneris, N. Chatani, J. Kim, S. Chang, B. Punji, L. L. Schafer, D. G. Musaev, J. Wencel-Delord, C. A. Roberts, R. Sarpong, Z. E. Wilson, M. A. Brimble, M. J. Johansson, L. Ackermann, *Nat. Rev. Methods Primers* 2021, 1, 43.
- [66] B. D. Barve, Y.-H. Kuo, W.-T. Li, *Chem. Commun.* 2021, 57, 12045–12057.
- [67] Q. Shao, K. Wu, Z. Zhuang, S. Qian, J.-Q. Yu, *Acc. Chem. Res.* 2020, 53, 833–851.
- [68] P. Wedi, M. van Gemmeren, *Angew. Chem., Int. Ed.* 2018, 57, 13016–13027.
- [69] D. Wang, A. B. Weinstein, P. B. White, S. S. Stahl, *Chem. Rev.* 2018, 118, 2636–2679.
- [70] S. Fernández-Moyano, V. Salamanca, A. C. Albéniz, *Chem. Sci.* 2023, 14, 6688–6694.
- [71] T. Xu, S. Mal, M. van Gemmeren, *ACS Catal.* 2025, 15, 2735–2741.
- [72] L.-P. Xu, Z. Zhuang, S. Qian, J.-Q. Yu, D. G. Musaev, *ACS Catal.* 2022, 12, 4848–4858.
- [73] Z. Zhuang, S. Liu, J.-T. Cheng, K.-S. Yeung, J. X. Qiao, N. A. Meanwell, J.-Q. Yu, *Angew. Chem., Int. Ed.* 2022, 61, e202207354.
- [74] G. Naskar, M. Jeganmohan, *Org. Lett.* 2024, 26, 6580–6585.
- [75] J. Das, T. Pal, W. Ali, S. R. Sahoo, D. Maiti, *ACS Catal.* 2022, 12, 11169–11176.
- [76] J. Liu, L.-J. Huang, Z. Sun, J. Li, *Org. Chem. Front.* 2024, 11, 6393–6410.
- [77] J. Das, W. Ali, A. Ghosh, T. Pal, A. Mandal, C. Teja, S. Dutta, R. Pothikumar, H. Ge, X. Zhang, D. Maiti, *Nat. Chem.* 2023, 15, 1626–1635.
- [78] T. Pal, P. Ghosh, M. Islam, S. Guin, S. Maji, S. Dutta, J. Das, H. Ge, D. Maiti, *Nat. Commun.* 2024, 15, 5370.
- [79] C. Yuan, C. Jia, W. Zhang, Y. You, L. Zhu, Y. Dong, *Org. Lett.* 2024, 26, 8798–8802.
- [80] D. H. Dethe, V. Kumar, M. Shukla, *Chem. Sci.* 2023, 14, 11267–11272.
- [81] Y. Wang, X. Xu, B. Pang, L. Hao, G. Wu, Y. Ji, *Org. Lett.* 2022, 24, 6734–6739.
- [82] C. Yuan, C. Jia, X. Zhang, W. Zhang, Y. You, X. Xu, L. Zhu, Y. Chen, Y. Dong, L. Xu, *Org. Lett.* 2024, 26, 4877–4881.
- [83] R. Kumar, D. Parmar, Sarthi, D. Chandra, Sumit, A. K. Sharma, U. Sharma, *Mol. Catal.* 2024, 568, 114395.
- [84] S. B. Mohite, M. V. Mane, M. Bera, R. Karpoomath, *Chem. -Eur. J.* 2023, 29, e202302759.
- [85] F. Wei, Y. Zhang, *Org. Lett.* 2024, 26, 6209–6213.
- [86] M. Bakthadoss, T. T. Reddy, *Chem. Sci.* 2023, 14, 5880–5886.
- [87] H. Li, M. Yang, L. Jin, Y.-F. Yang, Y.-B. She, *J. Org. Chem.* 2021, 86, 13475–13480.
- [88] H. Wang, H. Li, X. Chen, C. Zhou, S. Li, Y.-F. Yang, G. Li, *ACS Catal.* 2022, 12, 13435–13445.
- [89] T. Bhattacharya, C. Teja, N. Kumar, K. K. Bhagat, G. K. Lahiri, P. Gupta, S. Tyagi, D. Maiti, *ACS Catal.* 2024, 14, 2216–2228.
- [90] S. Bag, S. Jana, S. Pradhan, S. Bhowmick, N. Goswami, S. K. Sinha, D. Maiti, *Nat. Commun.* 2021, 12, 1393.
- [91] N. Goswami, N. Kumar, S. Bag, P. Gupta, D. Maiti, *ACS Catal.* 2023, 13, 11091–11103.
- [92] J. Tang, J. Huang, G. Li, Z. Liu, S. He, Z. Jin, *Org. Lett.* 2024, 26, 6109–6113.
- [93] G. Li, Y. Yan, J. Tang, Q. Ma, J. Huang, X. Xu, Z. Jin, *Org. Lett.* 2024, 26, 4733–4737.
- [94] K. Ramakrishna, J. P. Biswas, S. Jana, T. K. Achar, S. Porey, D. Maiti, *Angew. Chem., Int. Ed.* 2019, 58, 13808–13812.
- [95] H. Shi, Y. Lu, J. Weng, K. L. Bay, X. Chen, K. Tanaka, P. Verma, K. N. Houk, J.-Q. Yu, *Nat. Chem.* 2020, 12, 399–404.
- [96] G. E. Fernandez, D. Maiti, D. J. Tantillo, *Chem. -Eur. J.* 2023, 29, e202300124.

- [97] T. K. Achar, K. Ramakrishna, T. Pal, S. Porey, P. Dolui, J. P. Biswas, D. Maiti, *Chem. -Eur. J.* **2018**, *24*, 17906–17910.
- [98] T. Yamada, K. Tanaka III, Y. Hashimoto, N. Morita, O. Tamura, *Adv. Synth. Catal.* **2023**, *365*, 3138–3148.
- [99] L. Zhou, H.-G. Cheng, L. Li, K. Wu, J. Hou, C. Jiao, S. Deng, Z. Liu, J.-Q. Yu, Q. Zhou, *Nat. Chem.* **2023**, *15*, 815–823.
- [100] M. Catellani, F. Frignani, A. Rangoni, *Angew. Chem., Int. Ed.* **1997**, *36*, 119–122.
- [101] F. Jia, C. Zhang, Y. Yang, X. Zheng, M. Shi, *Catal. Sci. Technol.* **2025**, *15*, 173–184.
- [102] C.-X. Liu, W.-W. Zhang, P. Yang, F. Zhao, Z. Feng, Q. Wang, S.-Z. Zhang, Q. Gu, S.-L. You, *Chem. Catal.* **2022**, *2*, 102–113.
- [103] D. A. Strassfeld, C.-Y. Chen, H. S. Park, D. Q. Phan, J.-Q. Yu, *Nature* **2023**, *622*, 80–86.
- [104] T. Sheng, G. Kang, T. Zhang, G. Meng, Z. Zhuang, N. Chekshin, J.-Q. Yu, *Angew. Chem., Int. Ed.* **2024**, *63*, e202408603.
- [105] V. G. Landge, A. Mishra, W. Thotamune, A. L. Bonds, I. Alahakoon, A. Karunaratne, M. C. Young, *Chem. Catal.* **2023**, *3*, 100809.
- [106] J. Rodrigalvarez, M. J. Gaunt, *ACS Catal.* **2024**, *14*, 18831–18840.
- [107] Z.-Y. Zhang, T. Zhang, Y. Ouyang, P. Lu, J. X. Qiao, J.-Q. Yu, *Chem. Sci.* **2024**, *15*, 17092–17096.
- [108] S. Mal, F. Jurk, K. Hiesinger, M. van Gemmeren, *Nat. Synthesis* **2024**, *3*, 1292–1298.
- [109] H. Wang, C. Zhou, Z. Gao, S. Li, G. Li, *Angew. Chem., Int. Ed.* **2023**, *62*, e202300905.
- [110] S. Wang, K. Chen, F. Guo, W. Zhu, C. Liu, H. Dong, J.-Q. Yu, X. Lei, *ACS Cent. Sci.* **2023**, *9*, 1129–1139.
- [111] S. Kaltenberger, M. van Gemmeren, *Acc. Chem. Res.* **2023**, *56*, 2459–2472.
- [112] P. Wedi, M. Farizyan, K. Bergander, C. Mück-Lichtenfeld, M. van Gemmeren, *Angew. Chem., Int. Ed.* **2021**, *60*, 15641–15649.
- [113] H. Chen, A. Mondal, P. Wedi, M. van Gemmeren, *ACS Catal.* **2019**, *9*, 1979–1984.
- [114] A. Mondal, H. Chen, L. Flämig, P. Wedi, M. van Gemmeren, *J. Am. Chem. Soc.* **2019**, *141*, 18662–18667.
- [115] A. Mondal, M. van Gemmeren, *Angew. Chem., Int. Ed.* **2021**, *60*, 742–746.
- [116] D. Zhao, P. Xu, T. Ritter, *Chem* **2019**, *5*, 97–107.
- [117] C. Zhao, S. Yang, Y. Cheng, R. Qu, X. Huang, H. Liu, *J. Org. Chem.* **2021**, *86*, 10526–10535.
- [118] S. K. Sinha, S. Panja, J. Grover, P. S. Hazra, S. Pandit, Y. Bairagi, X. Zhang, D. Maiti, *J. Am. Chem. Soc.* **2022**, *144*, 12032–12042.
- [119] M. Farizyan, R. de Jesus, J. Dey, M. van Gemmeren, *Chem. Sci.* **2023**, *14*, 4357–4362.
- [120] M. Farizyan, A. Mondal, S. Mal, F. Deufel, M. van Gemmeren, *J. Am. Chem. Soc.* **2021**, *143*, 16370–16376.
- [121] F. Deufel, M. van Gemmeren, *J. Chem. Educ.* **2024**, *101*, 3410–3417.
- [122] Y. Bairagi, S. Porey, S. V. C. Vummaleti, X. Zhang, G. K. Lahiri, D. Maiti, *ACS Catal.* **2024**, *14*, 15654–15664.
- [123] M. Tomanik, J.-Q. Yu, *J. Am. Chem. Soc.* **2023**, *145*, 17919–17925.
- [124] S. Porey, Y. Bairagi, S. Guin, X. Zhang, D. Maiti, *ACS Catal.* **2023**, *13*, 14000–14011.
- [125] J. M. González, X. Vidal, M. A. Ortuño, J. L. Mascareñas, M. Gulías, *J. Am. Chem. Soc.* **2022**, *144*, 21437–21442.
- [126] X. Yu, S. Liu, L. Wang, Y. Li, M. Huang, Z.-Y. Yan, H.-C. Li, Q. Zhang, X. Zhang, B.-F. Shi, *ACS Catal.* **2025**, *15*, 2540–2549.
- [127] A. Mondal, M. Díaz-Ruiz, F. Deufel, F. Maseras, M. van Gemmeren, *Chem* **2023**, *9*, 1004–1016.
- [128] N. Goswami, S. K. Sinha, P. Mondal, S. Adhya, A. Datta, D. Maiti, *Chem* **2023**, *9*, 989–1003.
- [129] C. Pinilla, A. C. Albéniz, *Eur. J. Inorg. Chem.* **2024**, *27*, e202400076.
- [130] J. M. Rawson, R. E. P. Winpenny, *Coord. Chem. Rev.* **1995**, *139*, 313–374.
- [131] E. J. Kang, E. Lee, *Chem. Rev.* **2005**, *105*, 4348–4378.
- [132] J.-L. Yan, L. Hu, Y. Lu, J.-Q. Yu, *J. Am. Chem. Soc.* **2024**, *146*, 29311–29314.
- [133] L. Hu, G. Meng, J.-Q. Yu, *J. Am. Chem. Soc.* **2022**, *144*, 20550–20553.
- [134] R. Khawaled, A. Bruening-Wright, J. P. Adelman, J. Maylie, *Pflügers Arch. Eur. J. Physiol.* **1999**, *438*, 314–321.
- [135] X.-L. Yang, S. Zhang, Q.-B. Hu, D.-Q. Luo, Y. Zhang, *J. Antibiot. (Tokyo)* **2011**, *64*, 723–727.
- [136] J. Zhao, J. Feng, Z. Tan, J. Liu, J. Zhao, R. Chen, K. Xie, D. Zhang, Y. Li, L. Yu, X. Chen, J. Dai, *J. Nat. Prod.* **2017**, *80*, 1819–1826.
- [137] S. Qian, Z.-Q. Li, M. Li, S. R. Wisniewski, J. X. Qiao, J. M. Richter, W. R. Ewing, M. D. Eastgate, J. S. Chen, J.-Q. Yu, *Org. Lett.* **2020**, *22*, 3960–3963.
- [138] L.-P. Xu, S. Qian, Z. Zhuang, J.-Q. Yu, D. G. Musaev, *Nat. Commun.* **2022**, *13*, 315.
- [139] M.d. E. Hoque, J. Yu, *Angew. Chem., Int. Ed.* **2023**, *62*, e202312331.
- [140] Z. Wang, L. Hu, N. Chekshin, Z. Zhuang, S. Qian, J. X. Qiao, J.-Q. Yu, *Science* **2021**, *374*, 1281–1285.
- [141] B. R. Albuquerque, S. A. Heleno, M. B. P. P. Oliveira, L. Barros, I. C. F. R. Ferreira, *Food Funct.* **2021**, *12*, 14–29.
- [142] W.-T. Wu, L. Zhang, S.-L. You, *Chem. Soc. Rev.* **2016**, *45*, 1570–1580.
- [143] Z. Qiu, C.-J. Li, *Chem. Rev.* **2020**, *120*, 10454–10515.
- [144] Z. Li, H. S. Park, J. X. Qiao, K.-S. Yeung, J.-Q. Yu, *J. Am. Chem. Soc.* **2022**, *144*, 18109–18116.
- [145] Z. Li, J.-Q. Yu, *J. Am. Chem. Soc.* **2023**, *145*, 25948–25953.
- [146] J. Muzart, *Eur. J. Org. Chem.* **2010**, *2010*, 3779–3790.
- [147] G. Dumonteil, S. Berteina-Raboin, *Catalysts* **2022**, *12*, 86.
- [148] M. De Paolis, I. Chataigner, J. Maddaluno, in *Ster. Alkene Synth.* (Ed: J. Wang), Springer Berlin Heidelberg, Berlin, Heidelberg **2012**, pp. 87–146.
- [149] G. Meng, L. Hu, H. S. S. Chan, J. X. Qiao, J.-Q. Yu, *J. Am. Chem. Soc.* **2023**, *145*, 13003–13007.
- [150] T. Sheng, G. Kang, Z. Zhuang, N. Chekshin, Z. Wang, L. Hu, J.-Q. Yu, *J. Am. Chem. Soc.* **2023**, *145*, 20951–20958.
- [151] E. Vitaku, D. T. Smith, J. T. Njardarson, *J. Med. Chem.* **2014**, *57*, 10257–10274.
- [152] L. Yang, X. Wang, M. Zhang, S. Li, X. Fang, G. Li, *Org. Chem. Front.* **2023**, *10*, 3760–3765.
- [153] K. Murakami, S. Yamada, T. Kaneda, K. Itami, *Chem. Rev.* **2017**, *117*, 9302–9332.
- [154] G. Meng, Z. Wang, H. S. S. Chan, N. Chekshin, Z. Li, P. Wang, J.-Q. Yu, *J. Am. Chem. Soc.* **2023**, *145*, 8198–8208.
- [155] S. Jeong, C. Lee, J. M. Joo, *Adv. Synth. Catal.* **2024**, adsc.202401139.
- [156] G. Meng, J.-L. Yan, N. Chekshin, D. A. Strassfeld, J.-Q. Yu, *ACS Catal.* **2024**, *14*, 12806–12813.
- [157] L. Hu, G. Meng, J.-Q. Yu, *J. Am. Chem. Soc.* **2022**, *144*, 20550–20553.
- [158] G. Kang, D. A. Strassfeld, T. Sheng, C.-Y. Chen, J.-Q. Yu, *Nature* **2023**, *618*, 519–525.
- [159] P. Wang, P. Verma, G. Xia, J. Shi, J. X. Qiao, S. Tao, P. T. W. Cheng, M. A. Poss, M. E. Farmer, K.-S. Yeung, J.-Q. Yu, *Nature* **2017**, *551*, 489–493.
- [160] C. Yuan, X. Wang, L. Jiao, *Angew. Chem., Int. Ed.* **2023**, *62*, e202300854.
- [161] C.-H. Yuan, L. Jiao, *Org. Lett.* **2024**, *26*, 29–34.
- [162] C. Yuan, X. Wang, K. Huang, L. Jiao, *Angew. Chem., Int. Ed.* **2024**, *63*, e202405062.
- [163] N. Goswami, N. Kumar, P. Gupta, D. Maiti, *ACS Catal.* **2024**, *14*, 3798–3811.
- [164] L. Wang, N. Wang, W. Zhang, X. Cheng, Z. Yan, G. Shao, X. Wang, R. Wang, C. Fu, *Signal Transduct. Target. Ther.* **2022**, *7*, 48.
- [165] M. Muttenthaler, G. F. King, D. J. Adams, P. F. Alewood, *Nat. Rev. Drug Discovery* **2021**, *20*, 309–325.
- [166] Z.-L. Hou, Y. Tang, Y. Lu, B. Yao, *ACS Catal.* **2024**, *14*, 11026–11033.
- [167] S. K. Sinha, N. Goswami, Y. Li, S. Maji, D. Raja, A. Suseelan Sarala, S. Guin, R. S. Paton, D. Maiti, *ACS Catal.* **2024**, *14*, 12681–12693.
- [168] J. E. Parker, A. G. S. Warrilow, H. J. Cools, C. M. Martel, W. D. Nes, B. A. Fraaije, J. A. Lucas, D. E. Kelly, S. L. Kelly, *Appl. Environ. Microbiol.* **2011**, *77*, 1460–1465.
- [169] P. Gergely, B. Nuesslein-Hildesheim, D. Guerini, V. Brinkmann, M. Traebers, C. Bruns, S. Pan, N. S. Gray, K. Hinterding, N. G. Cooke, A. Groenewegen, A. Vitaliti, T. Sing, O. Luttringer, J. Yang, A. Gardin, N. Wang, W. J. Crumb Jr, M. Saltzman, M. Rosenberg, E. Wallström, *Br. J. Pharmacol.* **2012**, *167*, 1035–1047.
- [170] R. W. Schrier, P. Gross, M. Gheorghiadu, T. Berl, J. G. Verbalis, F. S. Czerwicz, C. Orlandi, *N. Engl. J. Med.* **2006**, *355*, 2099–2112.
- [171] H.-C. Shen, J.-J. Li, P. Wang, J.-Q. Yu, *Chem. Sci.* **2024**, *15*, 15819–15824.
- [172] M. Abbod, N. Safaie, K. Gholivand, M. Mehrabadi, M. Bonsaii, A. A. E. Valmoozi, *Chem. Biol. Technol. Agric.* **2021**, *8*, 48.
- [173] S. Hkiri, C. Gourlaouen, S. Touil, A. Samarat, D. Sémeril, *New J. Chem.* **2021**, *45*, 11327–11335.
- [174] L. Yi, T. Zhao, J. Bu, J. Long, Q. Yang, *Org. Lett.* **2024**, *26*, 4132–4136.
- [175] S. M. Bachrach, *J. Org. Chem.* **2008**, *73*, 2466–2468.
- [176] Z. Xu, Z. Li, C. Liu, K. Yang, H. Ge, *Molecules* **2024**, *29*, 259.
- [177] C. Pinilla, M. García-Zarza, A. C. Albéniz, *Org. Chem. Front.* **2025**, *12*, 467–477.
- [178] K. Jia, J. Wang, X. Wang, C. Jiang, *Syn Lett* **2025**.
- [179] A. Dutta, M. Jeganmohan, *Org. Lett.* **2023**, *25*, 6305–6310.

- [180] T. Bi, Y. Cui, S. Liu, H. Yu, W. Qiu, K.-Q. Hou, J. Zou, Z. Yu, F. Zhang, Z. Xu, J. Zhang, X. Xu, W. Yang, *Angew. Chem., Int. Ed.* **2024**, *63*, e202412296.
- [181] K. D. Sipps, W. A. Gibbs, E. R. Sayfutyarova, J. L. Kuo, *ACS Catal.* **2024**, *14*, 18045–18054.
- [182] L. Jin, Y. Li, Y. Mao, X. B. He, Z. Lu, Q. Zhang, B. F. Shi, *Nature Commun.* **2024**, *15*, 4908–4918.
- [183] M. Liu, B. Qiu, Z. Zhang, Y. Zheng, J. Yuan, H. Li, X. Zhang, *J. Org. Chem.* **2024**, *89*, 8023–8034.
- [184] Z. Fan, D. A. Strassfeld, H. S. Park, K. Wu, J. Q. Yu, *Angew. Chem., Int. Ed.* **2023**, *62*, e202303948.
- [185] A. Shen, R. Bao, C. Shen, S. Cen, Z. Zhang, *Org. Lett.* **2024**, *26*, 10671–10677.
- [186] J. Dey, S. Kaltenberger, M. van Gemmeren, *Angew. Chem., Int. Ed.* **2024**, *63*, e202404421.
- [187] J. Dey, M. van Gemmeren, *Synlett* **2024**, *35*, 2191–2200.
- [188] H. Targhan, A. Rezaei, A. Aliabadi, A. Ramazani, Z. Zhao, H. Zheng, *Sci. Rep.* **2024**, *14*, 536–548.
- [189] M. H. Sayahi, A. Serajian, S. Bahadorikhalili, M. Mahdavi, *Sci. Rep.* **2024**, *14*, 26325–26337.
- [190] L. Chen, S. Zhang, Y. Yang, X. Wang, W. Lan, Z. Chen, W. Gong, Q. Nie, W. Cao, Z. Meng, *RSC Adv.* **2024**, *14*, 37928–37932.
- [191] J. Fichez, M. I. Lapuh, L. Truong, H. Oulyadi, F. Buttard, T. Besset, *Adv. Synth. Catal.* **2024**, *366*, 2811–2822.
- [192] L. Hu, G. Meng, X. Chen, J. S. Yoon, J. R. Shan, N. Chekshin, D. A. Strassfeld, T. Sheng, Z. Zhuang, R. Jazzar, G. Bertrand, K. N. Houk, J. Q. Yu, *J. Am. Chem. Soc.* **2023**, *145*, 16297–16304.
- [193] C. Valderas, K. Naksomboon, M. Á.n. Fernández-Ibáñez, *ChemCatChem* **2016**, *8*, 3213–3217.
- [194] K. Naksomboon, C. Valderas, M. Gómez-Martínez, Y. Álvarez-Casao, M. Á. n. Fernández-Ibáñez, *ACS Catal.* **2017**, *7*, 6342–6346.
- [195] K. Naksomboon, E. Gómez-Bengoa, J. Mehara, J. Roithová, E. Otten, M. Á.n. Fernández-Ibáñez, *Chem. Sci.* **2023**, *14*, 2943–2953.
- [196] K. Naksomboon, J. Poater, F. M. Bickelhaupt, M. Á. n. Fernández-Ibáñez, *J. Am. Chem. Soc.* **2019**, *141*, 6719–6725.
- [197] K.e-Z. Deng, W.-L. Jia, M. Ángeles Fernández-Ibáñez, *Chem. -Eur. J.* **2022**, *28*, e202104107.
- [198] V. Sukowski, M. Van Borselen, S. Mathew, B. de Bruin, M.Á.N. Fernández-Ibáñez, *Angew. Chem., Int. Ed.* **2024**, *63*, e202317741.
- [199] V. Sukowski, M. Van Borselen, S. Mathew, M. Á.n. Fernández-Ibáñez, *Angew. Chem., Int. Ed.* **2022**, *61*, e202201750.
- [200] K.e-Z. Deng, V. Sukowski, M. Á.n. Fernández-Ibáñez, *Angew. Chem., Int. Ed.* **2024**, *63*, e202400689.
- [201] E. González-Fernández, N. Marinus, J. Dhankhar, A. Linden, I. Čorić, *Chem. -Eur. J.* **2024**, *30*, e202401215.
- [202] S. S. Ng, W. H. Pang, O. Y. Yuen, C. M. So, *Org. Chem. Front.* **2023**, *10*, 4408–4436.
- [203] T. Imamoto, *Chem. Rev.* **2024**, *124*, 8657–8739.
- [204] F. Garnes-Portolés, S. Sanz-Navarro, J. Ballesteros-Soberanas, A. Collado-Pérez, J. Sánchez-Quesada, E. Espinós-Ferri, A. Leyva-Pérez, *J. Org. Chem.* **2023**, *88*, 5962–5971.
- [205] X. Lv, M. Wang, Y. Zhao, Z. Shi, *J. Am. Chem. Soc.* **2024**, *146*, 3483–3491.
- [206] C. Gu, C. M. So, *Adv. Sci.* **2024**, *11*, 2309192.
- [207] B. Mondal, R. Naskar, J. Bag, S. Garai, R. Maity, *Organometallics* **2024**, *43*, 2486–2494.
- [208] Y.-J. Zhang, X.-S. Wang, J. Cao, L.-W. Xu, *Green Chem.* **2024**, *26*, 8360–8366.
- [209] J. Yao, L. Shao, X. Huo, X. Wang, *Sci. China Chem.* **2024**, *67*, 882–889.
- [210] C. Debnath, S. R. Bhoi, S. Gandhi, *Org. Biomol. Chem.* **2024**, *22*, 4613–4624.
- [211] X.-X. Wang, L. Jiao, *J. Am. Chem. Soc.* **2024**, *146*, 25552–25561.
- [212] S. P. Rezgui, J. Farhi, H. Yu, Z. P. Sercel, S. C. Virgil, B. M. Stoltz, *Chem. Sci.* **2024**, *15*, 12284–12290.

Manuscript received: April 11, 2025

Revised manuscript received: June 4, 2025

Accepted manuscript online: June 4, 2025

Version of record online: ■ ■ ■